

RETURNING MATERIALS:
Place in book drop to remove this checkout from your record. FINES will be charged if book is returned after the date stamped below.

# THE DEVELOPMENT AND APPLICATION OF POST-SECTOR BEAM DEFLECTION IN TIME-RESOLVED ION MOMENTUM SPECTROMETRY

Ву

Brian Allen Eckenrode

## **A DISSERTATION**

Submitted to
Michigan State University
in partial fulfillment of the requirements
for the degree of

**DOCTOR OF PHILOSOPHY** 

**Department of Chemistry** 

1988

## **ABSTRACT**

# THE DEVELOPMENT AND APPLICATION OF POST-SECTOR BEAM DEFLECTION IN TIME-RESOLVED ION MOMENTUM SPECTROMETRY

By

#### Brian Allen Eckenrode

Post-sector beam deflection has propelled time-resolved ion momentum spectrometry (TRIMS), a form of mass spectrometry/mass spectrometry (MS/MS), to a greater realization of its analytical potential. TRIMS combines magnetic sector and time-of-flight analyzers to give energy-independent mass determination, and to enable separation of parent ions and products of metastable or collisionally activated dissociations. In the time-resolving section of this mass spectrometer, ion packet formation by beam deflection is shown to be superior to formation by ion source pulsing. Simultaneous time and momentum resolutions of 650 and 500 were achieved. Loss in detectability over that obtained using the magnetic sector without time resolution is only a factor of 65, despite the fact that the ion beam is on only 0.01% of the time. Precise beam intensity profiles as a function of magnetic field strength and arrival time are obtained.

TRIMS, in combination with time-array detection, (TAD), offers the unique capability to collect a complete MS/MS data field (all the daughter ions of all the parent ions) in a single sweep of the magnet. In TRIMS, observation of all arrival times for all values of the magnetic field strength produces a two-dimensional field from which all MS/MS data can be obtained. For components of a mixture, separated by chromatography, complete MS/MS data can now be collected.

Evaluation of the TRIMS-TAD instrument with regard to data quality, integrity and speed under raw data acquisition conditions is reported. To demonstrate the GC-MS/MS capability of TRIMS-TAD, a ten-second acquisition of the complete fragmentation map for methyl stearate is presented.

TRIMS can provide accurate mass assignments. The fundamental properties of momentum and velocity can be measured leading to an energy-independent ion mass assignment. Relative standard deviation values for n-decane stable ion mass assignments are typically less than 0.20 % with relative mass assignment errors not exceeding 3 parts per thousand.

TRIMS provides an alternate technique for the determination of the kinetic energy released in metastable or collisionally activated dissociations. The measured energy profiles for stable ions and the energy distribution profiles for daughter ions appear in the expected shape and location in the B-t data field. The energy release values calculated from the TRIMS data for selected compounds compare well with those in the literature.

To my beautiful and loving wife **JoAnne** 

#### **ACKNOWLEDGMENTS**

I thank the Lord my God for giving me the parents I have, guiding me into the field of analytical chemistry, and helping me to attain the level of Ph. D. in this field. My parents raised me with love and support. They instilled in me a good set of moral values, a desire to be the best, and the spirit and strength to be the best I could be. To them I give a thank-you too big for words.

I would like to thank the educators who have influenced me through the years. My high school chemistry teachers, Mr. Pawlowski and Mr. Harack, with their humorous and innovative approach to teaching, sparked my interest in chemistry. Professors Annino, McCarthy, Dinan, Stanton, VanVerth, and Bieron taught me to build on the fundamentals of chemistry and helped me to prepare for advanced research.

Professors Watson and Enke lead me along the research path described in this thesis. Dr. Jack Watson has worked to develop me into a capable mass spectrometrist. His skill as a scientist and a manager has opened my mind to several areas of bio-analytical chemistry. Dr. Christie Enke has taught me to read and write scientific publications very critically and precisely. He is technically superb with creative insights and a gift for expressing them. Both professors encourage freedom in research and this freedom allowed me to fail and falter as well as to discover and pursue ideas. This research philosophy has made me a very independent scientist and the experience will be invaluable in the world of industry or academe.

Dr. Jack Holland has been a great "coach" of the ITR and TRIMS project.

We have had several discussions that have helped me tremendously. I would

also like to thank Dr. Stille for participating in my defense in place of another fine professor. Dr. Eeroi.

Several others deserve a great deal of thanks. These include my family and relatives, my wife JoAnne and her family, and my close friends: Pat Roach, Joe Durick, Bob Kean and Tim Rydel. Their love and support has made the rough times in graduate school a little smoother.

Lastly, the friends I have made in graduate school that have helped shaped my intellect and personality, deserve thanks. My friends include the research groups of Watson, Enke, and Allison, the Facility staff, the ITR group, Marty Rabb, and Russ Geyer. Special thanks go to Bruce Newcome, Mike Davenport, Hugh Gregg, Norm Penix, Mark Victor, Keiji Asano, Pete Palmer, Rob Engerer, Ron Lopshire, George Yefchak and Kevin McNitt. We all may be moving on, but friendships are forever.

# TABLE OF CONTENTS

LIST OF FIGURES	. viii
LIST OF TABLES	, xvi
CHAPTER IINTRODUCTION	1
Research Goals	1
MS/MS INSTRUMENTATION	4
MS/MS - spatial based	7
The Double-focusing Geometry for MS/MS - spatial based	10
Fourier Transform Ion Cyclotron Resonance	46
Instruments - temporal based	18
First Generation	18
TIME-SLICE AND TIME-ARRAY DETECTION METHODS	. 29
Time-slice	. 29
REFERENCES	33
OLIARTER II	26
CHAPTER II	. 36
Post-sector Beam Deflection	36
Source Pulsing	, , 30 , , 42
Post-source pulsing	48
Resolution	56
Detectability	61
SIM data recording	62
Magnet Control	63
B-t data field acquisition	64
TRIMS-ITR Interface boards	. 64
Algorithm for mass assignments	75
REFERENCES	77

CHAPTER III  MASS ASSIGNMENT CAPABILITY OF TRIMS  Introduction  Theoretical Principles  Translational energy loss independence  Mass assignments in magnetic sector instruments  Mass assignments in time-of-flight instruments  PRECISION AND ACCURACY OF MASS ASSIGNMENTS	78 78. 79.
Stable ion mass assignments	.8
DVANTAGES OF TRIMS FOR MASS ASSIGNMENTS	.84 .85
REFERENCES	. 86
CHAPTER IV	.89 .89
detectability, and acquisition time	. 89
NSTRUMENTATION FÓR TRIMS-TAD	.94
Experimental Setup	. 98 101
MS/MS data quality determination	10
MS/MS data integrity and speed assessment	11(
Selected reaction monitoring	114
acquisition	110
TUTURE OPPORTUNITIES FOR TRIMS-TAD	118 110

CHAPTER VKINETIC ENERGY RELEASE MEASUREMENT WITH TRIMS-TAD	
Introduction	
INSTRUMENT OPERATION WHEN STUDYING KINETIC ENERGY RELEASE KINETIC ENERGY RELEASE RESULTS	124
CONCLUSION	133
CHAPTER VIFUTURE APPLICATIONS OF TRIMS-TAD	136
Introduction	136
GENERAL SYSTEM IMPROVEMENTS	138
System (ACES) and TRIMS-TAD	139

5

# **LIST OF FIGURES**

Figure 1.1 An MS/MS spectrum is typically obtained by fragmenting a selected ion and collecting the resulting ion current. In this way a daughter mass spectrum is produced, providing another dimension of information.  Reprinted from reference 16
Figure 1.2 MS/MS can provide an added dimension of information producing a 3-dimensional "fingerprint" of the compound. The complete MS/MS data field is shown for the protonated molecular ion of dimethylmorpholino phosphoramidate (DMMPA).  Reprinted from reference 21
Figure 1.3 In a typical MS/MS instrument, two stages of mass separation are employed. A sequential manner of analysis with ion formation, parent ion selection, parent ion dissociation and daughter ion selection followed by ion detection is achieved, yielding either additional structure information or mixture component identification
<u>Figure 1.4</u> A <u>Triple-Quadrupole Mass Spectrometer (TQMS) illustrating two stages of mass filtration separated by a single stage of ion reaction/collision. lonization can be performed under electron impact (EI) or chemical ionization (CI) conditions, among others9</u>
Figure 1.5 A. Mass Analyzed Ion Kinetic Energy Spectrometer (MIKES) illustrating ion selection, selected ion fragmentation followed by daughter ion analysis
Figure 1.6 Controlled analyzer scanning MS/MS. Two dimensional metastable map of ions in the decan-1-ol (molecular weight 158) electron impact spectrum. The electric sector is stepped followed by fast repetitive scanning of the magnet. The dots indicate the detection of a metastable ion.  Adapted from reference 37

Figure 1.7: Process of acquiring a complete MS/MS data field with different tandem mass filter instruments. The arrows inside the data boundaries show the incremental, and thus sequential, operation required to achieve a full field acquisition by these techniques.  TQMS = triple quadrupole mass spectrometer MIKES = mass analyzed ion kinetic energy spectrometer (reverse geometry) EB = forward geometry double-focusing mass spectrometer (linked scan)
Figure 1.8 FT-MS/MS radio-frequency pulse sequence. Approximately 40 msec is required to isolate a particular parent ion in the analyzer cell of an FTMS instrument. This parent ion is excited to a known energy for collision. Approximately 50 msec is required for parent excitation, collision, and daughter ion detection. This pulse sequence is performed in a background of argon collision gas (1 x 10-6 to 1 x 10-5 torr)
Figure 1.9 The dispersion of collisionally dissociated ions in a magnetic sector and time-of-flight mass spectrometers.  p = parent, d = daughter
Figure 1.10 A magnetic field strength sweep of a selected mass region of benzonitrile. At approximately 980 DAC units the stable ions at mass 56 and the ions from the 103>96 metastable decomposition are superimposed. The TRIMS technique would allow for the separation of these ions, and therefore, lead to an unambiguous mass assignment for compound structure analysis
Figure 1.11 Ion separation by momentum and velocity in TRIMS. Daughter ions from the same parent appear at the same arrival time but are dispersed according to their momenta. Stable ions have shorter arrival times than daughter ions of the same momentum because of their greater initial velocity 22
Figure 1.12 The values of momentum and velocity are compared for the benzonitrile metastable reaction discussed in Figure 1.9.  KE = kinetic energy, v = velocity, mv = momentum

Figure 1.13 The <i>B-t</i> data field for TRIMS showing the expected locus of points for different types of ions.  Adapted from reference 1
Figure 1.14 MS/MS scan modes available with TRIMS. In every case, the value on the mass axis in the resulting mass spectrum is obtained from the combination of <i>B</i> and <i>t</i> at which the ion current is detected
Figure 1.15 The MS/MS data field generated by the TRIMS instrument. The horizontal lines represent ion arrival-time spectra acquired at a particular magnetic field strength (B). The heavy arrow indicates that only one sweep of the magnet is required to collect the full MS/MS data field and that the magnet is swept simultaneously with the arrival-time data acquisition. Interrogation of this field (post-processing) provides the characteristic MS/MS scans
Figure 1.16 Comparison of time-slice detection and time-array detection. A simulated time-of-flight mass spectrum is shown for n-butane, using a flight-tube length of 100 cm and an accelerating voltage of 3,000 V. In time-slice detection, only one time window is measured for each pulse event, thereby requiring multiple pulses to construct the complete spectrum. In time-array detection, the complete spectrum is acquired following each pulse event
Figure 1.17 Block diagram of the integrating transient recorder (ITR). TOF transients are digitized, summed, reduced to hall, time, intensity triplets, and stored as a scan file. With parallel processing this sequence can occur at approximately 180 Hz

Figure 2.1 : Three basic ion formation possibilities found in the source of any mass spectrometer: (a), initial spatial spread, (b), spread in magnitude of initial kinetic energies, and (c), angular distribution of the initial kinetic energies (worst case shown) also known as "the turn-around time"
Figure 2.2 Results of TRIMS (first generation) operated with source pulsing40
Figure 2.3 Final ion velocity as a function of total flight time for mass 71 at several extraction voltages with ion source pulsing
<u>Figure 2.4</u> Ion pulse formation by deflection of a continuous beam across an aperture. D = separation between deflection plates; S = aperture width; V' = deflection voltage; $\Delta tof_p$ = width in time of ion packet passing through the aperture [15]
Figure 2.5 Four "snapshots" from a model of ion trajectories in a beam deflection assembly. This is the deflection plate region with a plate spacing of 2 mm, slit width of 2 cm, length to slit of 1.5 m, mass of 1000 u, an energy of 3500 eV and a 100 V deflection pulse applied
Figure 2.6 Deflection of a continuous ion beam removes the resolution limiting effects of spatial spread and turn-around time
Figure 2.7 Diagram of the beam deflection assembly constructed for the LKB-9000. The assembly is built on the existing exit slit housing
Figure 2.8 Schematic of the fast square wave plate driver. This circuit generates the pulses which create the ion packet for TOF analysis
Figure 2.9 (a) Top view of the ion path through the instrument. (b) Top view of the deflection slit assembly

<u>Figure 2.10</u> A schematic representation of the ion momentum and time dispersion characteristics of the modified magnetic sector mass spectrometer55
Figure 2.11 Plot showing the 92+> 91+ metastable decomposition product of toluene as well as the stable ion at mass 90. This is a single sweep of the time axis while the magnet is set to pass mass 90
Figure 2.12 Plot of the ion current representing the 142+> 112+ and 142+> 113+ metastable decomposition products of the molecular ion of n-decane. The time of arrival of the parent is held constant and the magnetic field is swept. Five hundred pulses were averaged for each of 40 sweeps of the magnet. These data result from background subtraction and smoothing (m/Δm for the magnetic field axis is ≈500)
Figure 2.13 Contour of the molecular ion region of toluene. Isomass ions of higher velocity arrive at the detector at a higher magnetic field strength and in less time than slower ions of the same mass. This effect is more pronounced for metastable or CAD reactions in TRIMS because of the energy spread that results from these processes
Figure 2.14 Three-dimensional view of the molecular ion region of toluene65
Figure 2.15 Block diagram of the TRIMS-ITR interface board. This board communicates with the signal in/command out (SIN/COUT) board on the VME bus of the ITR
Figure 2.15 a. Schematic of the TRIMS-ITR interface board
Figure 2.16 Block diagram of the optically-isolated ADC board that communicates with the TRIMS-ITR interface board. This circuitry allows the ITR to sense the magnetic field strength at any time and synchronize this data with ion arrival time information
Figure 2.16 a. Schematic of the optically-isolated ADC board 70

Figure 2.17 Block diagram of the DAC interface to the ITR from the TRIMS instrument. This circuit allows the ITR to control the magnetic field strength in step-wise fashion
Figure 2.17 a. Schematic of the DAC interface board
Figure 2.18 Hall voltage plotted as a function of the square root of mass. The relationship is linear and can be used to calibrate the TRIMS instrument 7
Figure 2.19 Results from the digitized Hall voltage vs m <sup>1/2</sup> . A linear fit is evider and agrees well with the analog data presented in Figure 2.18. Thes measurements indicate a properly functioning Hall-read interface

Figure 4.1 Detailed diagram of the <i>B-t</i> data field acquisition process. At each magnetic field strength increment, multiple TOF transients are summed to produce a scan. The full <i>B-t</i> data field thus consists of several scans for a single sweep of the magnetic field strength
Figure 4.2 A schematic of the TRIMS-TAD instrument. The TAD data system is comprised of an integrating transient recorder (ITR) and control hardware 93
Figure 4.3 a The ITR data system consists of several modules which all communicate over a VME bus. Data flow begins at the top with transient digitization and summation occurring via "command-status" control modules. The data-out board can move data across the bus to a reduction module or to disk for storage
Figure 4.3 b The custom sum and store circuitry module of the ITR data system. Each bank contains an adder, RAM (1K x 24-bit) and a 24-bit latch. One bank sums successive transients while the other bank outputs the previously summed spectrum to the reduction hardware or storage
Figure 4.3 c The data reduction processor module of the ITR data system. RAM is configured so that specific addresses correspond to specific time windows. This time-mapped memory is operated on by several contral processing units (CPUs) in parrallel. The Hall voltage value is read from the VME bus via the TRIMS-ITR Hall interface board. The processed data are then moved to storage in a Hall voltage, flight time, intensity triplet format
Figure 4.4 Transient summation capability of the ITR. The magnet is set to pass ions of mass 90 and the stable ions at this mass are observed (at 18.16 $\mu$ sec) as well as the 92 to 91 metastable ions (at 18.36 $\mu$ sec). Different numbers of sums (as indicated) were acquired and compared
Figure 4.5 S/N versus the square root of the number of summed transients for mass 41 of n-decane. Each data point was determined from the average of three separate measurements of the variation in the ion peak height. The reciprocal of the peak height relative standard deviation is the S/N value
Figure 4.6 These are the rotation matricies which transform the original x, y, z data coordinates. For the RX, RY or RZ matricies the x, y, and z values are in radians.  S = global scaling factor T = absolute x, y, z global translation constant

Figure 4.7 Composite plot of IMAX-IMIN (the "total ion current") as a function of the magnetic field strength. At each value of the magnetic field strength the difference between the maximum and the minimum intensity is plotted. This type of plot is convenient for examining the full MS/MS data field
Figure 4.8 a Scan #599 was selected from the composite data of Figure 4.7. This is the stable ion at mass 56 of n-decane
Figure 4.8 b Scan #973 was selected from the composite data of Figure 4.7. This scan was selected to observe the signal-to-background for low abundant ions at mass 100 of n-decane
Figure 4.8 c Scan #474, also selected from the data in Figure 4.7, shows the stable ion at mass 44, plus the metastable reaction 113> 71 of n-decane which occurs at approximately the same apparent mass
Figure 4.9 Complete unimolecular fragmentation field observed for n-decanol. The daughter (metastable) ion intensities have been multiplied by five 111
Figure 4.10 Postulated fragmentation reactions in n-decanol112
Figure 4.11 A selected reaction monitoring experiment with TRIMS-TAD. A mixture of benzene and chlorobenzene was separated by gas chromatography and subjected to MS/MS. The selected reaction was the 78> 77 metastable decomposition of benzene (peak at 17.93 μsec); the stable ion of mass 76 is represented by a peak at 17.71 μsec Four scans were chosen from the 1000 total scans and the data are described in the text
Figure 4.12 A complete MS/MS map of methyl sterate acquired in 10 seconds. This is a top view of the B-t data field. A wide-bore capillary column was used for the chromatographic introduction to the TRIMS-TAD instrument

Figure 5.1 Representation of the <i>B-t</i> data field for the metastable loss of chlorin from the molecular ion of 2,4 dichlorotoluene
Figure 5.2 Observed contour in the <i>B-t</i> data field for the reaction represented i Figure 5.1
Figure 5.3 Energy release profile from the metastable loss of chlorine from 2, dichlorotoluene
<u>Figure 5.4</u> Energy profile for the molecular ion of para-chlorotoluene. The energy width at half-height is approximately 7 electron volts
Figure 5.5 Energy release profile of the metastable loss of chlorine from benzy chloride
Figure 6.1 Overall chemical structure elucidation scheme incorporating TRIMS

5

# LIST OF TABLES

3.1	Stable ion mass assignments
3.2	Precision and accuracy of stable ion mass assignments
5.1	Kinetic energy release of chlorine under unimolecular conditions

## CHAPTER I

:

#### INTRODUCTION

## Research Goals

Make no little plans; they have no magic to stir men's blood.

Daniel Burnham

A breakthrough in mass spectrometric instrumentation has occurred with the development of an instrument that provides the capability for mass spectrometry/mass spectrometry (MS/MS) [1,2]. The instrument employs ion pulsing with time-resolved detection in a magnetic sector mass spectrometer; the technique has been coined, "time-resolved ion momentum spectrometry," (TRIMS). Ions that fragment in the field-free region between the source and the magnetic sector maintain the velocity of the parent, but due to the loss of mass, have a lower momentum. At the setting of the magnetic field at which they appear, they have a longer flight time than ions of the same momentum which had not fragmented. Thus, flight time resolution is able to separate all fragmentation products from stable ions as well as provide clear identification of the parent and daughter ion relationships. Compared to more conventional MS/MS techniques, TRIMS offers several advantages. However, it is also plagued with limitations. One of the limitations will be addressed in this thesis, namely the lack of adequate mass resolution and detectability due primarily to space and energy effects inherent with source pulsing[3].

In the first generation of the TRIMS development, ion trapping followed by source pulsing was employed to improve sensitivity as well as provide time encoding for the ion beam exiting the source of the instrument. This configuration proved the feasibility of the TRIMS technique for MS/MS studies, but suffered because the mass resolution along each dispersive axis, namely momentum and velocity, was poor [4]. At the onset of this research the highest mass resolution recorded was approximately 100, using the full-width-at-half-maximum (FWHM) definition of resolution. In addition, ion profiles in the magnetic field-time (*B-t*) data field were reversed from that expected theoretically.

A goal of the present research is to address the ion focusing problems observed with source pulsing by employing post-sector beam deflection. With beam chopping at the exit slit of the magnetic sector instrument, the resolution limiting phenomena present with source pulsing are reduced or eliminated. This modification enhances both the resolution and sensitivity of the instrument and provides the theoretically predicted beam intensity profiles as a function of magnetic field strength and ion arrival time [5].

A second goal of this research is to verify the mass assignment capability of the TRIMS instrument. Theoretically in a TRIMS instrument, an ion's mass can be assigned independent of its energy. Mass assignments on a single-focusing magnetic sector mass spectrometer or a time of flight (TOF) mass spectrometer alone are hampered by a spread of ion energies in the source [6]. A TRIMS instrument is a magnetic sector-TOF hybrid and any energy changes in the source are compensated by the determination of the ion's momentum and velocity. Relative standard deviation values for n-decane stable ion mass

assignments are typically less than 0.20 % with relative mass assignment errors not exceeding 3 parts per thousand.

A third and major goal involves interfacing the TRIMS instrument to a time-array detection (TAD) system for high speed acquisition of the complete MS/MS data field on samples with a brief residence time in the source [7,8]. The complete MS/MS data field is defined as a data matrix containing all the daughter ions of all the parent ions. This is a two-dimensional data field that yields a great deal of compound structure information. The problem addressed with this research concerns collection of the MS/MS data field in a short time frame, *i.e.*, compatible with chromatography, for GC-MS/MS. Current mass spectrometric instrumentation has not been able to achieve this acquisition speed primarily because of the inherent analyzer scanning required for MS/MS analysis. TAD with TRIMS has answered this challenge with complete MS/MS data field acquisition in under 10 seconds [9,10].

The fourth and final goal of this research is to explore kinetic energy release measurements for isomer differentiation. A characteristic and measurable energy release accompanies uni- or bi-molecular decomposition. This kinetic energy release is different for different chemical compounds and can be useful for identifying isomers [11,12]. Intensity values in the TRIMS data field can be converted into an energy distribution from which kinetic energy release values can be determined [13,14]. The measured energy profiles for stable ions and the energy distribution profiles for daughter ions appear in the expected shape and location in the *B-t* data field.

In summary, this thesis sequentially addresses each of the goals described above. MS/MS instrumentation is first introduced with an emphasis on current data acquisition limitations. The TRIMS instrument is presented as a possible solution to these limitations with the potential for high speed MS/MS full field acquisitions. Further development of the TRIMS instrument is discussed with regard to a beam chopping modification resulting in the post-sector beam deflection experimentation. The results of this change revived TRIMS as an analytical technique and led to a continuation of the experiments first proposed by J.T. Stults, J.F. Holland and C.G. Enke [1]. The experiments, applications, and results of the second generation TRIMS, specifically, improved mass assignment, high speed GC/MS/MS, and kinetic energy release are presented. Finally, the future prospects for TRIMS is presented in light of its integration into a complete automated chemical structure elucidation system being developed in this laboratory [15].

## **MS/MS INSTRUMENTATION**

The TRIMS technique shares many of the attributes common to those of conventional MS/MS techniques. With MS/MS it is possible to generate daughter mass spectra for each ion in a stable ion spectrum [16-20]. An example of this is shown in Figure 1.1 [16]. These daughter spectra can be used to elucidate the structure of a particular parent ion and thereby provide an added dimension of information (see Figure 1.2) [21]. MS/MS also has some features analogous to a separation technique, similar to those of gas chromatography in GC/MS. One employs the first MS to separate a mixture of ions according to mass, and the

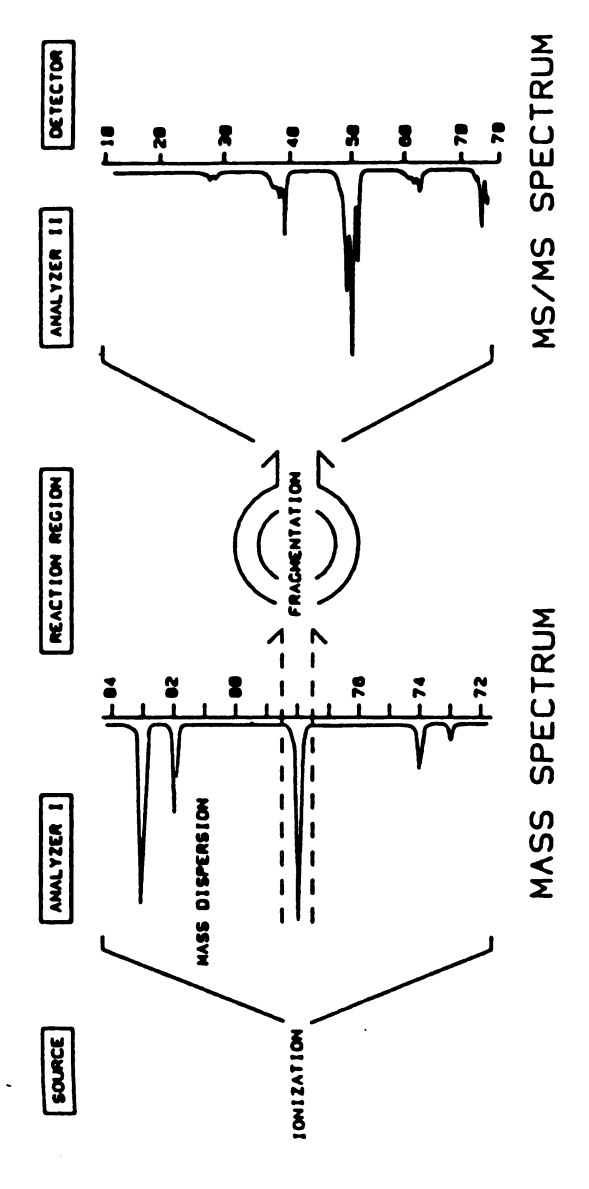
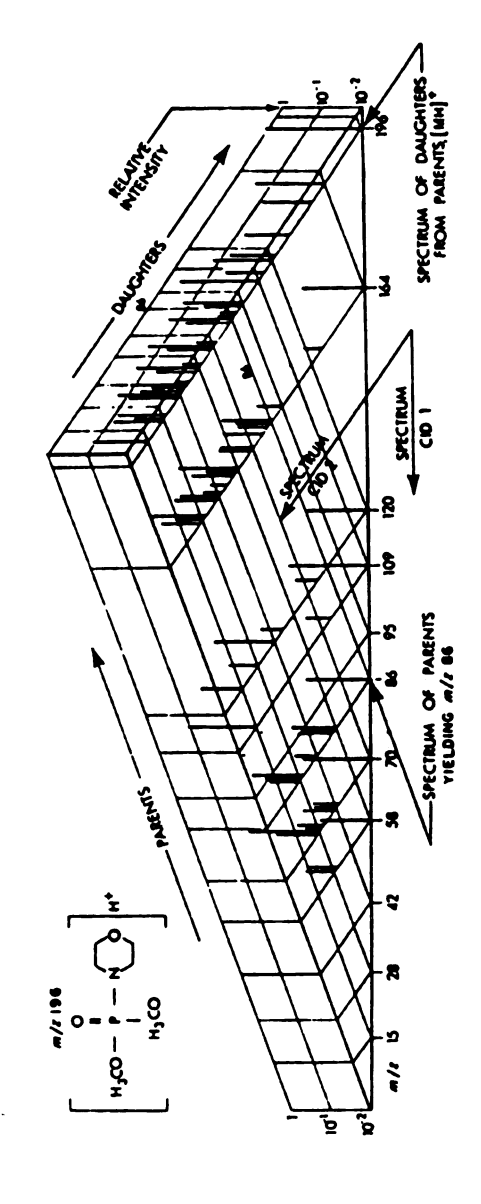


Figure 1.1 An MS/MS spectrum is typically obtained by fragmenting a selected ion and collecting the resulting ion current. In this way a daughter mass spectrum is produced, providing another dimension of information. Reprinted from reference 16.



:

Figure 1.2 MS/MS can provide an added dimension of information producing a 3-dimensional "fingerprint" of the compound. The complete MS/MS data field is shown for the protonated molecular ion of dimethylmorpholino phosphoramidate (DMMPA).

Reprinted from reference 21.

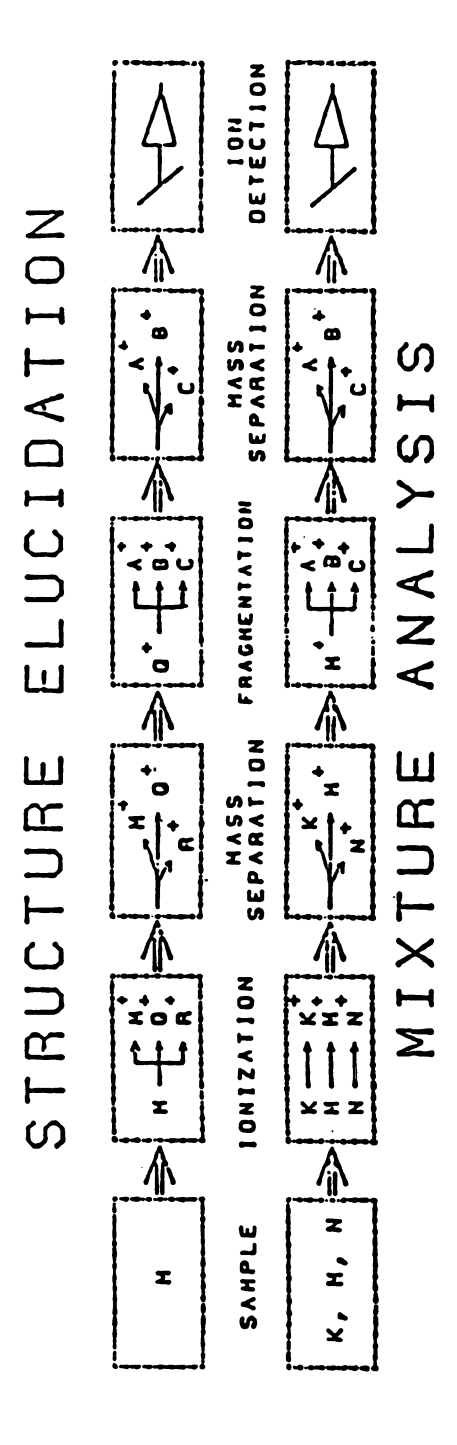
second MS to identify each component. Figure 1.3 illustrates a mass separation scheme for:structure elucidation and mixture analysis achieved by MS/MS. It is not surprising then, that tandem mass spectrometry has become a powerful analytical technique having a wide variety of chemical, biochemical and environmental applications [22-29].

# Triple Quadrupole Mass Spectrometers for MS/MS Spatial based

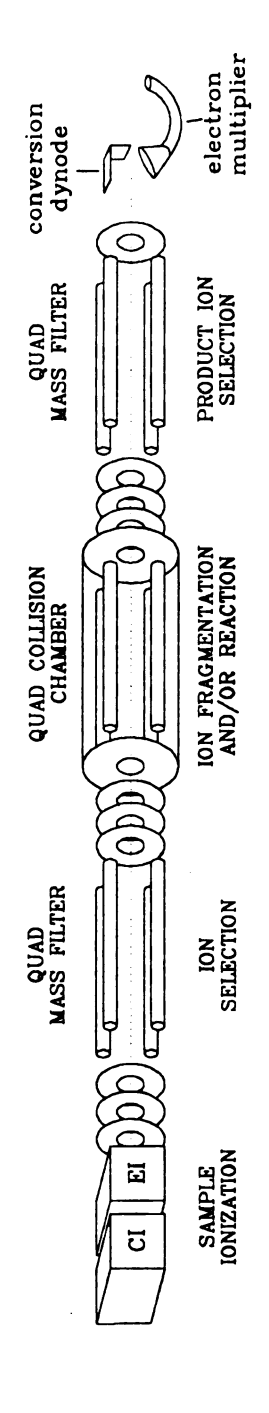
Conventional MS/MS instruments usually consist of a series of two or more mass selective devices in tandem with one or more collision chambers. In these instruments a mass filter selects a parent ion of interest, the ion is fragmented by collision with a target gas, and the mass spectrum of the resulting daughter ion is scanned by a second mass filter [30-32]. A tandem quadrupole MS/MS (TQMS) instrument is shown in Figure 1.4. The first quadrupole provides parent ion selection from the source and the third quadrupole provides daughter ion selection from the collision cell. The second quadrupole is not operated as a mass filter, but provides selective ion containment for the low-energy collision process. In complex mixture analysis, the unit mass resolution selection of both parent and daughter ions provides extremely specific detection of particular sample compounds [21,24]. The capability to assign accurate masses to all daughter ions of each possible parent ion from a given molecule is a powerful aid to structure analysis [25].

The collection of the complete MS/MS spectrum shown in Figure 1.2 requires multiple scans. This is most often achieved by collecting a daughter scan for

:



selection, parent ion dissociation and daughter ion selection followed by ion detection is achieved, yielding either additional structure information or mixture Figure 1.3 In a typical MS/MS instrument, two stages of mass separation are employed. A sequential manner of analysis with ion formation, parent ion component identification.



:

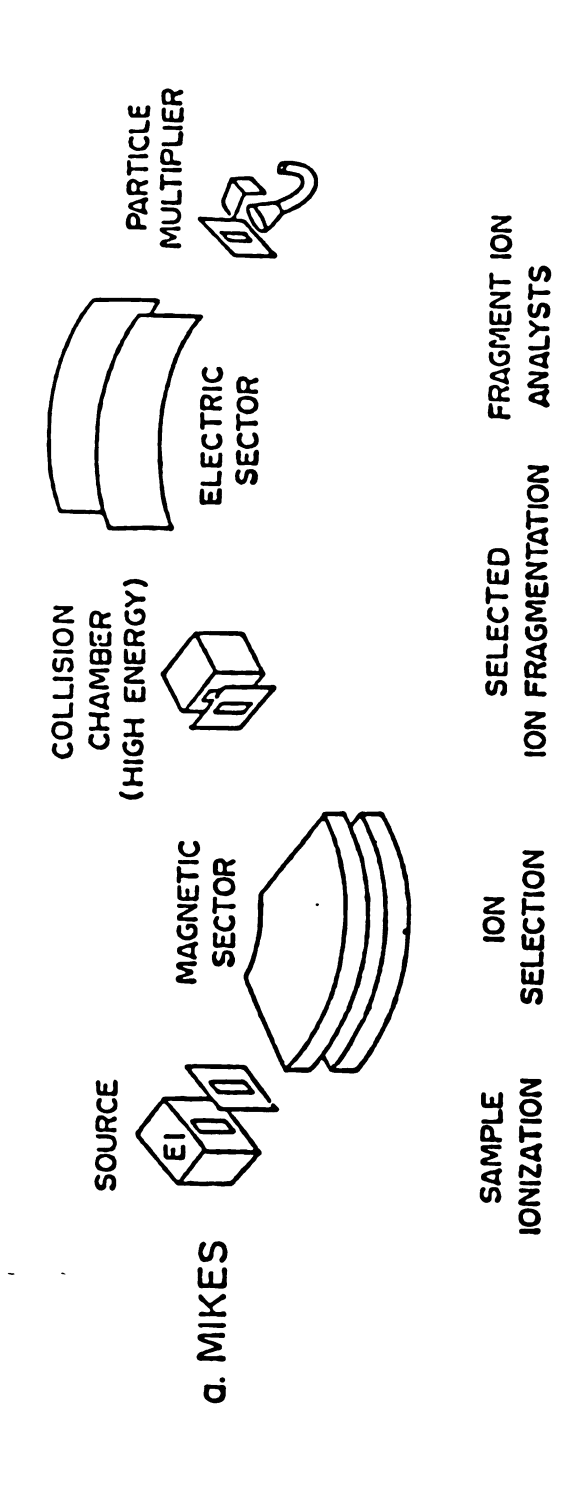
Figure 1.4 A Triple-Quadrupole Mass Spectrometer (TQMS) illustrating two stages of mass filtration separated by a single stage of ion reaction/collision. Ionization can be performed under electron impact (EI) or chemical ionization (CI) conditions, among others.

each increment of the parent mass. A more efficient way is to do one normal MS scan and then collect one daughter spectrum for each of the parent peaks detected. It is desirable to be able to perform automatically a variety of sequences of single-scan modes.

When particular sample components are present only briefly (as with GC/MS/MS or selective volatilization from a solids probe) only a limited amount of data can be collected while each component is present. Selected reaction monitoring can be employed with the first and third quadrupoles set for a particular parent-daughter combination to provide some spectral information. The TQMS instrument is thus limited in its ability to collect complete MS/MS fragmentation maps in a short time frame. The maximum spectral data available during a capillary GC peak is only a few scans for reasonable sensitivities.

# The Double-focusing Geometry for MS/MS Spatial based

The unique features of double-focusing mass spectrometers allow one to make use of a number of different types of scans which can be useful for MS/MS analyses. In an instrument of forward geometry (e.g., JEOL HX110 or Kratos MS50), the electric sector precedes the magnetic sector, and a collision cell is placed at or near the source slit. In an instrument of reverse geometry (e.g., the VG ZAB-2F), the magnetic sector precedes the electric sector and the collision cell is placed at or near the source slit for some types of scans, or at the intermediate focal point for other types of scans. An illustration of a reversed geometry double-focusing instrument is shown in Figure 1.5. This is a mass



:

Figure 1.5 A. Mass Analyzed Ion Kinetic Energy Spectrometer (MIKES) illustrating ion selection, selected ion fragmentation followed by daughter ion analysis.

analyzed ion kinetic energy spectrometer (MIKES). The magnetic sector acts as the first mass analyzer to allow selection of a parent ion. This selected ion enters the intermediate focal point for collision with a gas such as helium. The resulting daughter ions are energy resolved in the electric sector and detected. This sequential MS/MS analysis scheme is very similar to the TQMS instrument except the double-focusing instruments operate in the high energy (>1KV accelerating potential) regime.

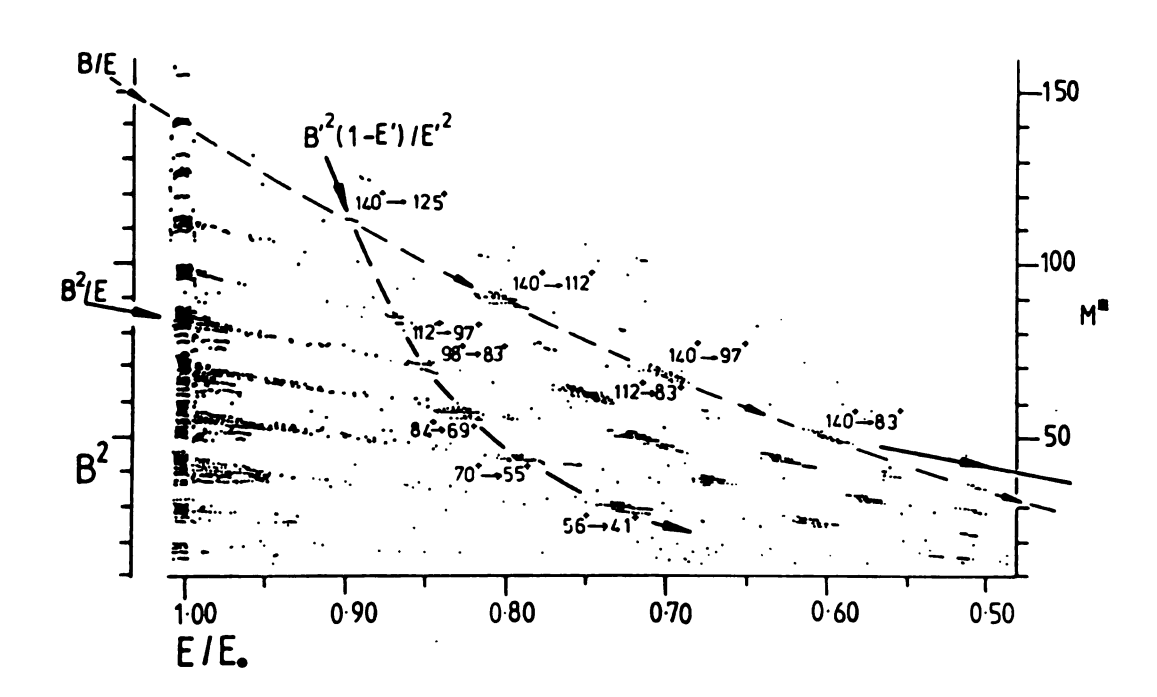
Various linked scans can be performed in double-focusing instruments to yield parent-daughter relationship information. A B/E (B = magnetic field strength, E = electric field strength) scan may be used on instruments of either forward or reverse geometry and allow the collection of daughter ions,  $m_2$ +, formed from parent ions,  $m_1$ +, m the field-free region between the source and the first sector. The B/E linked scan operates such that the accelerating potential is held constant and B and E are scanned simultaneously to keep the ratio B/E constant throughout the scan. The scan gives a spectrum of all daughter ions,  $m_2$ +, formed from a chosen parent,  $m_1$ + [33]. The instrument is set up for normal operation such that under conditions specified by V<sub>1</sub>, E<sub>1</sub> and B<sub>1</sub>,  $m_1$ + ions are collected.

The linked scan processes required for the collection of an entire MS/MS data field limits the data collection rate of double-focusing instruments. If a mixture is investigated in which information is required on a large number of ions, the linked scan procedure can be time-consuming and wasteful of sample. The B/E and other available scans are merely different methods of investigating the ion intensity at different points within the B, E plane. Different methods have been described [34-36] to plot all metastable ions (ions undergoing uni-molecular

decompositions in the first field-free region) occurring with the B, E plane. An example of a data field is shown in Figure 1.6 [37,38]. This MS/MS data field was acquired by fast repetitive scanning of B and stepping E under computer control and using time-to-mass correlation with automatic data acquisition and display. Several minutes were required for this acquisition. This figure illustrates the vast amount of MS/MS information available for a single compound that can be missed and therefore not used when sequential-type MS/MS analyses are performed. Sample constraints can limit the time available to collect this field and thus experimental trade-offs can result.

Figure 1.7 illustrates the strategies for acquisition of a complete MS/MS map on the three popular mass filter instruments described above. The tandem filter nature of the spatial instrumentation imposes a requirement of multiple time-consuming scans in order to obtain MS/MS analyses. In TQMS and MIKES instruments, a complete scan of the second stage of mass analysis is required to yield a single daughter spectrum. For unknown compounds, incrementing along the primary spectrum followed by a scan of the electric sector or quadrupole is required. Although scanning the second stage requires only 50 to 100 msec, a 500 dalton mass range cannot be accommodated in the time available with chromatographic separation. Linked scanning in a forward geometry instrument can require from 0.25 to 1.0 sec per daughter scan because a magnet is inherently slower to scan and also coordination with the electric sector is time consuming. If many different ions could be detected simultaneously, the possibilities for much faster map acquisition could be improved [28].

:



<u>Figure 1.6</u> Controlled analyzer scanning MS/MS. Two dimensional metastable map of ions in the decan-1-ol (molecular weight 158) electron impact spectrum. The electric sector is stepped followed by fast repetitive scanning of the magnet. The dots indicate the detection of a metastable ion. Adapted from reference 37.

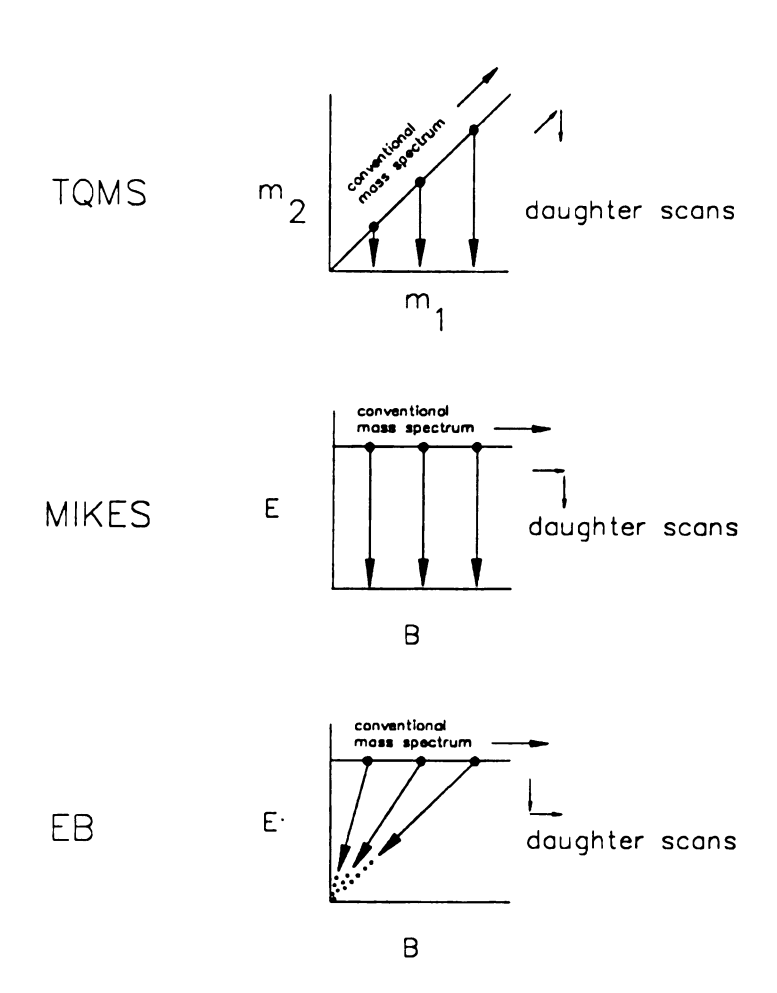


Figure 1.7 Process of acquiring a complete MS/MS data field with different tandem mass filter instruments. The arrows inside the data boundaries show the incremental, and thus sequential, operation required to achieve a full field acquisition by these techniques.

TQMS = triple quadrupole mass spectrometer

MIKES = mass analyzed ion kinetic energy spectrometer

:

(reverse geometry)
EB = forward geometry double-focusing mass spectrometer (linked scan)

# Fourier-transform Ion Cyclotron Resonance Instruments for MS/MS Analysis Temporal based

In Fourier Transform Mass Spectrometry (FTMS) there are no slits, flight tubes or spatially separate first-stage and second-stage analyzers. All of the ions are formed by a pulsed electron beam (or laser) and stored (trapped) inside a single analyzer cell. The cyclotron frequencies of an ensemble of ions are measured, and these are then used to calculate a mass spectrum [39]. The Fourier transform method retains all the capabilities of the conventional ICR technique, but it has the advantage of being able to acquire a mass spectrum orders of magnitude faster. An FTMS instrument is a multi-channel mass spectrometer because all the ions are accelerated and detected at the same time.

MS/MS was first reported in an ion cyclotron resonance instrument by Kaplan in 1968 [40]. In 1971, McIver and associates [41] used a pulse of RF power in a trapped ion analyzer cell to accelerate parent ions to known energies and controlled the collision energy by varying the RF irradiation level. A broadband bridge detector allowed the detection of CAD (collisionally activated dissociation) ions for MS/MS analysis. The entire process (ionization, parent ion selection, collision, and analysis of the resulting daughter ions) as illustrated in Figure 1.8 for a single parent ion, without pumping collision gas in and out, can require 100-200 ms/transient. For daughter ion analysis of 10 peaks in the primary spectrum with 25 transients averaged for each daughter spectrum the total time for a complete MS/MS data field acquisition would be a minimum of approximately 25

5

QUENCH

ELECTRON BEAM

ISOLATE PARENT

EXCITE PARENT

COLLISION

DAUGHTER DETECTION

RECEIVE

<u>Figure 1.8</u> FT-MS/MS radio-frequency pulse sequence. Approximately 40 msec is required to isolate a particular parent ion in the analyzer cell of an FTMS instrument. This parent ion is excited to a known energy for collision. Approximately 50 msec is required for parent excitation, collision, and daughter ion detection. This pulse sequence is performed in a background of argon collision gas  $(1 \times 10^{-6} \text{ to } 1 \times 10^{-5} \text{ torr})$ .

seconds. Nevertheless, two promising FT-MS/MS techniques have been recently developed and soon this analysis time may be reduced [42,43].

#### **TRIMS**

#### First Generation

To answer the instrumental challenges discussed above. TRIMS was developed to offer a potentially much faster method for generation of the multidimensional MS/MS data through simultaneous ion momentum and velocity dispersion. To get a feeling for the evolution of the TRIMS instrument, it is helpful to begin with a discussion of the separate dispersive capabilities of each analyzer involved. TRIMS is a hybrid MS/MS geometry instrument, which means that it is comprised of a combination of magnetic sector and time-of-flight (TOF) mass spectrometer characteristics. Figure 1.9 illustrates the collision induced dissociation (CID or collisionally activated dissociation (CAD)) process and the resulting ion fragment dispersion in both the magnetic and TOF instruments. The subscript, p, denotes a parent ion attribute represented with mass or velocity. The ion shown entering the collision region is a parent ion with its corresponding charge and momentum. Upon dissociation in the collision region, daughter ions are generated (subscript d) which retain the velocity of their parent. magnetic sector instrument alone, these daughter ions are separated according to their momentum. A major problem with this arrangement for MS/MS analysis is that other parent ions in the primary mass spectrum (stable ions) will overlap with the separated daughter ions that arose from heavier parents (see Figure 1.10). In a TOF instrument alone, the daughter ions are not separated because the velocities of all the fragments (including the parent ion) are virtually the same.

:

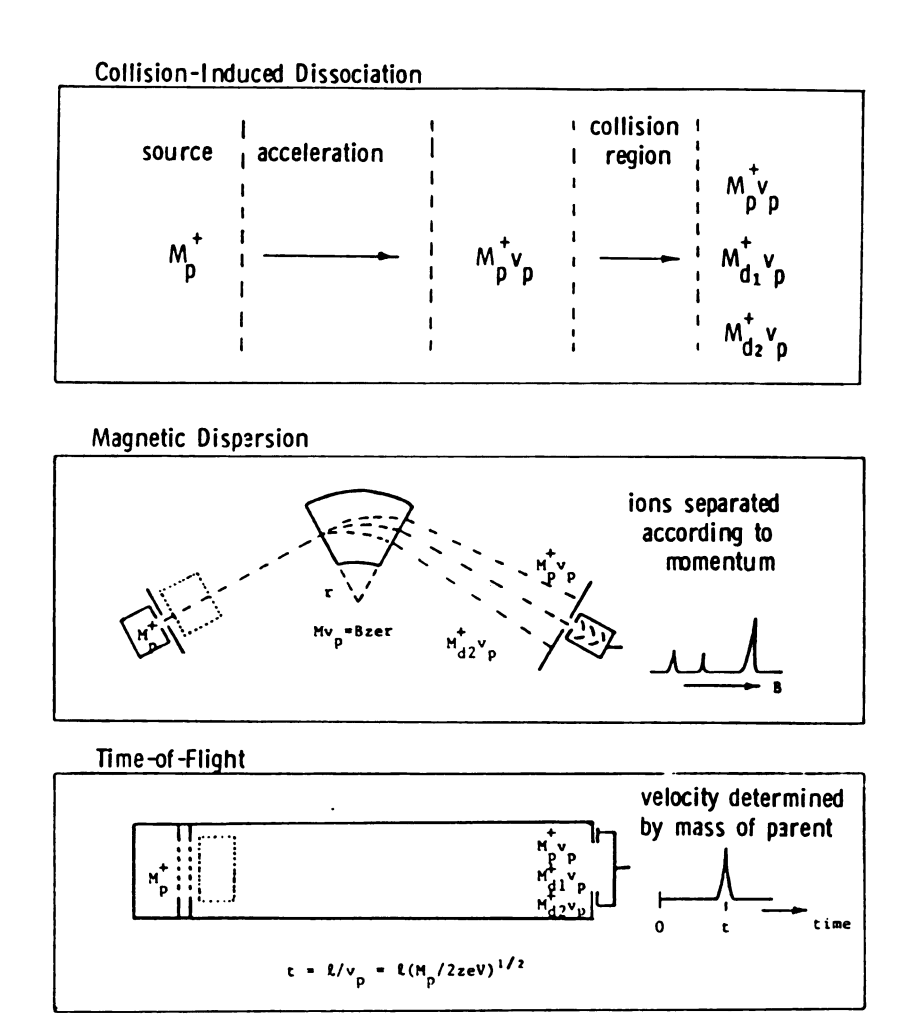


Figure 1.9 The dispersion of collisionally dissociated ions in a magnetic sector and time-of-flight mass spectrometers. p = parent, d = daughter.

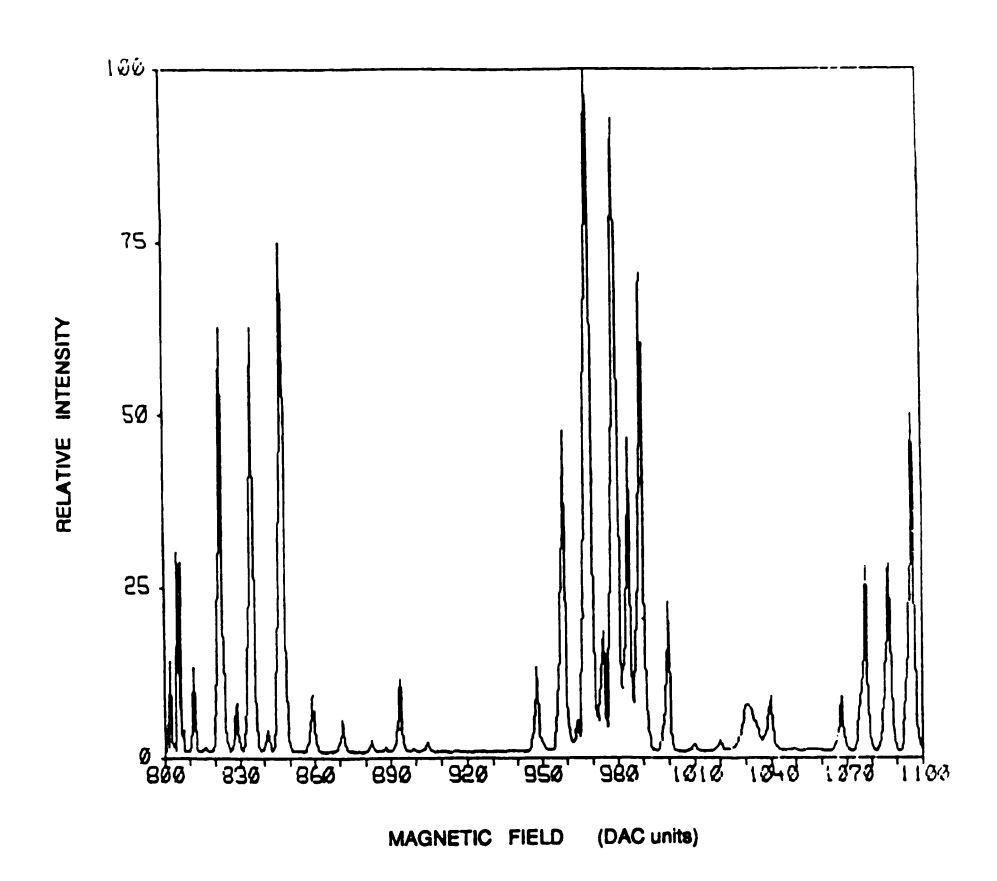


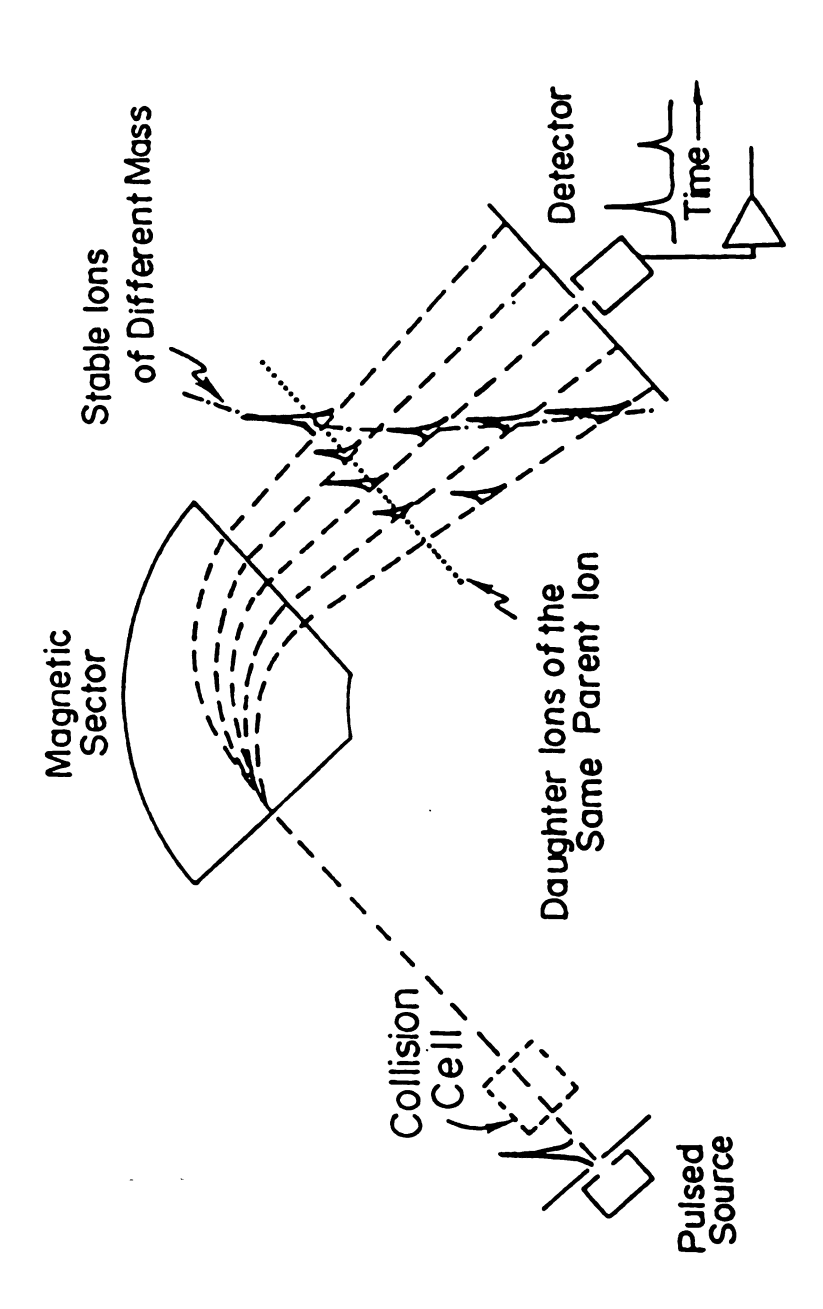
Figure 1.10 A magnetic field strength sweep of a selected mass region of benzonitrile. At approximately 980 DAC units the stable ions at mass 56 and the ions from the 103-->96 metastable decomposition are superimposed. The TRIMS technique would allow for the separation of these ions, and therefore, lead to an unambiguous mass assignment for compound structure analysis.

However, by combining the mass dispersive features of the two types of mass spectrometers (momentum and velocity), daughter ions can be separated from their parent and other stable ions.

The TRIMS instrument provides analysis of ion momentum (proportional to the magnetic field strength) with the combination of a pulsed ion beam and a time-resolved detection system providing the analysis of ion velocity (inversely proportional to the TOF). If the ion is a daughter ion formed by metastable decomposition or CAD in the field-free region preceding the magnet, the daughter ion mass is correctly assigned by its momentum-velocity coordinate. It is known that the velocity of a daughter ion will be nearly the same as that of its precursor (parent) ion since the kinetic energy release, due to the fragmentation process, and the kinetic energy loss, due to collisional activation, alter the velocity only slightly [11]. Therefore, all daughter ions from the same parent mass will traverse the magnetic field with nearly the same velocity, but they and their parent will be dispersed according to their momenta (see Figure 1.11). Figure 1.12 illustrates numerically the relationship of velocity and momentum for a particular fragmentation reaction in benzonitrile. The TRIMS instrument can resolve the daughter ions from their parent and all other stable ions that have 3500 eV of kinetic energy.

The theoretical principles of the TRIMS technique have been developed and are-discussed in detail elsewhere [1,4]. The fundamental mass assignment function results from a combination of TOF and momentum equations and is:

$$m/z = Bt(er/d) \tag{1.1}$$



:

Figure 1.11 lon separation by momentum and velocity in TRIMS. Daughter ions from the same parent appear at the same arrival time but are dispersed according to their momenta. Stable ions have shorter arrival times than daughter ions of the same momentum because of their greater initial velocity.

## **BENZONITRILE**

:

## stable ion

mass = 76.0KE = 3500 eVv = 94,286 m/smv =  $7.2 \times 106$ 

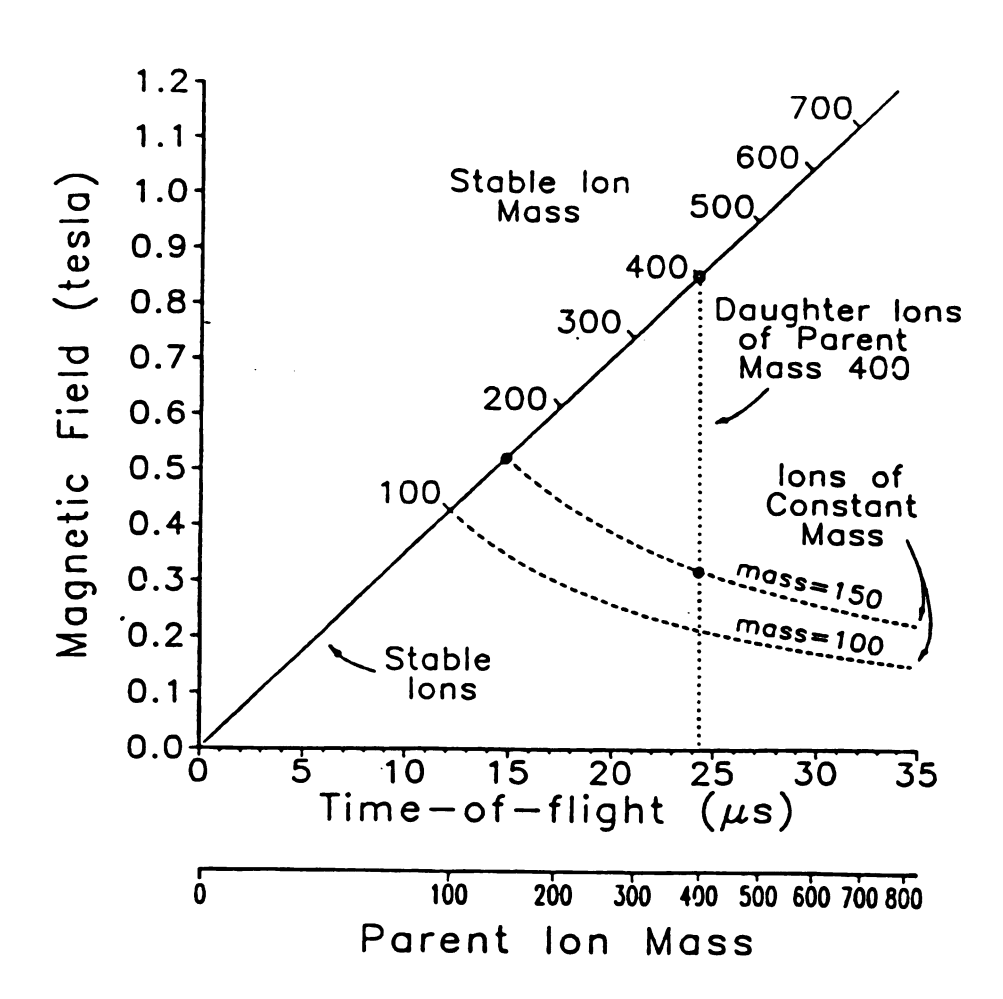
Figure 1.12 The values of momentum and velocity are compared for the benzonitrile metastable reaction discussed in Figure 1.9. KE = kinetic energy, v = velocity, mv = momentum.

where m is ion mass, z is ion charge, B is the corrected magnetic field strength, t is the corrected time-of-flight, e is the electronic charge, r is the radius of the magnetic sector and d is the ion flight distance. The combination of a momentum analyzer and a velocity analyzer produces a mass-to-charge ratio that is independent of the ion energy. Simultaneous measurement of the ion momentum with a magnetic sector and measurement of the ion velocity by TOF is another method of determining ion mass.

The TRIMS magnetic field-flight time (*B-t*) data field is shown in Figure 1.13. This figure is a computer generated plot of the *B-t* data field for an instrument with an accelerating potential of 3500V, a flight distance of 1.0m, and a magnetic sector radius of 0.2m. Each location on the plane represents the field and time values at which a specific ion would be found. For example, all daughter ions of the same parent mass will have a similar velocity and therefore a similar time-of-flight. This is shown by a vertical line for all daughters of parent mass 400. All daughter ions of the same mass but derived from different parents will have the same value of *Bt*, according to equation 1.1. Stable ions appear at the point where the parent mass is equal to the daughter mass. They all have the same nominal energy, 3500 eV.

Time sweeps, magnetic field sweeps, or linked sweeps can be performed with the *B-t* data field (see Figure 1.14). If the detection system is set to sample only ions that traverse the flight path with the velocity of a particular parent ion, a sweep of the magnetic field will permit detection of the daughter ions that arise from that parent. These daughter ions will be of lower masses and therefore will

-



<u>Figure 1.13</u> The B-t data field for TRIMS showing the expected locus of points for different types of ions. Adapted from reference 1.

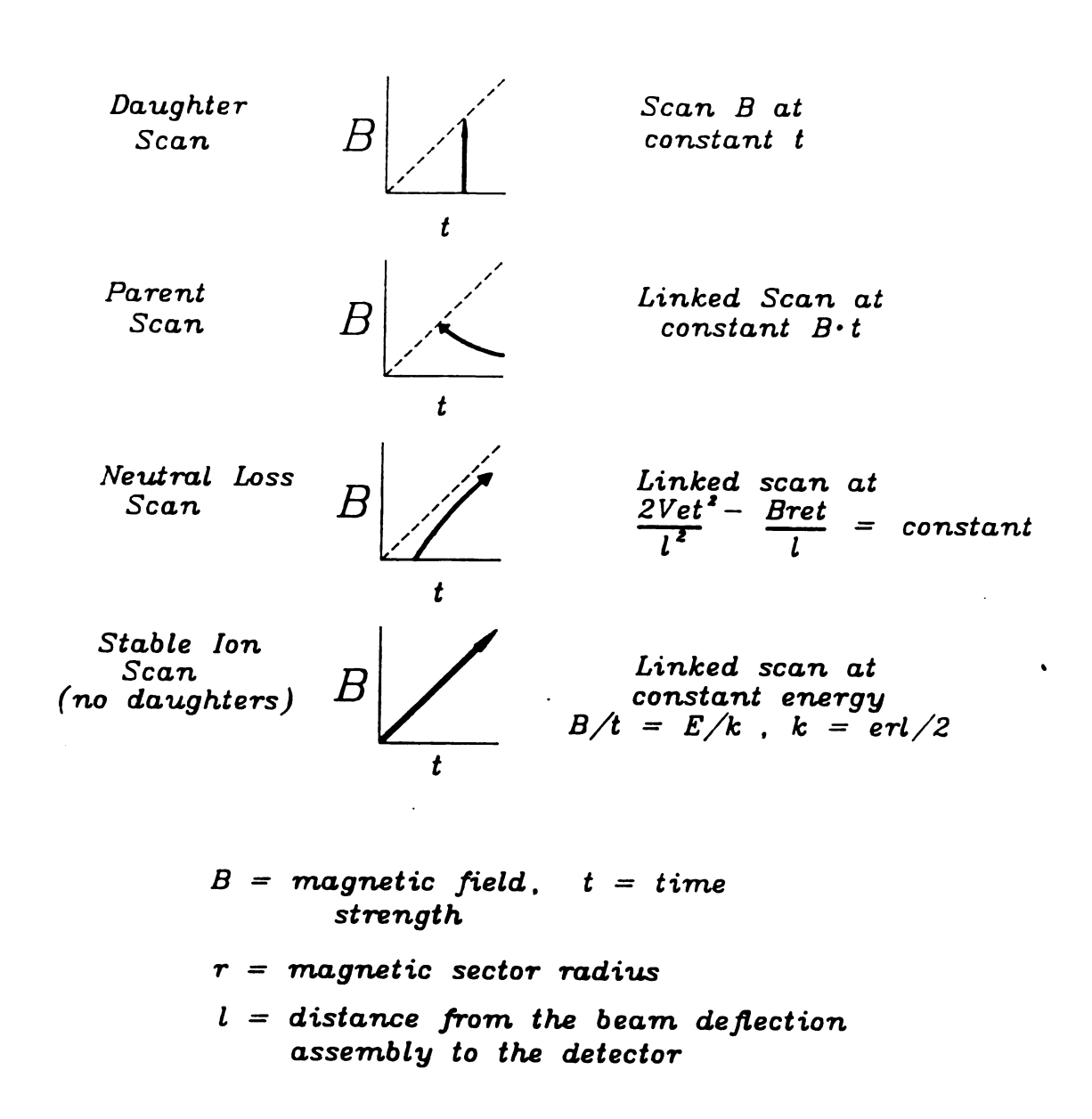


Figure 1.14 MS/MS scan modes available with TRIMS. In every case, the value on the mass axis in the resulting mass spectrum is obtained from the combination of B and t at which the ion current is detected.

appear at lower mcmenta. Any of the MS/MS scans (parent, daughter and neutral loss) can be accomplished (employing time-slice detection, (TSD)) and selected portions of the two-dimensional TRIMS data field can be investigated.

# Potential for full MS/MS field acquisition

With further inspection, it can be seen that TRIMS offers the unique potential to collect the complete MS/MS data field in a single sweep of the magnet (see Figure 1.15). By observation of all arrival times for all values of the magnetic field strength a two-dimensional data field is produced from which all MS/MS data can be obtained. As the magnetic field is swept through the desired mass range, ion flight times are measured for every hall-effect voltage measurement. If all possible time channels are sampled in a 100 µsec transient for each increment along the magnetic field, then a complete MS/MS data field acquisition is possible in the time for a single sweep of the magnet. For 1000 magnet increments an entire MS/MS map could theoretically be acquired in 100 msec. Interrogation of the full field will yield particular parent, daughter, or neutral loss information. For example, a daughter scan can be extracted (post-processing) from this data field by locating all the ions that have the same flight time as the chosen parent ion. This is shown by the vertical line in Figure 1.15. TRIMS, therefore, can provide the complete MS/MS data field in one sweep of the magnet.

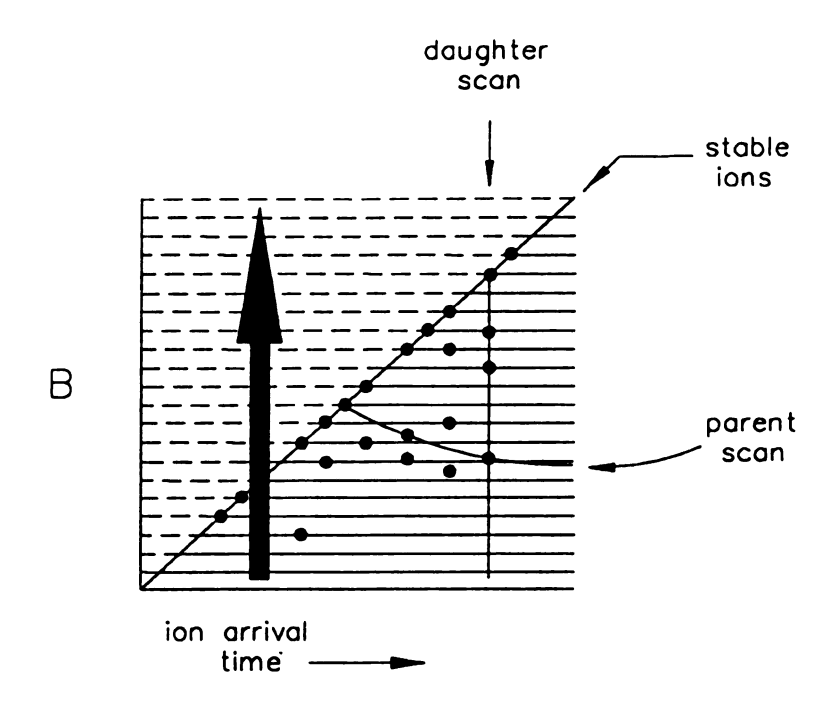


Figure 1.15. The MS/MS data field generated by the TRIMS instrument. The horizontal lines represent ion arrival-time spectra acquired at a particular magnetic field strength (B). The heavy arrow indicates that only one sweep of the magnet is required to collect the full MS/MS data field and that the magnet is swept simultaneously with the arrival-time data acquisition. Interrogation of this field (post-processing) provides the characteristic MS/MS scans.

# TIME-SLICE AND TIME-ARRAY DETECTION METHODS Time-Slice

TRIMS can provide the complete MS/MS data field very rapidly, but unless the detection system can handle the data rate and data volume, no advantage over conventional MS/MS techniques will be evident. Two common time-resolved detection techniques are time-slice detection (TSD) and the previously mentioned time-array detection (TAD). Figure 1.16 illustrates the differences between TSD and TAD. In TSD, timed amplitude measurements are made which measure the amplitude of the ion signal during a narrow time "window" at a specific delay time after a start signal. By monotonically increasing the delay time after successive beam deflection (pulse) events, a spectrum can be acquired. A boxcar integrator with a delay generator are normally used to make these measurements. As shown in Figure 1.16 only one time slice or window is sampled after each pulse and many pulses are required to obtain a full spectrum (10,000 in the TOF application, or 1 spectrum/second). Signal averaging during each time-slice can further increase the analysis time.

# Time-Array

In TAD, the ion signal amplitude is effectively measured for all of the detection windows following each pulse, and thus, a multi-channel advantage is obtained. A transient recorder can be used to achieve this function. However, conventional transient recorders are limited either by the maximum repetition rate for signal averaging or by the time required to download the acquired transient

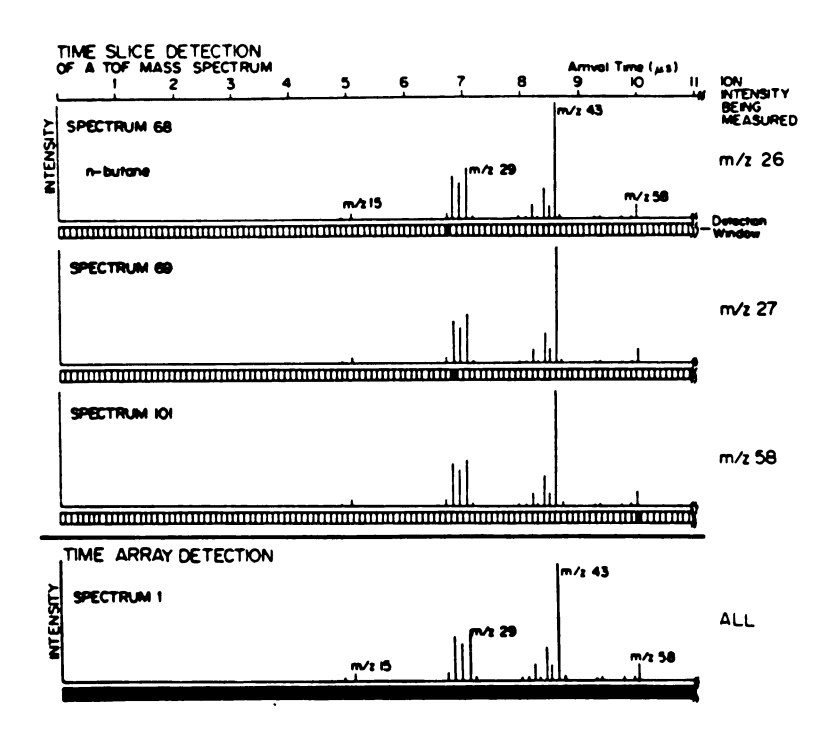
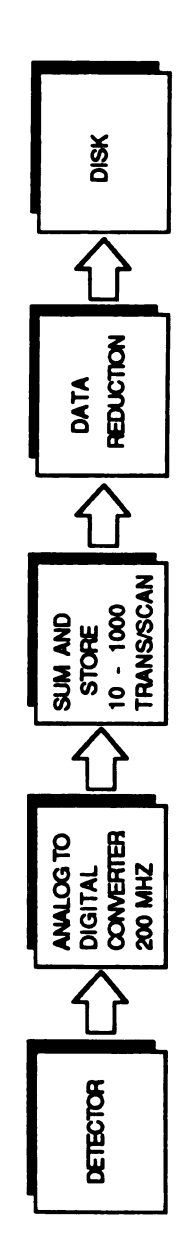


Figure 1.16 Comparison of time-slice detection and time-array detection. A simulated time-of-flight mass spectrum is shown for n-butane, using a flight-tube length of 100 cm and an accelerating voltage of 3,000 V. In time-slice detection, only one time window is measured for each pulse event, thereby requiring multiple pulses to construct the complete spectrum. In time-array detection, the complete spectrum is acquired following each pulse event.

before another one can be acquired. In fact, due to the fundamental limitation in computer bus data transfer rate the transfer time between transients far exceeds the time of each transient. Only 1-100 transients/second can be obtained presently, or less than one transient out of a thousand in the TOF application. Thus, much valuable information is lost. Therefore, an integrating transient recorder (ITR) was developed that allows the continuous acquisition and summation of transient events [44,45].

A block diagram of the ITR is shown in Figure 1.17. The ion signal is digitized by a flash analog-to-digital converter (ADC). The detected and digitized transients are summed together, to improve ion statistics, and become one scan. The scans are reduced to Hall voltage, time, intensity triplets in the data reduction section and moved to storage. More details on the ITR data system can be found in chapter four.

The ITR is required to reach the goal of acquiring a complete MS/MS fragmentation field in a brief time frame for GC-MS/MS. TRIMS in combination with TAD meets the data rate and data volume challenges and offers a unique ability to conquer them.



:

Figure 1.17 Block diagram of the integrating transient recorder (ITR). TOF transients are digitized, summed, reduced to hall, time, intensity triplets, and stored as a scan file. With parallel processing this sequence can occur at approximately 180 Hz.

## CHAPTER I

#### REFERENCES

- 1. Stults, J.T.; Holland, J.F.; Enke, C.G. Anal. Chem. 1983, 55, 1323-1330.
- 2. Stults, J.T.; Myerholtz, C.A.; Newcome, B.H.; Enke, C.G.; Holland, J.F. *Rev. Sci. Instrum.* 1985, 56, 2267-2273.
- 3. Stults, J.T.; Holland, J.F.; Watson, J.T.; Enke, C.G. *Int. J. Mass Spectrom. Ion Proc.* 1986, 71, 169-181.
- 4. Stults, J.T. Ph.D. Thesis, Michigan State University, 1985.
- 5. Eckenrode, B.A.; Watson, J.T.; Enke, C.G. Holland, J.F. *Int. J. Mass Spectrom. Ion Proc.* 1988, 83, 177-187.
- 6. Wiley, W.C.; McLaren, I.H. Rev. Sci, Instrum. 1955, 26, 1150.
- 7. Eckenrode, B.; Newcome, B.; Ericksone E.; Yefchak, G.; Davenport, M.; Holland, J. ASMS Fall Workshop, Washington D.C. Nov. 9-10, 1986.
- 8. Eckenrode, B.A.; Newcome, B.H., Watson, J.T.; Holland, J.F.; Enke, C.G. *FACSS 14th Annual Meeting*, Detroit, Mi. Oct. 4-9, 1987.
- 9. Eckenrode, B.A.; Watson, J.T.; Holland, J.F.; Enke, C.G. ASMS Conference on Mass Spectrometry and Allied Topics, June 5-10, 1988, San Francisco, CA. p. 952.
- 10. Eckenrode, B.A.; Victor, M.A.; Watson, J.T.; Enke, C.G.; Holland, J.F. *Anal. Chem.* in press.
- 11. Cooks, R.G.; Beynon, J.H.; Caprioli, R.M.; Lester, G.R. "Metastable lons," Elsevier: New York, 1973.
- 12. Voyksner, R.D.; Hass, J.R.; Bursey, M.M. Anal. Chem. 1983, 55, 914-920.
- 13. Stults, J.T.; Enke, C.G.; Holland, J.F. ASMS Conference on Mass Spectrometry and Allied Topics, May 27-June 1, 1984, San Antonio, TX.
- 14. Aviyente, V.; Shaked, M.; Feinmesser, A.; Gefen, S.; Lifshitz, C. Int. J. Mass Spectrom. Ion Proc. 1986, 70, 67-77.
- 15. Enke, C.G.; Wade, A.; Palmer, P.; Hart, K.J. *Anal. Chem.* 1987, 59, 1363A-1371A.
- 16. Cooks, R.G.; Glish, G.L. Chem. and Eng. News 1981, 30, 40.
- 17. McLafferty, F.W.; Bente, P.F.III; Kornfeld, R.; Tsai, Shih-Chuan; Howe, I. J. Am. Chem. Soc. 1973, 95, 2120.

- 18. McLafferty, F.W.; Kornfeld, R.; Haddon, W.F.; Levsen, K.; Sakai, I,; Bente, P.F.III; Tsai, Chih-Shuan; Shaddemage, J.D.R. *J. Am. Chem. Soc.* 1973, 95, 3886.
- 19. McLafferty, F.W.; Bockhoff, F.M. Anal. Chem. 1978, 50, 69-75.
- 20. Kondrat, R.W.; Cooks, R.G. Anal. Chem. 1978, 50, 81A.
- 21. Dawson, P.H.; French, J.G.; Buckley, J.A.; Douglas, D.J.; Simmons, D. *Org. Mass Spectrom.*, 1982, 17, 212-219.
- 22. Levsen, K.; Beckey, H.D. Org. Mass Spectrom. 1974, 9, 570-581.
- 23. Kruger, T.L.; Litton, J.F.; Cooks, R.G. Anal Lett. 1976, 9, 533-542.
- 24. Kruger, T.L; Litton, J.F.; Kondrat, R.W.; Cooks, R.G. *Anal. Chem.* 1976, 48, 2113-2119.
- 25. Dymerski, P.P.; McLafferty, F.W. J. Am Chem. Soc. 1976, 98, 6070.
- 26. Koppel, C.; McLafferty, F.W. J. Am. Chem. Soc. 1976, 98, 8293.
- 27. Holzmann, G.; Susilo, R.; Gmelin, R. Org. Mass Spectrom. 1982, 17, 165.
- 28. McLafferty, F.W. Ed., "Tandem Mass Spectrometry," John Wiley and Sons: New York, 1983.
- 29. Yost, R.; Fetterolf, A. Mass Spectrom. Rev. 1983, 2, 1-45.
- 30. Yost, R.A.; Enke, C.G. J. Am. Chem. Soc. 1978, 100, 2274-2275.
- 31. Yost, R.A.; Enke, C.G. Anal. Chem. 1979, 51, 1251A-1263A.
- 32. Yost, R.A.; Enke, C.G.; McGilvery, D.C.; Smith, D.; Morrison, J.D. *Int. J. Mass Spectrom. Ion Phys.* 1979, 30, 127-36.
- 33. Bruins, A.P.; Jennings, K.R.; Stradling, R.S.; Evans, S. *Int. J. Mass Spectrom. Ion Phys.*, 1978, 26, 395.
- 34. Shannon, T.W.; Mead, T.E.; Warner, C.G.; McLafferty, F.W. *Anal Chem.* 1967, 39, 1748.
- 35. Kiser, R.W.; Sullivan, R.E.; Lupin, M.S. Anal. Chem. 1969, 41, 1958.
- 36. Coutant, J.C.; McLafferty, F.W. Int. J. Mass Spectrom. Ion Phys. 1972, 8, 323.
- 37. Mason, R.S.; Farncombe, M.J.; Jennings, K.R.; Scrivens, J. Int. J. Mass Spectrom. Ion Phys. 1982, 44, 91.
- 38. Warburton, G.R.; Mason, R.S.; Farncombe, M.J. Org. Mass Spectrom. 1981, 16, 507.

- 39. Comisarow, M.B.; Marshall, A.G. Chem. Phys. Lett. 1974, 25, 282.
- 40. Kaplan, F. J. Am. Chem. Soc. 1968, 90, 4483.
- 41. McIver, R.T.Jr.; Ledford, E.B.Jr.; Junter, R.L. *J. Chem. Phys.* 1980, 72, 2535.
- 42. McLafferty, F.W.; Stauffer, D.B.; Loh, S.Y.; Williams, E.R. *Anal. Chem.* 1987, 59, 2212.
- 43. Pfandler, P.; Bodenhausen, G.; Rapin, J.; Walser, M.; Gaumann, T. *J. Am. Chem. Soc,* 1988, 110, 5625-5628.
- 44. Holland, J.F.; Enke, C.G.; Allison, J.; Stults, J.T.; Pinkston, Newcome, B. H.; J.D.; Watson, J.T. *Anal. Chem.* 1983, 55, 997A-1012A.
- 45. Enke, C.G.; Newcome, B.H.; Holland, J.F. U.S. Patent #4, 490, 806.

## CHAPTER II

## **SECOND GENERATION TRIMS**

## **Post Sector Beam Deflection**

Well done is better than well said.

Ben Franklin

# ion focusing in TRIMS

TRIMS presents an interesting instrumental challenge in that both time-of-flight (TOF) and magnetic sector ion optics must be optimized simultaneously. In each type of mass spectrometer, the ions have a finite spatial spread and a distribution of kinetic energies (see Figure 2.1). Ions accelerated from different planes of the ion source (those perpendicular to the analyzer axis) experience different fractions of the accelerating voltage and therefore have different kinetic energies as they exit the source. Ions originating from the same plane of the ion source exhibit a range of initial kinetic energies which become superimposed upon the kinetic energy acquired during acceleration. In addition, a "turn-around" time exists which results from a difference in flight times between ions originating in the same plane of the ion source with kinetic energies of the same magnitude but of opposite sign. These effects must be compensated in order to improve resolving power.

Unlike the conventional TOF instrument, in which the goal of focusing is to achieve the same flight time for all ions of the same mass, the goal of focusing in a magnetic sector instrument is to achieve the same velocity for all ions of the same mass. In a magnetic sector instrument, this is accomplished by using a

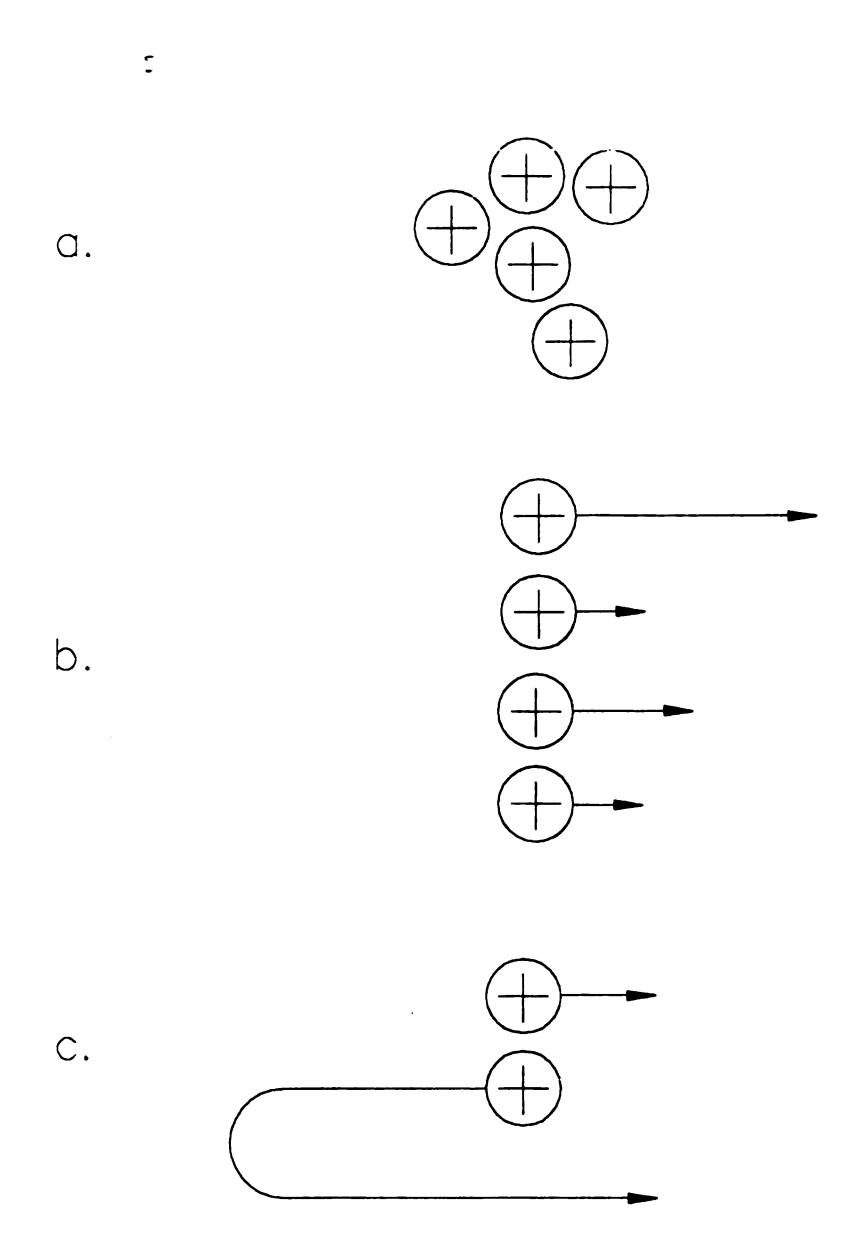


Figure 2.1 Three basic ion formation possibilities found in the source of any mass spectrometer: (a), initial spatial spread, (b), spread in magnitude of initial kinetic energies, and (c), angular distribution of the initial kinetic energies (worst case shown) also known as "the turn-around time".

large accelerating voltage, which makes the initial energy negligible, and by using a small extraction voltage (usually less than 10 V) to minimize energy differences of ions formed in the different planes of the ion source. (The group of ions constituting the total ion beam from the ion source enters the sector magnetic field with a total kinetic energy equal to the value of the accelerating potential. The extraction potential is a fraction of the accelerating potential and is measured between the source block and the first lens of the focusing apparatus.) However, when a sudden application of the source voltage is used to extract a packet of ions from the source in TOF mass spectrometry, much larger extraction voltages are needed to reduce the turnaround time. In fact, the optimum extraction voltage for source pulsing with TOF mass spectrometry is determined by the space focusing condition [1]. With TRIMS, ion velocity must be measured by determining the delay time between pulse formation at the beam deflector and the ion arrival time at the detector. Thus, a very narrow packet of ions must be created in the flight path prior to the detector to make the arrival time an accurate measurement of the velocity. Regardless of the method chosen to create the packet, it is essential to maintain the ion optics of the magnetic sector instrument so as not to reduce the magnetic field resolution.

# Source Pulsing

Pulsed ion extraction and ion beam deflection are two ways of generating a packet of ions. In pulsed ion extraction, the negative space charge of the electron beam is used to trap the ions after their formation, thus increasing sensitivity [2-4]. The electron beam is operated continuously and an extraction pulse accelerates the accumulated ions out of the source at discrete intervals.

lon trapping followed by source pulsing was attempted with TRIMS (first generation) and found to exhibit severe limitations in overall resolving power (for example see Figure 2.2) [5]. The initial spatial distribution of ions in the source produced ion intensity profiles in the magnetic field-time (*B-t*) data field that were opposite to those expected from simple TRIMS theory. It was found that, to achieve good time resolution, a high extraction voltage was necessary to reduce the contribution of the turnaround time, but this resulted in poor magnetic field (momentum) resolution. Conversely, to achieve good momentum resolution, a low extraction voltage was needed to reduce the spread of ion energies and velocities, but the time resolution was degraded under these conditions (see Figure 2.3). The same ion energy effects discussed by Wiley and McLaren [1] plagued the TRIMS instrument in this pulsing mode. Thus, it was decided to try post-source ion beam deflection as a means of creating the required narrow packet of ions for accurate velocity measurement.

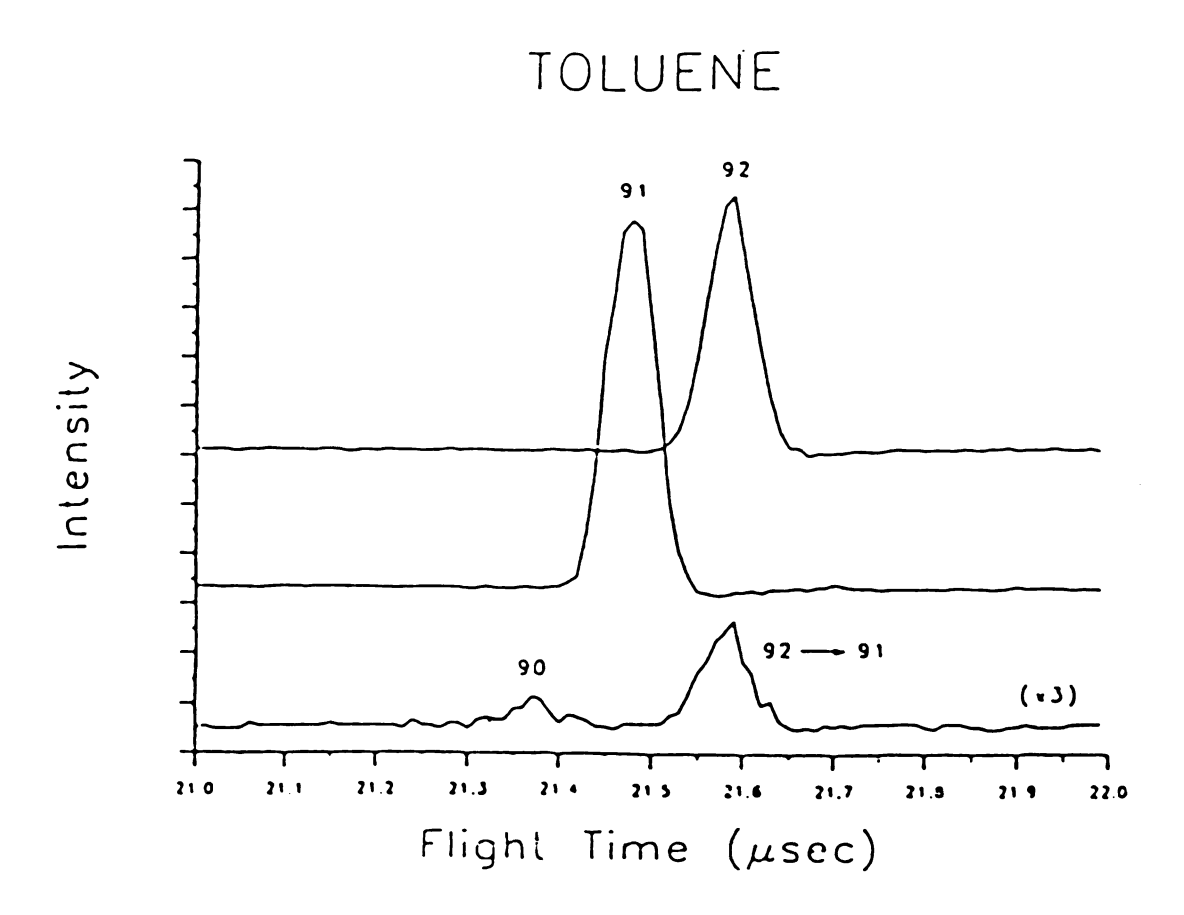


Figure 2.2 Results of TRIMS (first generation) operated with source pulsing.

97750 (33V) (66V) 97500 FINALgood momentum (100V) ION97250 resolution poor velocity (130V) **VELOCITY** resolution 97000 (m/s)96750 good velocity resolution poor momentum 96500 (220V) resolution 96250 16.6 16.8 17.0 17.2 17.4 17.6 FLIGHT TIME (µs)

<u>Figure 2.3</u> Final ion velocity as a function of total flight time for mass 71 at several extraction voltages with ion source pulsing.

## Post-source Pulsing

The beam deflection method for ion packet production (pulsing) offers the advantage that the spatial spread and turnaround time effects are no longer resolution-limiting phenomena and thus the diametric problems in resolving power for ion source pulsing discussed above are reduced. The initial TRIMS implementation employed beam deflection following the entrance slit of an LKB-9000 mass spectrometer. Unfortunately, this met with little success due primarily to mechanical difficulties in modifying the instrument so close to the ion source [6]. Therefore, it was decided to deflect the ion beam after the exit slit of the instrument (post-sector) [7]. The ion beam is swept across the width of a deflection slit placed a fixed distance from the deflection plates.

The theory of obtaining short bursts of ions from an ion beam was first developed in the 1960s by Fowler and Good [8]. They found that all methods of producing pulses by "sweeping" a continuous beam past a stationary aperture introduce an energy spread. A complementary relationship between beam quality and pulse duration exists such that the shortness of burst duration is always obtained at some cost in beam quality. Also fringing fields, nonhomogeneous fields related to surface imperfections, and diffraction effects exist at the edge and surface of each deflection plate and their strengths increase in magnitude as the deflection voltage increases. As portions of the ion packet pass through different equipotential surfaces of the fringing fields, they may acquire differing amounts of kinetic energy.

Fowler and Good described the process of extracting bursts of ions from a monoenergetic ion beam as beam chopping. The ion burst duration was found to

be related to the beam cross section and a quantity, writing speed (ws), which is defined as:

$$ws = (aperture\ width)/t_0$$
 (2.1)

where to is the time of entry of an ion into the deflector plates.

In spite of the early attempts [9-11] beam deflection was not used with great success for organic mass spectrometry until the work of Bakker [12,13]. He points out that any ions travelling in a horizontal beam between vertical deflecting plates at the instant an electrical field change occurs will experience both downward and upward directed forces. The motion of these ions is dependent on their exact position between the deflection plates at the time of field change.

Figure 2.4 is a conceptual diagram of the beam deflection event. A pulse is applied to one deflection plate while the other is held at a reference voltage. The deflection pulse is generated such that the positive-to-negative voltage change is symmetrical about the voltage of the other plate. (This diagram is somewhat misleading because it suggests that an infinitely fast risetime pulse will produce an infinitely thin ion packet. A finite ion packet width will always be produced no matter how fast the pulse is.)

A more detailed "picture" of ion motion in a deflection plate is shown in Bakker's paper [12]. George Yefchak has modelled ion's in the deflection region the results of which are illustrated in Figure 2.5 [14]. His model considered a collimated beam of mono-energetic ions which pass between the plates, so the ions are deflected off the flight axis. If the electric field is reversed, the beam is

-

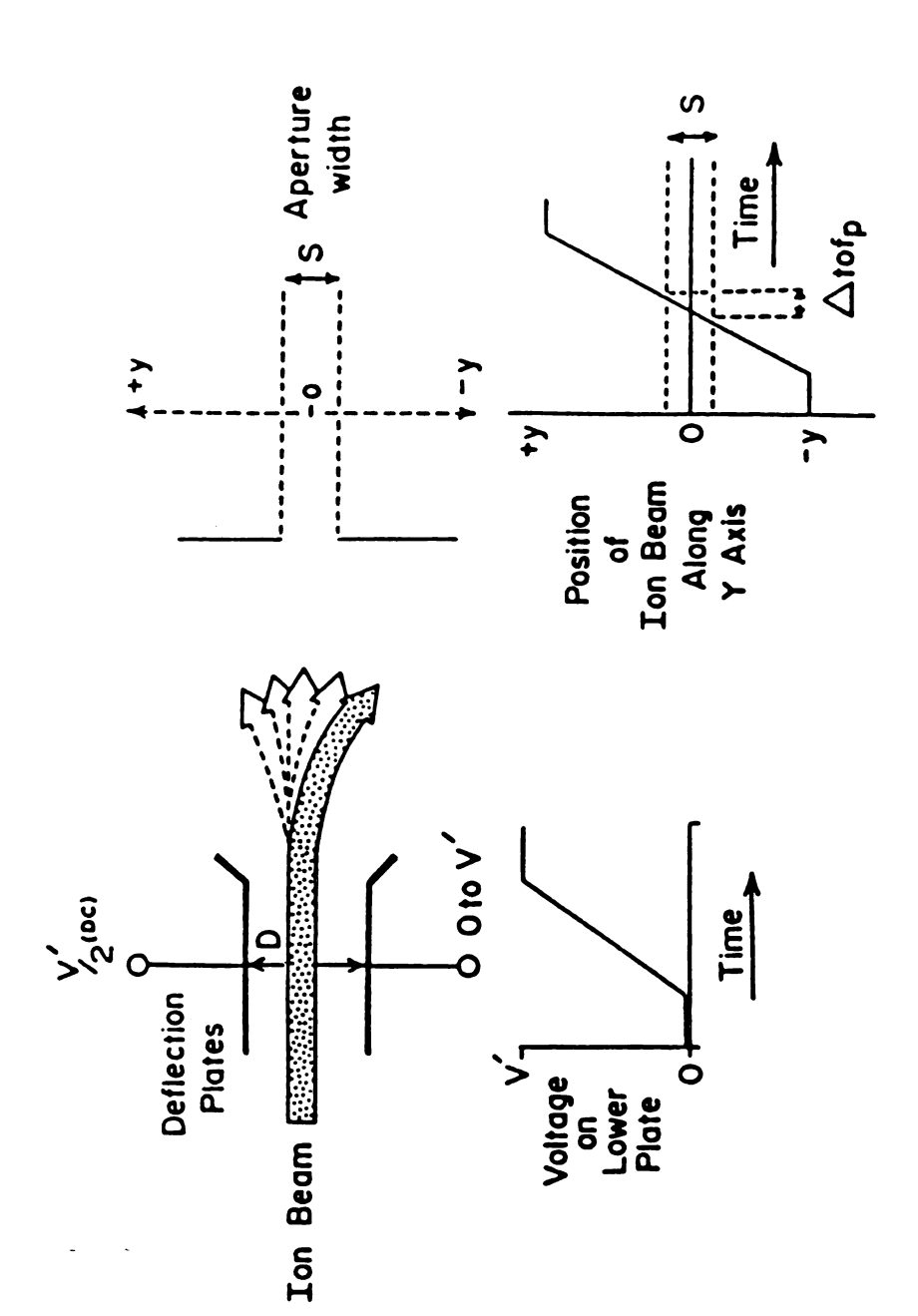


Figure 2.4 Ion pulse formation by deflection of a continuous beam across an aperture. D = separation between deflection plates; S = aperture width; V' = deflection voltage;  $\Delta tof_p$  = width in time of ion packet passing through the aperture [15].

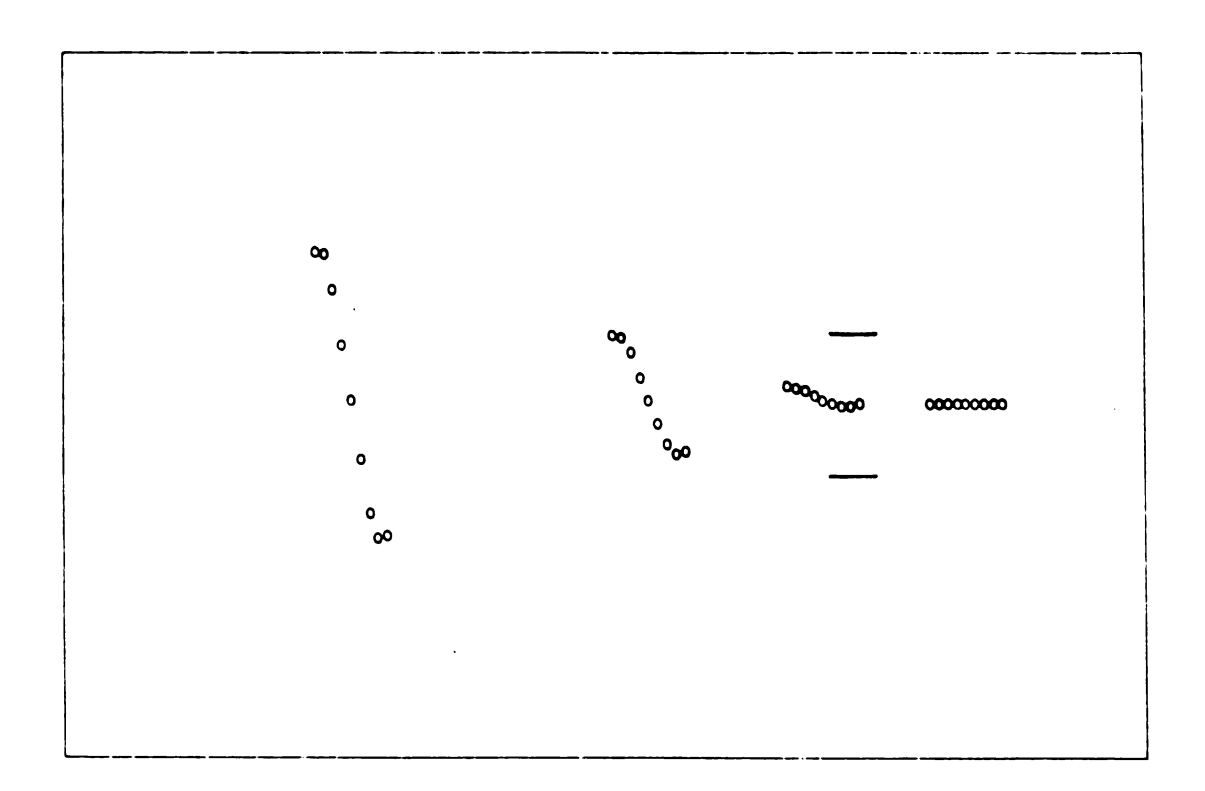


Figure 2.5 Four "snapshots" from a model of ion trajectories in a beam deflection assembly. This is the deflection plate region with a plate spacing of 2 mm, slit width of 2 cm, length to slit of 1.5 m, mass of 1000 u, an energy of 3500 eV and a 100 V deflection pulse applied.

eventually deflected in the opposite direction. For a short time, however, a "kink" occurs in the beam since ions which were in the deflection plate region when the field reversal occurred experience nearly equal forces in the two directions and thus leave the plates traveling nearly parallel to the original flight axis. Ions exactly in the middle of the plates will experience no net change in their velocity, but will be displaced slightly off axis due to a difference in initial conditions. These positive ions at first did not have any up or down velocity components, but at the deflection voltage change, acquired this component, and thus, are changed in position. If a slit is placed across the flight axis past the deflection plates, a packet of ions will emerge through the slit.

Bakker [12,13] derived an equation relating the ion bunch duration,  $\Delta t_{p}$ , to the deflection parameters. He assumes that the rise-time of the deflection pulse is short compared to the transit time of the ions in the deflection plates (5 nsec vs 1-2  $\mu$ sec) and that the drift space is large compared with the length of the deflection plates (1 m vs 1-2 cm). With the above assumptions his equation reduces to:

$$\Delta t_p = (B + S)D (2mU)^{1/2}/2V'L (e)^{1/2}$$
 (2.2)

where B is the width of the ion beam, L is the flight tube length, m is the mass, U is the accelerating voltage, e is the charge on an electron and the other variables are shown in Figure 2.4.

The time resolution in the time-of-flight measurement is necessarily limited by the ion bunch duration. The maximum resolution is given by  $R = t/(2 \Delta t_p)$  in which t is the TOF of the ion and, thus, Bakker arrived at:

$$R = L2V'/2DU(B+S)$$
 (2.3)

for the resolution attainable with square wave beam deflection. Bakker also derived an equation relating the ion intensity as:

$$I \propto (B+S)DU/V'Ld$$
 (2.4)

where *d* is the length of the deflection plates. Bakker assumed that the energy spread of the ions within the continuous ion beam is negligible. Pinkston [14] addresses this problem and presents an excellent description of the factors involved in designing a beam deflection assembly.

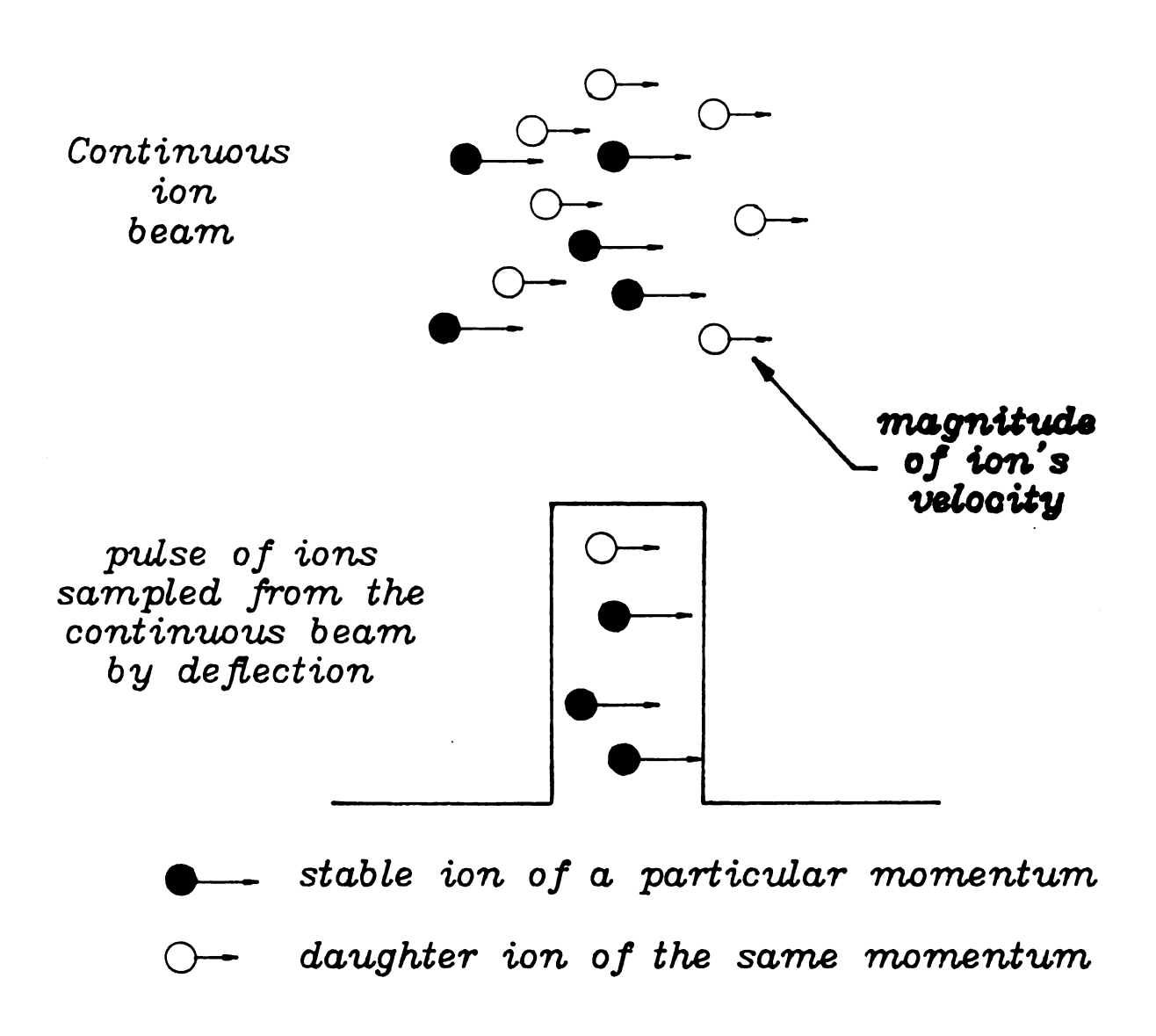
Interpretation of equations 2.2 and 2.3 above reveals that the deflection voltage, V, cannot be too large otherwise sensitivity will suffer. The flight tube and the deflection plate length limit the sensitivity as well. Increasing the deflection plate length to insure a uniform electrical field is offset by the possibility of losing ions by collision with the plate itself. The distance between the plates is similarly related to the degree of ion loss. An optimum assembly could be arrived at most efficiently by simulation. At the time of designing the TRIMS assembly, modelling programs with a time dimension feature did not exist. It was decided to follow the recommendation of Pinkston [15] in designing a simple pair of deflection plates and a deflection slit.

## Beam Deflection in TRIMS

Bakker [12,13] and Pinkston et al. [16] have explored deflection methods and, in particular, have experimented with a set of gating plates to improve time resolution. By varying the rate at which the deflection voltage changes through a reference voltage (usually ground), the resolution/sensitivity trade-off can be changed.

Beam deflection in TRIMS after full acceleration effectively samples the ion beam at a given instant as illustrated in Figure 2.6. The sampled ion packet consists of ions with the same momentum and a distribution of velocities. Beam chopping does nothing to effect the kinetic energy spread of ions within the beam and therefore the mass resolution will be limited. However, mass assignment in the TRIMS instrument is not hampered by an induced or initial kinetic energy spread because the simultaneous measurement of both momentum and velocity makes mass determination independent of ion energy (equation 1.1).

Deflection of the ion beam after it has left the source and acceleration region allows a direct measure of ion velocity; this method does not include measurement of the ion acceleration time (as with source pulsing). With beam deflection, the ion source is operated under the conditions and configuration of a normal magnetic sector mass spectrometer. This gives the advantage of operating the instrument with maximal magnetic field resolution and sensitivity under normal focusing conditions. Thus, the magnetic field and TOF features of TRIMS can be optimized independently.



<u>Figure 2.6</u> Deflection of a continuous ion beam removes the resolution limiting effects of spatial spread and turn-around time.

A single pair of deflection plates and a slit (deflection slit) comprise the beam deflection assembly (see Fig. 2.7). The technique for post-sector beam deflection required modification of the exit slit and flange assembly of the LKB-9000. Four phenolic rods mounted directly on the housing provide support for the two rectangular copper deflection plates. The plate dimensions are 2.0 cm x 0.6 cm x 1.3 cm, with a separation of 0.2 cm. An ultrahigh vacuum ceramic-metal quad-minithru feedthru (Ceramaseal, Inc.) was mounted on a flange to provide the electrical connection to the plates. All electrical leads were made as short as possible to minimize pulse distortion.

The circuit driving the deflection plates provides a variable pulse amplitude and a variable pulse duration. A  $\pm 25$  V square wave with a frequency of 5 kHz is typically used and is applied to one plate while the other plate is held at ground potential. Each edge of the square wave has a rise or fall time of approximately 10 ns. Ions are transmitted during the pulse transition (edge) through ground. Thus, an ion packet is transmitted to the detector every 100  $\mu$ sec (every edge) and only when both deflection plates are at the same electrical potential.

The deflection circuitry and associated hardware is shown in Figure 2.8. A pulse is supplied to the edge-triggered 7474 flip flop in the circuit diagram. Each pulse alternately produces a positive and negative going edge. Each edge triggers a monostable which creates two pulses 4.7 µsec wide and one half cycle apart. Each of these pulses is the input to two CMOS clock drivers (DS0026) capable of driving the large input capacitance of the output field-effect transistors (FET). The upper and lower FETs are alternately switched on by the 47 µsec pulses to create a very fast square wave whose amplitude is determined by the magnitude of the output supplies.

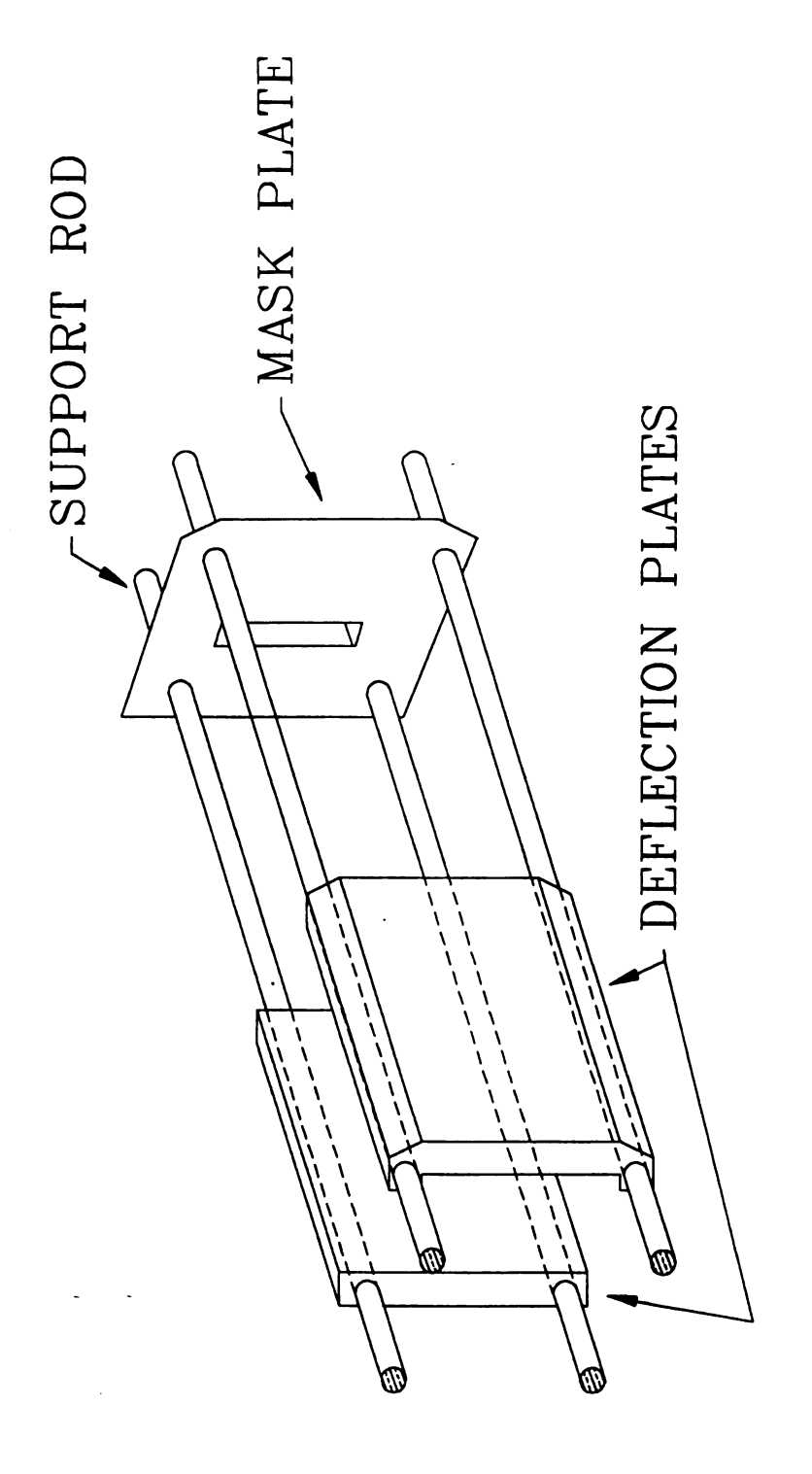
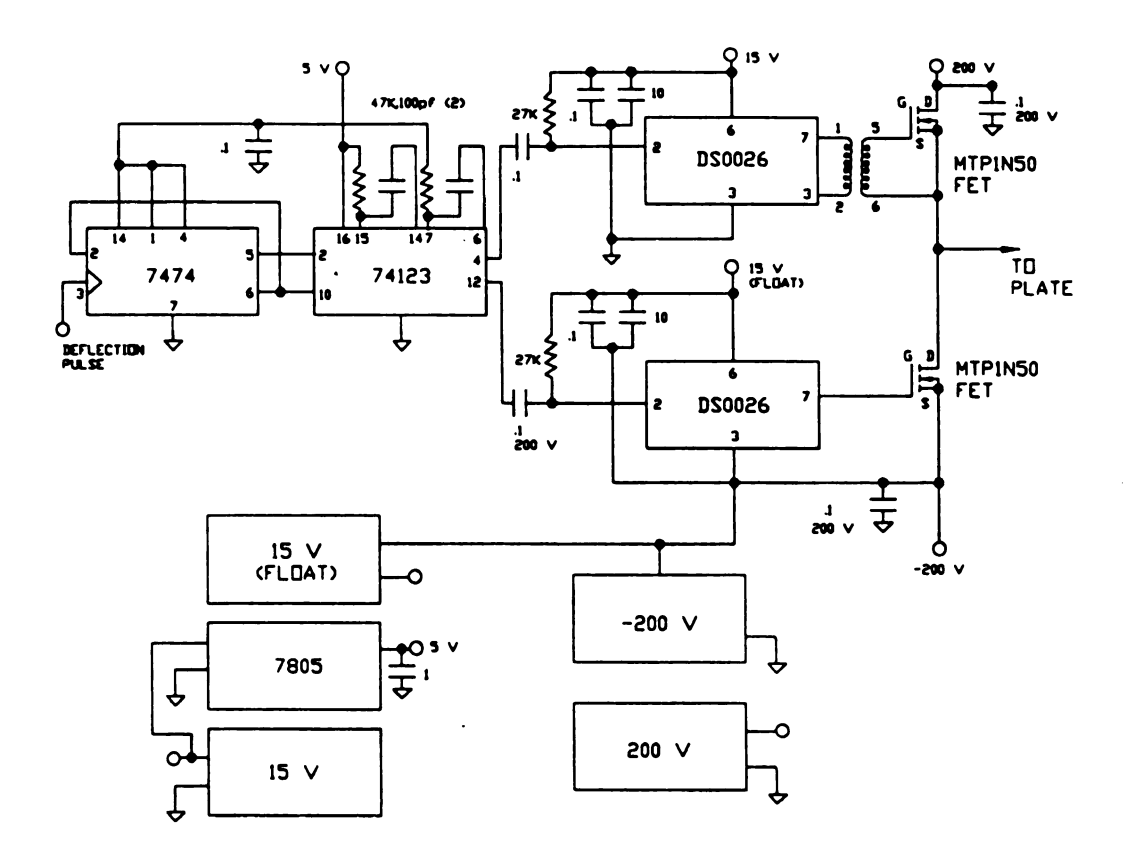


Figure 2.7 Diagram of the beam deflection assembly constructed for the LKB-9000. The assembly is built on the existing exit slit housing.



<u>Figure 2.8</u> Schematic of the fast square wave plate driver. This circuit generates the pulses which create the ion packet for TOF analysis.

The supper transistor (MTP1N50) is isolated from the driver by a transformer (PE1983X) to facilitate the swing of its source without disturbing the driver. The lower output FET does not require this isolation because its source is fixed at the negative supply voltage. This fact, however, requires that this driver's 15 volt supply should float on the negative supply. The 0.1 µf input capacitor to the lower driver is required to isolate the monostable from the -200 volts at which this driver is operating. The upper input coupling capacitor is present for symmetry although is not strictly required.

A multi-plate gating system is not required here because the rise and fall times of the deflection pulse are sufficiently matched so as not to adversely affect the peak shape. The slit serves to reduce the voltage required to deflect the ion beam out of the large collection area of the detector and to limit background ions from reaching the detector.

Figure 2.9 shows the location of the beam chopper relative to the LKB-9000. For ion velocity measurement with improved resolution, a 1.55 m flight tube was added beyond the exit slit of the instrument. Figure 2.10 is a schematic representation of the second generation TRIMS instrument. The time-resolving stage is completely separate from the magnetic sector, but the TRIMs theory discussed in chapter one still applies. Although ion velocity measurements are made after the magnetic sector, all equations developed previously for mass assignment remain valid because the ion velocity in the post-sector flight tube is the same as that through the magnet.

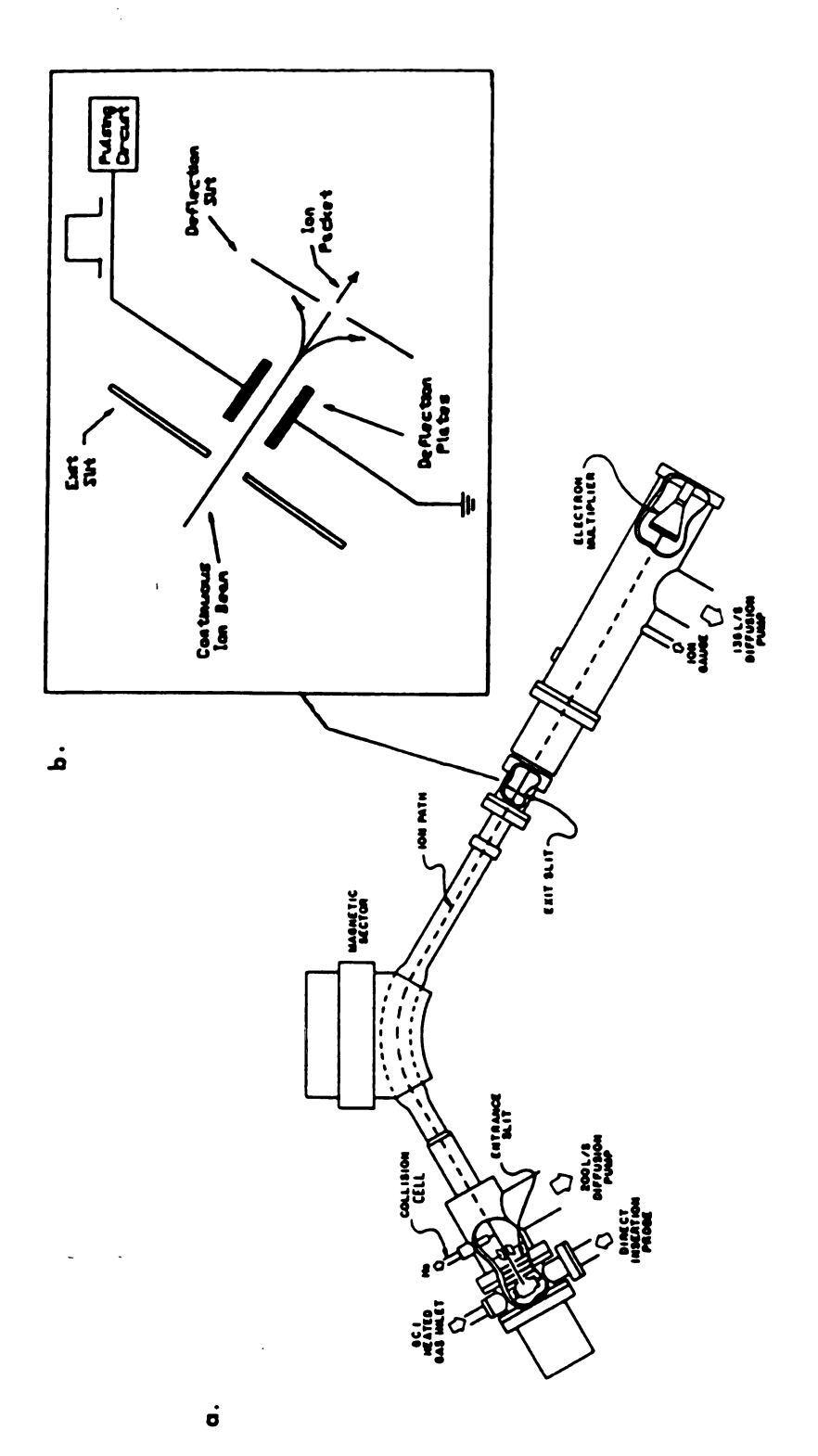
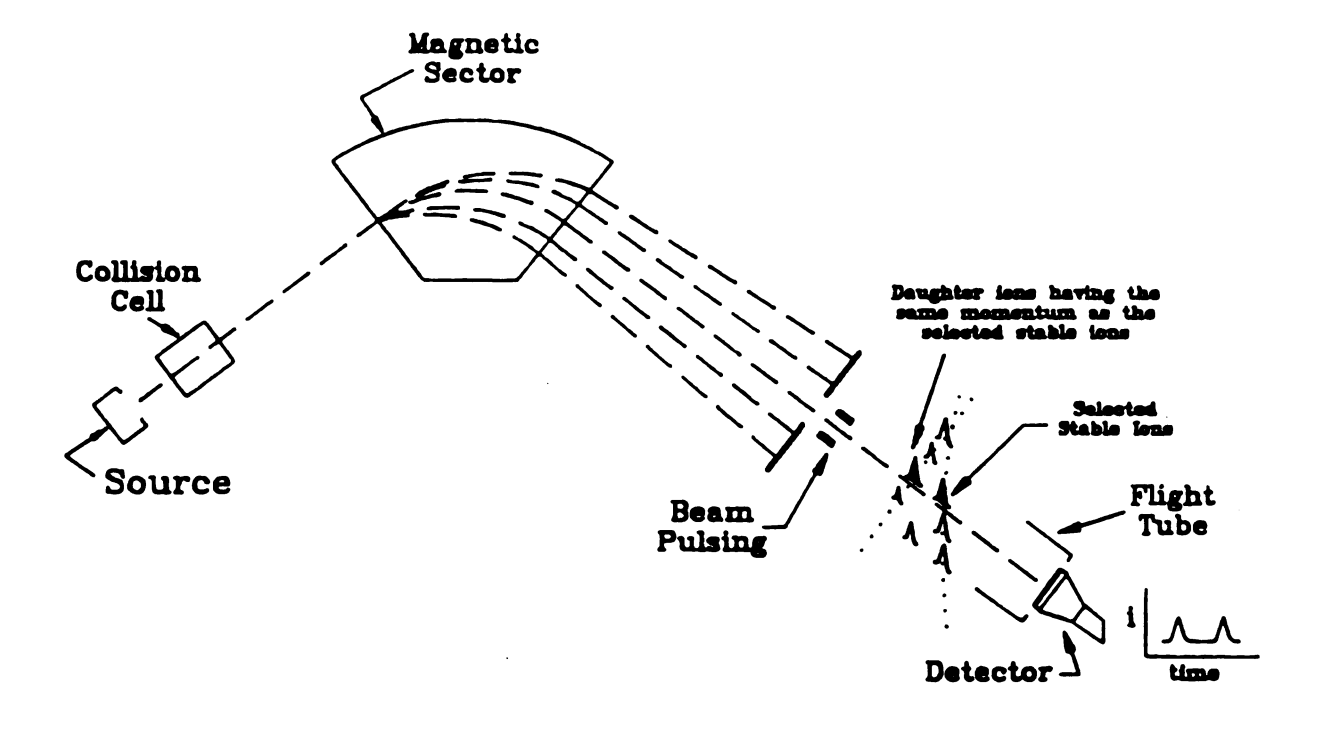


Figure 2.9 (a) Top view of the ion path through the instrument. (b) Top view of the deflection slit assembly.

# TRIMS Instrument



<u>Figure 2.10</u> A schematic representation of the ion momentum and time dispersion characteristics of the modified magnetic sector mass spectrometer.

All the measurements described in this chapter were performed with an 8088-based data system that controls the magnetic field and the sampled flight time and provides data acquisition with signal averaging. Data acquisition is accomplished with code written in FORTH [17]. The magnetic field is controlled by an optically isolated digital-to-analog converter and time-slice detection is possible through the use of a delay generator, a boxcar integrator, and the deflection circuitry, all under computer control (for further details see reference 18).

## EXPERIMENTAL RESULTS EMPLOYING BEAM DEFLECTION

## Resolution

Experiments were performed with the well-characterized metastable decompositions of n-decane and toluene. Figure 2.11 shows peaks for the 92-->91 metastable decomposition product of the molecular ion of toluene and the stable ions at mass 90. These ions appear at the same magnetic field strength (ion momentum) but at different arrival times. The daughter ions of mass 92 appear at approximately the same momentum as the stable ions at mass 90, but are separated in time because they arose from heavier and therefore slower parent ions (m/z=92). The inset in the figure shows precisely how these data were acquired. The use of the measured flight time of the daughter ion can be used to identify the mass of the parent from which the daughter originated. The equation used in this case is

$$m/z = 2Vet^2/d^2 \qquad (2.5)$$

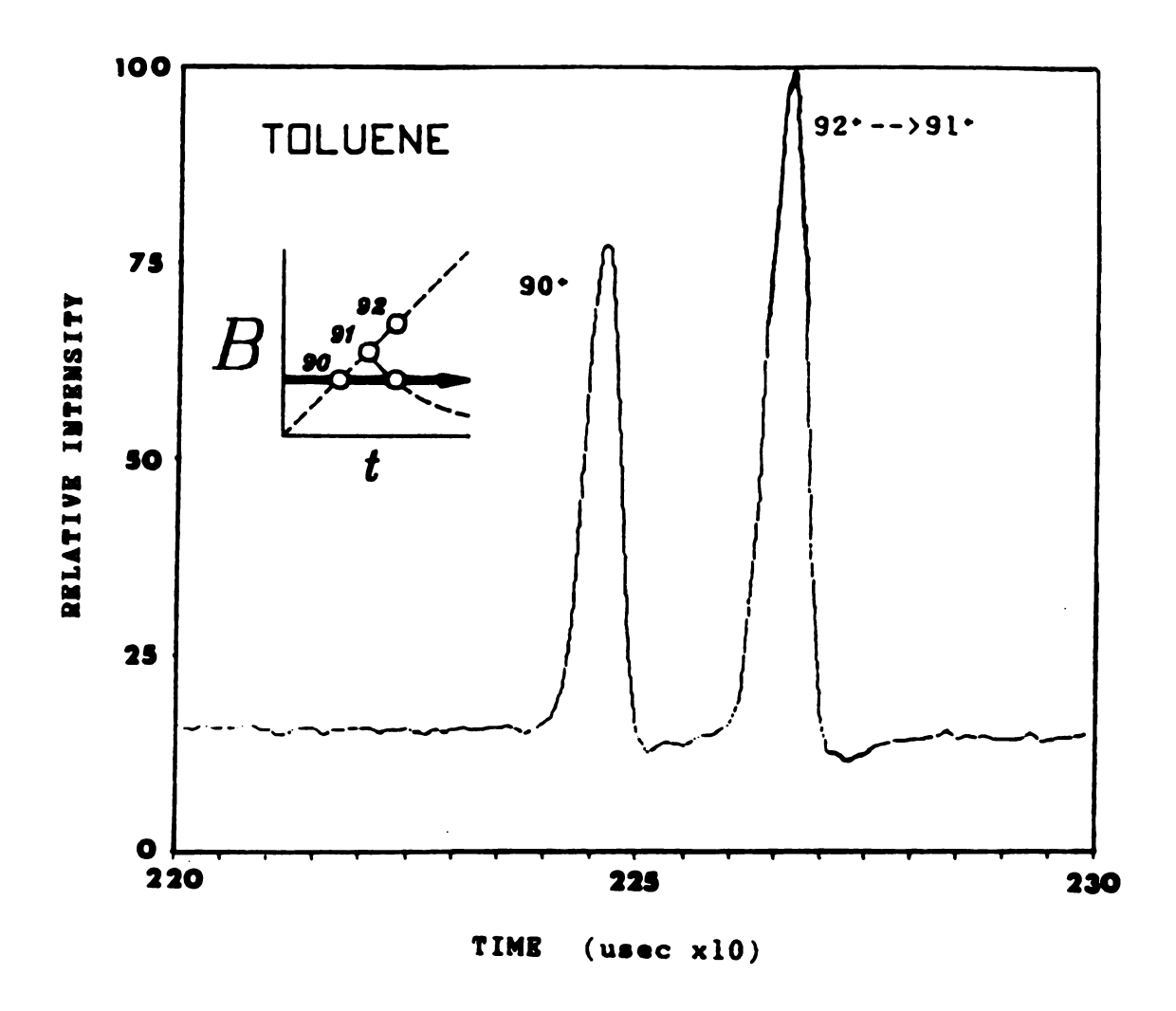


Figure 2.11 Plot showing the 92+ --> 91+ metastable decomposition product of toluene as well as the stable ion at mass 90. This is a single sweep of the time axis while the magnet is set to pass mass 90.

where V is the accelerating potential, t is the flight time, and d is the flight distance (measured from half way between the deflection plates to the detector). As measured from the separation of peaks representing the stable ions of mass 92 and 91 from toluene, the mass resolution on the time axis is approximately 650 (full width at half maximum definition (FWHM)).

Figure 2.12 is the result of scanning the magnetic field while sampling the arrival time at a fixed value corresponding to the arrival time of the stable ion of mass 142. Here, the peaks representing products of metastable decomposition of the molecular ion of n-decane (142-->112 and 142-->113) are separated with a mass resolution (FWHM) of approximately 500. This daughter ion resolution is primarily a function of the magnetic analyzer employed, its slit widths, and its focusing adjustments, and it could therefore be improved with better analyzer design.

A contour of the raw data obtained for mass 90 and 92-->91 daughter ion of toluene is shown in Figure 2.13. An additional feature of post-sector deflection is that it produces ion intensity profiles in the B-t data field that follow theoretical expectations [7]. Isomass ions with higher velocities should appear at higher magnetic field strengths (because mv = Bzer) and shorter flight times. This is borne out by observing the contour lines from slices of the B-t data field. These data can be used for kinetic energy release measurements of ion dissociation processes. More about this aspect can be found in Chapter five.

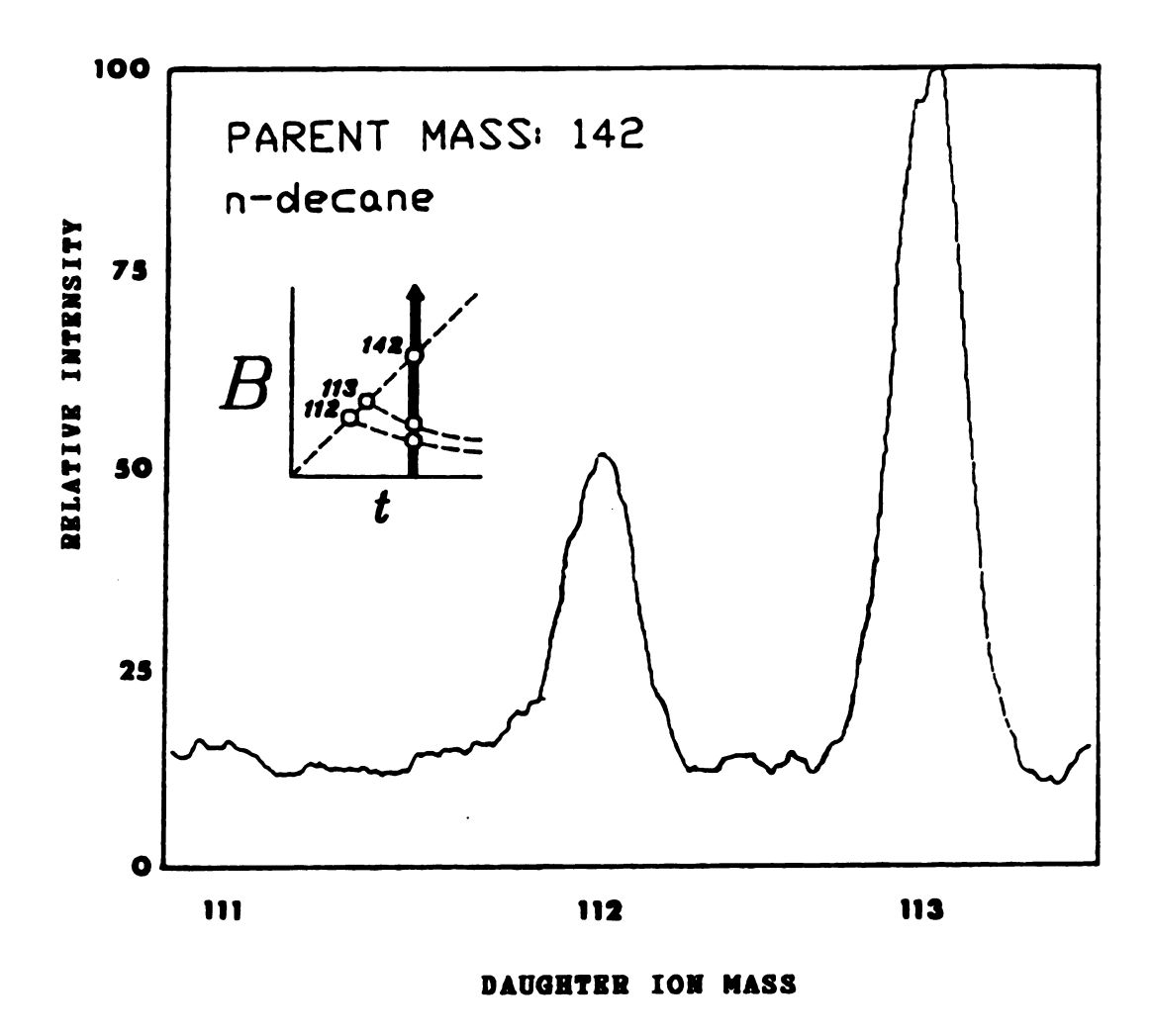
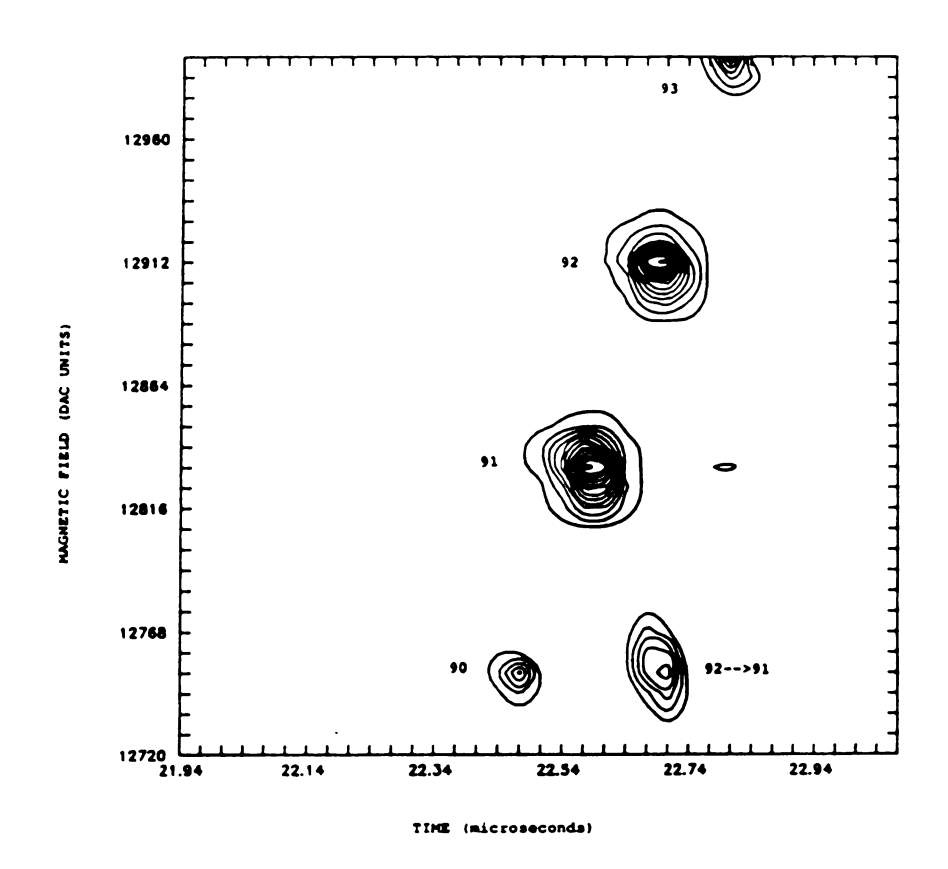


Figure 2.12 Plot of the ion current representing the 142+ --> 112+ and 142+ --> 113+ metastable decomposition products of the molecular ion of n-decane. The time of arrival of the parent is held constant and the magnetic field is swept. Five hundred pulses were averaged for each of 40 sweeps of the magnet. These data result from background subtraction and smoothing (m/ $\Delta$ m for the magnetic field axis is  $\approx$ 500).



<u>Figure 2.13</u> Contour of the molecular ion region of toluene. Isomass ions of higher velocity arrive at the detector at a higher magnetic field strength and in less time than slower ions of the same mass. This effect is more pronounced for metastable or CAD reactions in TRIMS because of the energy spread that results from these processes.

# Detectability

:

The detection limit obtained by selected ion monitoring (SIM) was compared with that obtained under similar conditions by post-sector beam deflection. The molecular ion of n-decane was monitored by first setting the appropriate magnetic field and arrival time and then collecting the ion current produced during chromatographic elution. The ion beam was deflected (post-sector) with a repetition rate of 10 kHz. A signal-to-background ratio of 4.6 was observed from 13 ng of n-decane. With SIM in continuous beam (not time-resolved) mode, 200 pg of sample was required to give the same ratio. Therefore, pulsing by beam deflection reduces the detectability by a factor of 65.

Deflection of a continuous ion beam has the disadvantage of permitting observation of only approximately 0.01% of the beam (due to the duty cycle). Sensitivity (coulombs detected per microgram of sample) must be 104 less in time-slice detection (TSD) than with continuous monitoring of the selected ion beam. However, the instantaneous current (during the appropriate time slice) is approximately equal for both methods. The measurement of current is noisier for TSD because of integration of current over 104 longer time in continuous mode and therefore a signal-to-noise improvement of approximately 100 (square root of the integration cycles) should be observed for continuous acquisition. The level of background is lower for TSD than for continuous mode because integration of the ion-current with boxcar detection circuitry at the proper time delay after deflection, enhances the current from reproducible arrival times over that from the random arrival times of ions producing background noise. Thus, this instrumental configuration with time resolution gives the advantage of synchronous detection and a consequent reduction in chemical noise. The level of chemical noise will depend on what other and how many ions can pass the momentum-filter. Therefore, despite a loss in signal strength of 10<sup>4</sup>, an overall loss in signal-to-background of less than 10<sup>2</sup> is realized over continuous beam operation. This seems a small price to pay for the vast increase in information obtained.

With post-sector deflection, the momentum and time regions of the instrument can be independently optimized. This resulted in a 150-fold improvement in detection limit over that obtained with source pulsing. Improved ion focusing has also contributed to the present low detection limit. This configuration takes advantage of the magnetic sector focusing properties since the deflection apparatus is at the focal point of the magnetic sector.

These results indicate that post-sector deflection provides good resolution and detection limit in both the momentum and velocity axes and eliminates the distortion in velocity determination previously observed with source pulsing. Beam deflection has the further advantage in that any ion source normally employed in a conventional magnetic sector instrument can be used (such as chemical ionization).

#### SOFTWARE MODIFICATIONS FOR TRIMS WITH TSD

# SIM data recording

Software modifications or additions have been made to the time-slice detection data system. A "word" called FOCUS-SIM was created to allow a more

accurate recording of SIM data. The magnet on the LKB-9000 mass spectrometer is old and its field strength tends to drift quite appreciably. When acquiring SIM data a drifting magnetic field strength can be disastrous. Any movement of the magnetic field strength will result in a lower than normal recording for the intensity or ion current. The new code operates by sweeping the magnetic field strength over a range of DAC values that encompass the mass of interest. As the sweep occurs (while the component is eluting from the chromatograph) a moving maximum is performed and the maximum value is recorded. This allows the magnetic field to shift slightly without causing ion detection problems. The code was successfully applied to methyl stearate SIM of mass 74.

# Magnet control

Magnet sweep rate control code was written to give the user a precise time control for magnet sweeping. A word called M-DELAY allows for a variable amount of time at each DAC element. By appropriate choice of this delay time various sweep rates can be achieved. The word GO-MAG executes the magnet sweep and returns the time in seconds for the specific DAC range swept.

## B-t field acquisition

A word called 1BT-FIELD allows acquisition of the full MS/MS data field. This code is actually used for collecting a small region of the *B-t* field because the full field acquisition would be too consuming of time and data storage space. The

values for the magnet DAC and time (in the *B-t* field) are set in the parameter editor. Execution of 1BT-FIELD can yield a plot similar to Figure 2.14 (a commercial software package called SURFER (Golden Software, Inc.) was used for this figure). This is the smoothed raw data of the molecular ion region of toluene. It is important to check the available storage space on the TSD system before execution 1BT-FIELD because there must be a sufficient number of records available.

#### HARDWARE FOR THE TRIMS-TAD INTERFACE

The ITR controls the synchronization of the collection of the time and magnetic field strength (Hall-effect) measurements. A start pulse to a chopper circuit initiates the production of an ion packet and serves as a zero time value for velocity measurement of the ions.

## TRIMS-ITR Interface boards

Two TRIMS-ITR interface boards were designed and constructed to accommodate the hall probe. Figure 2.15 is a block diagram of the address decoders (chips labelled 74F521) employed to function in a "status-in" and "command-out" (SIN/COUT) manner. Figure 2.15a is a schematic of this board. An MP-6912A (Analogic, Inc.) 12-bit analog-to-digital converter (ADC) data acquisition system was optically isolated from the ITR's high speed emmiter-coupled and transistor-transistor logic to provide noise immunity (a block diagram is shown in Figure 2.16). The ADC connections with line-drivers (chips labelled

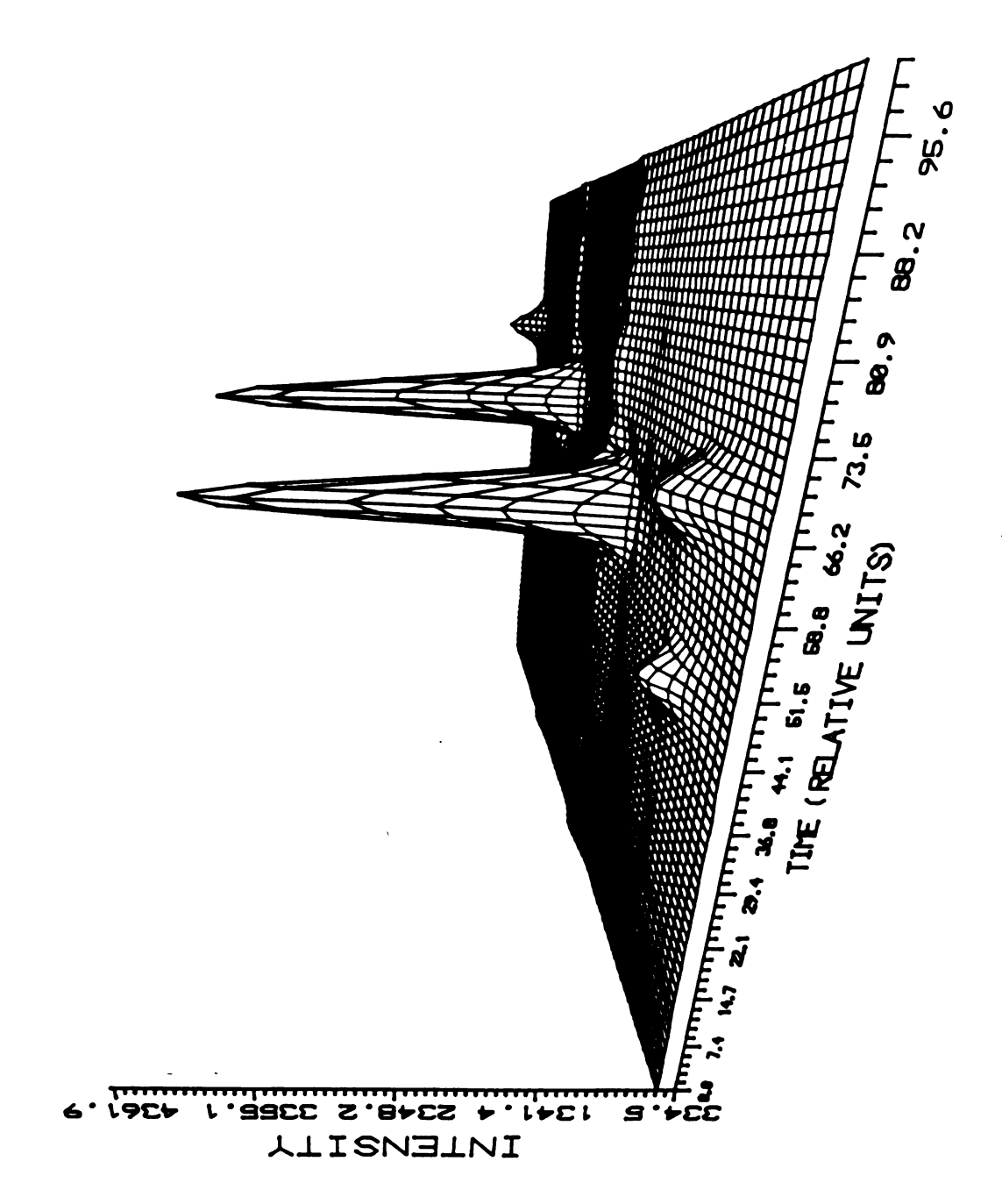


Figure 2.14 Three-dimensional view of the molecular ion region of toluene.

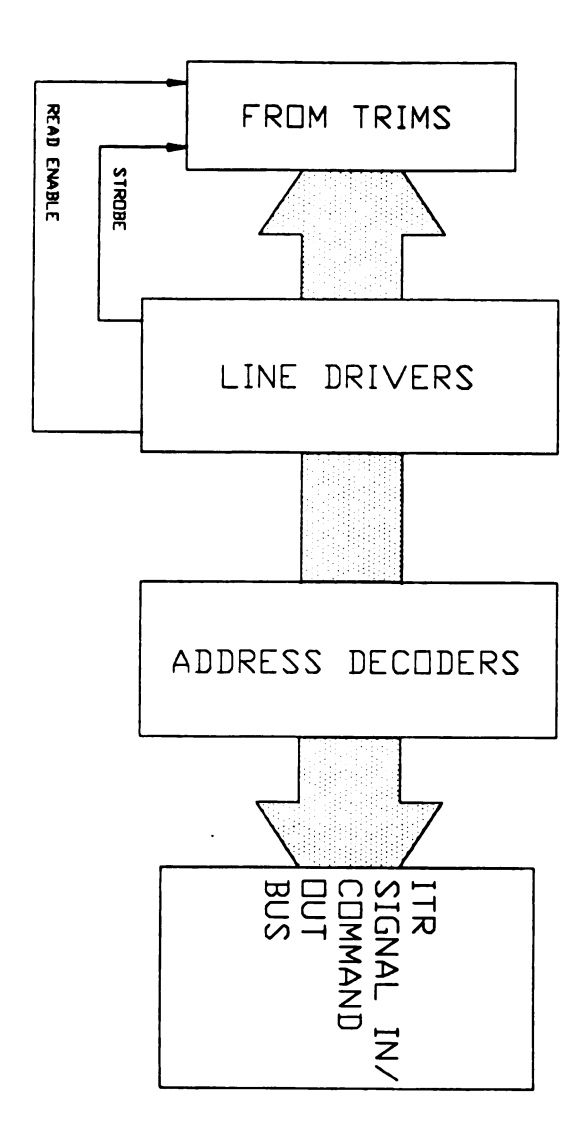


Figure 2.15 Block diagram of the TRIMS-ITR interface board. This board communicates with the signal in/command out (SIN/COUT) board on the VME bus of the ITR.

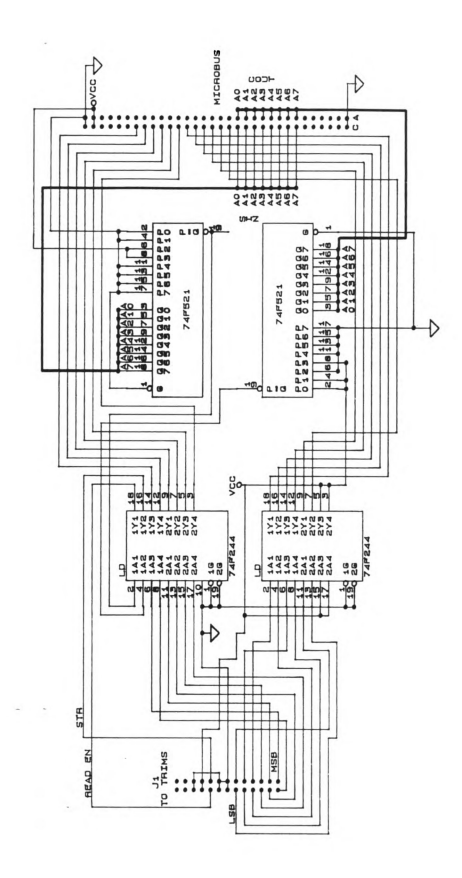


Figure 2.15 a. Schematic of the TRIMS-ITR interface board.

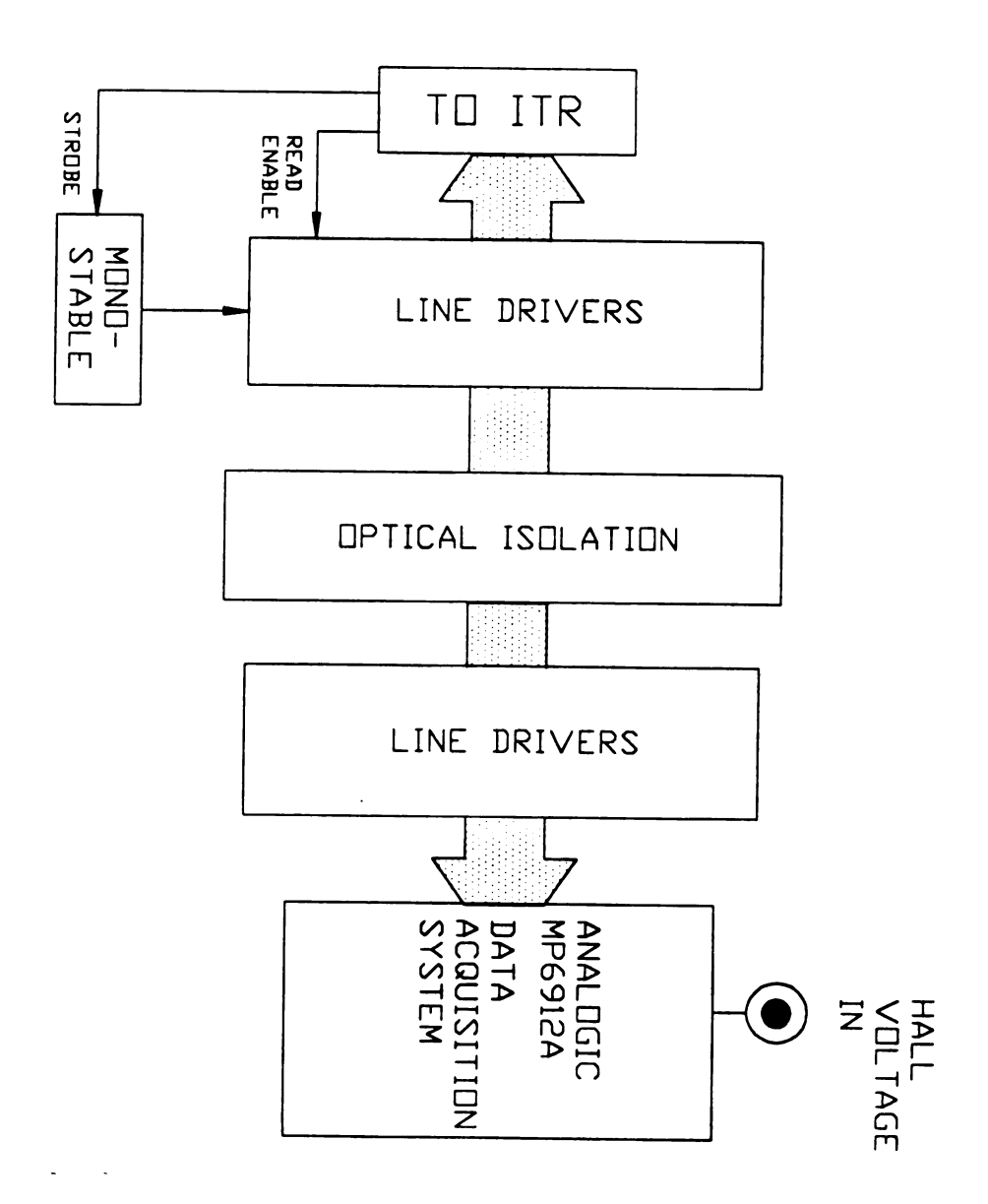


Figure 2.16 Block diagram of the optically-isolated ADC board that communicates with the TRIMS-ITR interface board. This circuitry allows the ITR to sense the magnetic field strength at any time and synchronize this data with ion arrival time information.

74F244) and optical isolation is shown in the schematic of Figure 2.16a. A digital-to-analog converter (DAC) interface was constructed as well to allow control of the magnetic field strength (via two latches labelled 74LS374) and a block diagram is shown in Figure 2.17. The schematic of the DAC interface board is illustrated in Figure 2.17a. The relationship of DAC vs mass on the TRIMS instrument has been demonstrated [6]. A DAC value (voltage) is linearly converted by the magnet current power supply circuitry into a current. This current is proportional to the magnetic field strength. Mass is proportional to the square of the magnetic field strength and it follows that the DAC value must be proportional to mass squared. A Hall-effect probe measures the magnetic field strength and produces a corresponding voltage. The Hall voltage should be proportional to the magnetic field strength that the ion experiences. A plot of Hall voltage versus mass 1/2 should be linear.

To test the functioning of the TRIMS-ITR Hall-effect sensor interface, the mass marker on the LKB-9000 was adjusted to set the magnet at particular masses. The Hall voltage was recorded from the digitized output of the ADC board (on the VME bus) as well as from a digital multimeter before entering the circuitry. The results of the analog Hall voltage measurement vs square root of mass is shown in Figure 2.18. The dashed line is a linear fit of the data to the equation y = B(0) + B1(x). The residual sum of squares is 0.0010. The results of the digitized Hall voltage measurement vs square root of mass is shown in Figure 2.19. The same fit was performed with a resulting residual sum of squares equal to 0.0016. These results indicate excellent agreement with established theory and also that the interface is functioning properly.

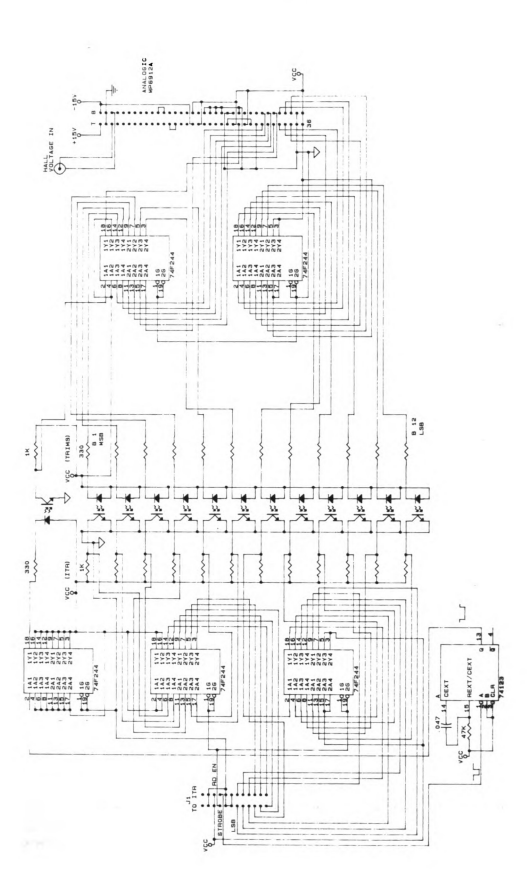


Figure 2.16 a. Schematic of the optically-isolated ADC board.

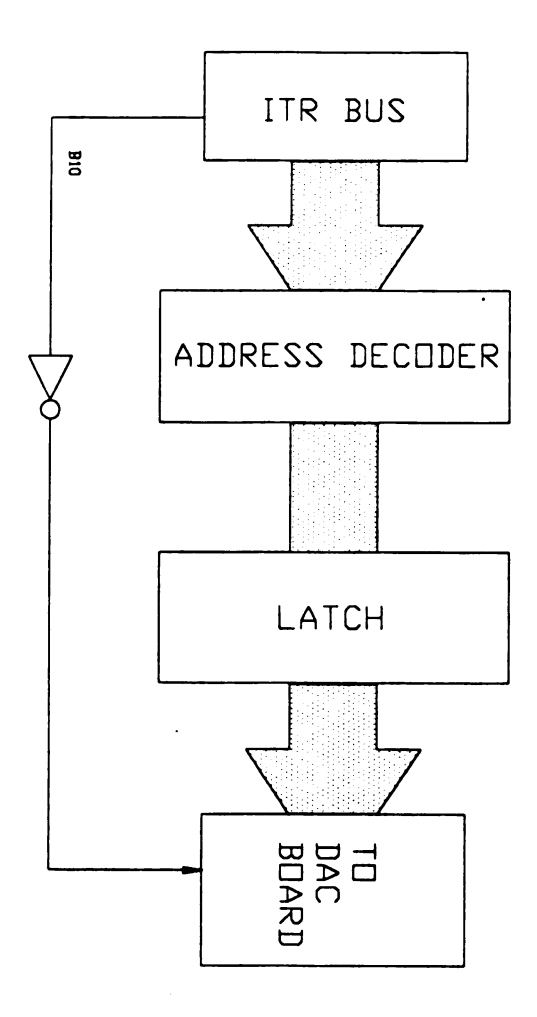


Figure 2.17 Block diagram of the DAC interface to the ITR from the TRIMS instrument. This circuit allows the ITR to control the magnetic field strength in a step-wise fashion.

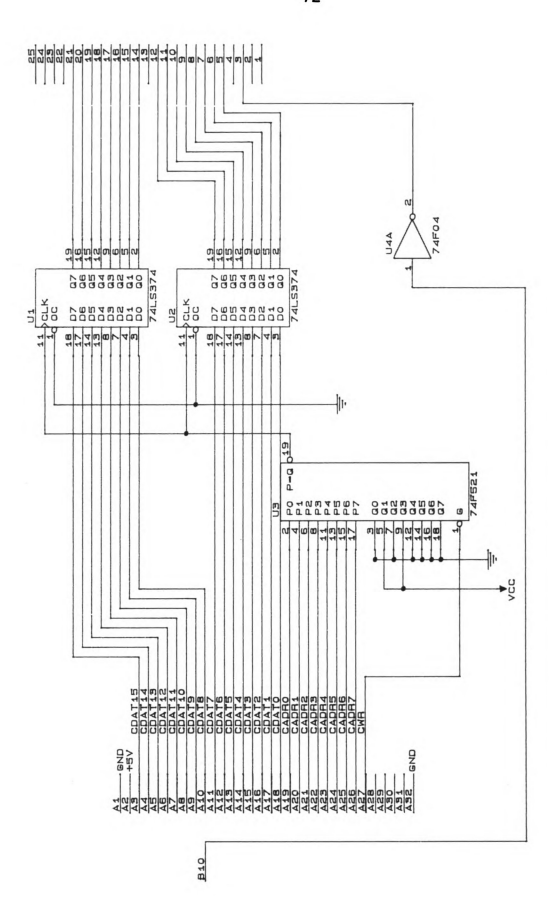


Figure 2.17 a. Schematic of the DAC interface board.

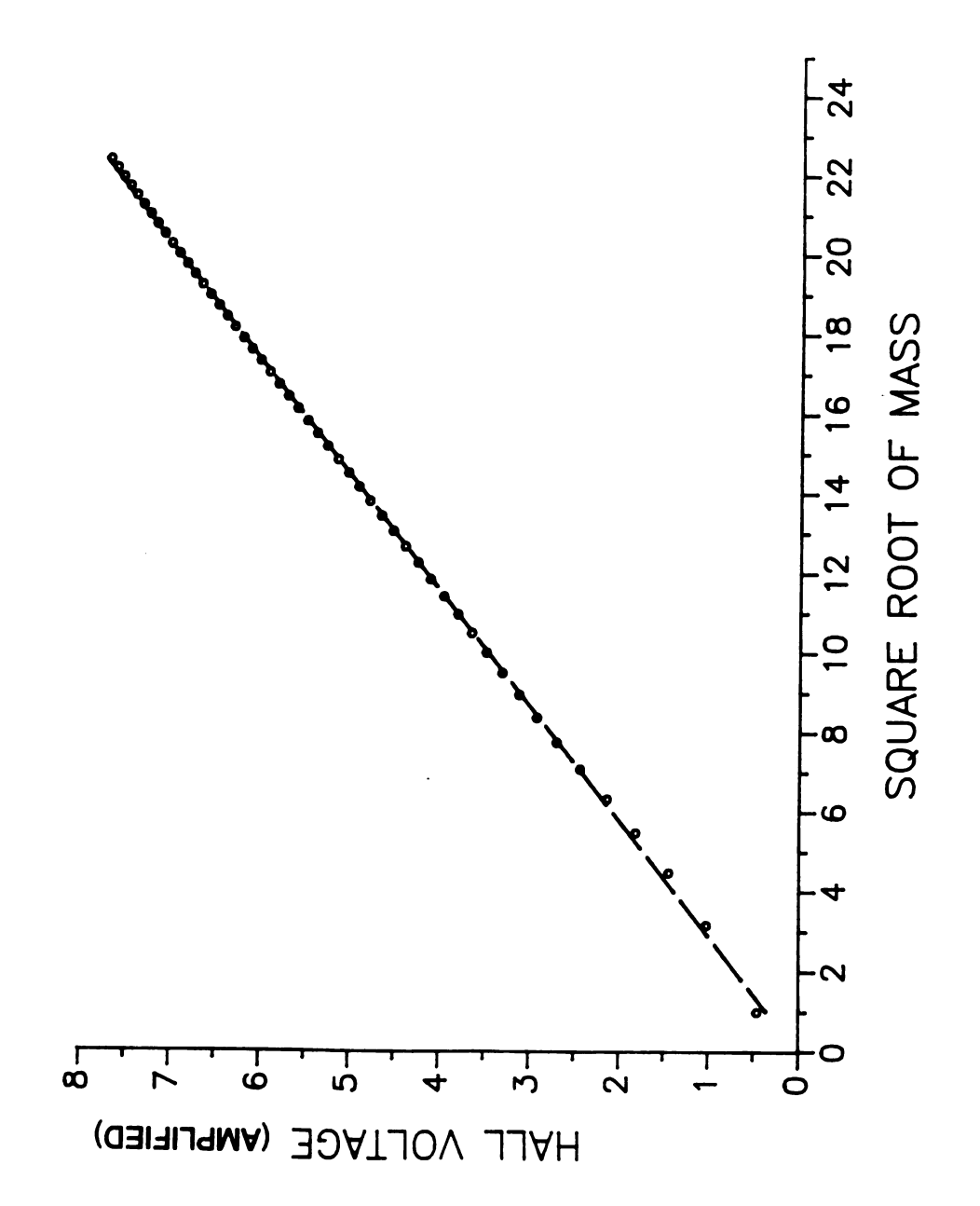


Figure 2.18 Hall voltage plotted as a function of the square root of mass. The relationship is linear and can be used to calibrate the TRIMS instrument.

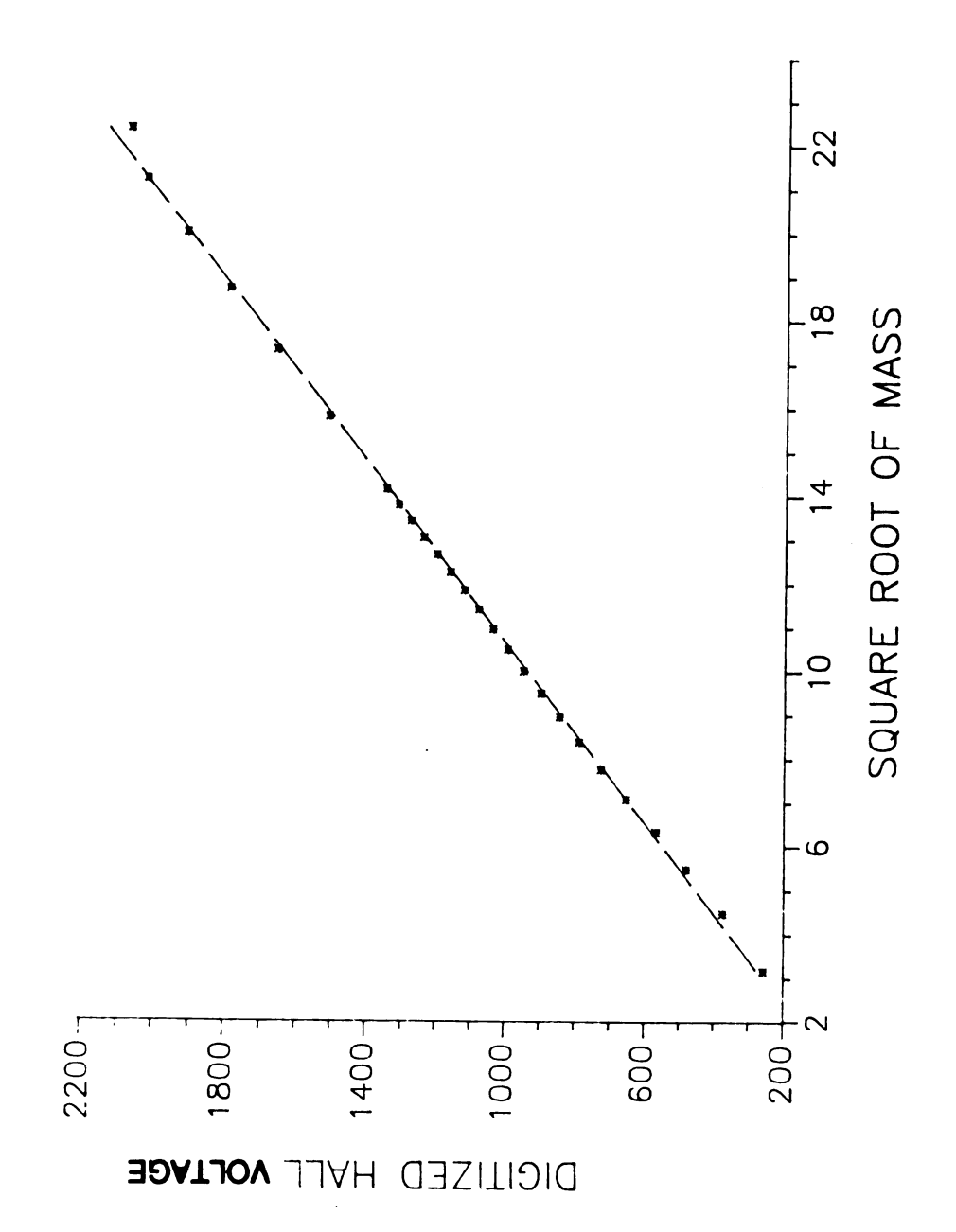


Figure 2.19 Results from the digitized Hall voltage vs m<sup>1/2</sup>. A linerar fit is evident and agrees well with the analog data presented in Figure 2.18. These measurements indicate a properly functioning Hall-read interface.

#### SOFTWARE FOR THE TRIMS-TAD INTERFACE

A VME 68000 based (Motorola, Inc.) control system communicates with the ITR through a common bus. This system contains the programs for highspeed post-processing of the MS/MS map results.

## Algorithm for mass assignments

The algorithm employed for ion mass assignments consists of three basic steps. First, the time-of-flight offset,  $t_{Off}$ , must be determined for the ions because equation (1.1) requires the real flight time of the ions (barring electrical delays, etc.). The user is prompted for two data points (assuming some knowledge of the data field),  $t_1$  and  $t_2$ , which are the flight times of two known stable masses in the field. These values are substituted into the following equations:

$$t_1 = k_1 m_1^{1/2} + t_{off}$$
 (2.5)

$$t_2 = k_1 m_2 1/2 + t_{off}$$
 (2.6)

$$t_2$$
- $t_1 = k_1(m_2^{1/2} - m_1^{1/2})$  (2.7).

Solving equation (2.7) for  $k_1$  and substitution into equations (2.5) or (2.6) will yield a close approximation to the  $t_{off}$  value. All flight times are then corrected in the data file.

An improvement on the values for  $k_1$  and  $t_{off}$  can be made at this stage. A TOF comparison is made for a **set** of known stable ions between the calculated and observed flight times. The expected TOFs are calculated using the approximate  $k_1$  and  $t_{off}$  determined above, and a regression is performed on **all** the observed stable ion flight times versus their  $m^{1/2}$  values. The regression yields more reliable  $k_1$  and  $t_{off}$  values. Subsequently all the flight times are corrected with the more reliable value for  $t_{off}$ .

The second step in the calibration or mass assignment process involves correction for the Hall probe measurement. Each data record contains a Hall voltage, a flight time, and an intensity and, thus, knowledge of the TOF values allows a regression on the stable ion *Hall voltages* versus  $m^{1/2}$  (linear relationship). This yields a *halloff* voltage which is used to correct all the Hall voltages in the data field.

The third and last step involves a determination of k3 from a modified version of equation (1.1) shown below:

$$m/z = (VHall, corr * timecorr) * k3$$
 (2.8)

where  $V_{Hall,COTT}$  is the corrected Hall voltage. A regression of the stable ion masses versus ( $V_{Hall,COTT}$  \*  $time_{COTT}$ ) yields a slope of k3 with an intercept very close to zero (within experimental error).

The Hall voltage and time correction factors along with the k3 value allow any ion in the MS/MS data field to be assigned a mass. Programs were written to display tables containing mass precision and accuracy determinations, thereby providing the operator with additional feedback on the quality of the mass assignments. The results of the programs for time-of-flight and magnetic field strength corrections are given in the following chapter.

# CHAPTER II

#### **REFERENCES**

- 1. Wiley, W.C.; McLaren, I.H., Rev. Sci. Instrum., 1955, 26, 1150.
- 2. Studier, M.H., Rev. Sci. Instrum., 1963, 34, 1367.
- 3. Herod, A.A.; Harrison, A.G., *Int. J. Mass Spectrom. Ion Phys.*, 1970, 4, 415.
- 4. Aviyente, V.; Shaked, M.; Feinmesser, A.; Gefen, S.; Lifshitz, C., Int. J. Mass Spectrom. Ion Phys., 1986, 70, 67-77.
- 5. Stults, J.T.; Holland, J.F.; Watson, J.T.; Enke, C.G., *Int. J. Mass Spectrom. Ion Processes*, 1986, 71, 169.
- 6. Stults, J.T., Ph.D. Thesis, Michigan State University, 1985.
- 7. Eckenrode, B.A.; Watson, J.T.; Enke, C.G.; Holland, J.F., *Int. J. Mass Spectrom. Ion Processes*, 1988, 83, 177-187.
- 8. Fowler, T.K.; Good, W.M., Nucl. Instrum. Meth., 1960, 7, 245.
- 9. Cameron, A.E.; Eggers, D.F., Rev. Sci. Instrum, 1948, 19, 605.
- 10. Takekoshi, J.; Turuoka, K.; Shimizu, S.; Bulletin of the Institute for Chemical Research, Kyoto University, 1951, 27, 52.
- 11. Wolff, M.M.; Stephens, W.E., Rev. Sci., Instrum., 1953, 24, 616.
- 12. Bakker, J.M.B., J. Phys. E: Sci. Instrum., 1973, 6, 785.
- 13. Bakker, J.M.B., *J. Phys. E: Sci. Instrum.,* 1974, 7,364.
- 14. Private Communication
- 15. Pinkston, J.D., *Ph.D. Thesis*, Michigan State University, 1985.
- 16. Pinkston, J.D.; Rabb, M.; Watson, J.T.; Allison, J., *Rev. Sci. Instrum.*, 1986, 57, 583.
- 17. Forth Inc., Hermosa Beach, CA 90254, U.S.A.
- 18. Stults, J.T.; Meyerholtz, C.A.; Newcome, B.H.; Enke, C.G.; Holland, J.F., *Rev. Sci., Instrum.*, 1985, 56, 2267.

#### CHAPTER III

## MASS ASSIGNMENT CAPABILITY OF TRIMS

Keep pace with the drummer you hear, however measured or far away.

Henry David Thoreau

#### Introduction

The measurement of the fundamental properties of momentum (mv) and velocity (v) for a particular ion yields its mass [1-3]. TRIMS allows the simultaneous measurement of an ion's momentum and velocity by a combination of magnetic dispersion and TOF analysis [4].

## Theoretical principles

The momentum measurement of the magnetic sector can be combined with the velocity measurement of TOF to yield any ion's mass independent of its energy. The mass relationship can be derived as follows:

$$mv = Bzk_1 \tag{3.1}$$

$$V = (1/\hbar)k_2$$
 (3.2)

and dividing equation (3.1) by (3.2) yields

$$m/z = Btk3 \tag{3.3}$$

where m is the ion's mass, B is the magnetic field strength, z is the charge, and t is the time-of-flight of the ion. The electronic charge, e, the ion flight path length,

d, and the radius of the magnetic sector, r, are incorporated into the three constants  $k_1$  (et),  $k_2$  (d), and  $k_3$  ( $k_1/k_2$ ). The resulting mass relationship is energy independent.

An important consequence of the energy independent mass determination is the capacity to accurately assign the mass for stable ions (those ions which do not change mass after acceleration from the source of a mass spectrometer) as well as metastable or daughter ions which change mass in the first field-free region between the ion acceleration region and the magnetic sector. This capacity for accurate mass assignment is important in mass spectrometry/mass spectrometry (MS/MS) which involves collisionally activated dissociation (CAD) of parent ions in the first field-free region to yield ions of different mass and energy. The nature of the fragmentation event can provide information about the parent ion structure, but it is imperative that the proper mass be assigned to the fragment (daughter) ions.

# Translational energy loss independence

Translational energy losses can occur with CAD resulting in inaccurate mass assignment of daughter ions for instruments with energy dependent (e.g. an electric sector) daughter ion mass determinations [5,6]. The energy independence due to the simultaneous measurement of velocity and momentum avoids mass assignment errors due to translational energy losses. For high mass compounds subjected to CAD for structure determination the variation in energy loss can be quite large (100 eV). It was found that the translational energy loss was different for different fragment ions formed from a given parent ion even under single collision conditions [5]. Since all fragment ions are not

characterized by the same energy loss, complicated scan laws are required in four-sector MS/MS instruments to assess parent-daughter relationships. The TRIMS instrument should assign the mass of an ion regardless of its translational energy loss.

# Mass assignments in magnetic sector instruments

Mass assignments on a single-focusing magnetic sector mass spectrometer are hampered by a spread of ion energies in the ion source. Typically the accelerating voltage is made very large to make the relative ion energy spread small. Nevertheless, the small variations in the energy of the ions leads to variations in their velocity which affect the precision with which their momentum can be determined. If greater energy variations occur, for example, in the field-free region preceding the magnet from either unimolecular dissociation and/or CAD, the problem is further exacerbated. Any other energy variations due, for example, to a particular ionization method such as fast atom bombardment, leads to a further decrease in the capacity of the instrument to obtain accurate assessment of an ion's mass.

# Mass assignments in time-of-flight instruments

Time-of-flight instruments suffer greatly from ion energy differences in the source [7]. Spatial and initial energy effects lead to reduced resolving power in TOF instruments due to the increased velocity spreads. The mass relationship in a TOF mass spectrometer indicates that the mass assignment is dependent on an ion's energy (as with the magnetic sector mass spectrometer). Any uncertainty in the ion's energy thus leads to a reduced precision in the assignment of its mass.

Independently, a TOF analyzer cannot separate ions that have changed mass while in the field-free flight tube from those that have not. The daughter ions travel with approximately the same velocity as their parent and their detection becomes superimposed on that of their parent ions. The greater distribution of energies among the daughter ions leads to broadened peaks in a TOF spectrum. The mass assignment for the daughter ions cannot be determined utilizing the classical field-free concepts of TOF-MS [8].

## PRECISION AND ACCURACY MASS ASSIGNMENT RESULTS

# Stable ion Mass Assignments

Several complete MS/MS data field acquisitions were performed on n-decane under unit mass resolution conditions in both momentum and velocity. From these data it was possible to calculate precision and accuracy for the measurement process. Each structure map consists of stable and daughter ions, all of which require accurate mass assignment. An example of the computer output for an n-decane map is shown in Table 3.1. This is a 30 second MS/MS data field acquisition with the resultant mass assignment errors shown. In this 30 second time span all the daughter ions of all the parent ions in n-decane were recorded. The composite results of eleven complete fragmentation maps for stable ion mass assignments are shown in Table 3.2. Relative standard deviation (RSD) values for the mass assignments are typically less than 0.20 % with relative mass assignment errors not exceeding 3 parts per thousand (ppt).

TABLE 3.1
STABLE ION MASS ASSIGNMENTS

ACTUAL MASS	MEASURED MASS	MASS ERROR	CORRECTED HALL	CORRECTED TIME (µs)	RELATIVE INTENSITY
29.039	29.079	0.0401	524	10.038	8146
43.055	42.988	-0.0672	636	12.228	19796
57.070	57.054	-0.0155	733	14.083	26408
71.086	71.103	0.0168	818	15.728	8991
85.101	84.968	-0.1335	894	17.198	6085
99.117	99.094	-0.0232	966	18.563	3023
113.133	113.156	0.0230	1033	19.823	2764
142.172	142.167	-0.0048	1158	22.218	3097

 $t_{\text{Off}} = 0.2969$ 

Halloff voltage = -21.474

 $k_3 = 0.00552$ 

TABLE 3.2

STABLE ION MASS ASSIGNMENT PRECISION AND ACCURACY

MASS	RSD (%)	RELATIVE MASS ERROR (ppt)
29.039	0.07	1.4
43.055	0.09	0.8
57.070	0.07	1.3
71.086	0.11	1.8
85.101	0.06	2.1
99.117	0.09	1.2
113.133	0.12	1.0
142.172	0.06	0.4

The precision of the Hall voltage, time, and  $k_3$  values can easily be assessed from the eleven maps. The  $k_3$  value was found to be 5.50 x 10<sup>-3</sup>  $\pm$  0.00002 da  $\mu$ sec<sup>-1</sup> fsu<sup>-1</sup> (fsu = magnetic field strength units) with an RSD of 0.24 %. All Hall voltage measurements were reproducible to 0.25 %. The time-of-flight measurement reproducibility was slightly better with a resulting RSD of 0.15 %. As shown in Table 3.2, the combination of Hall voltage (momentum) and time-of-flight (velocity) measurements resulted in high precision and accuracy.

## THE ADVANTAGES OF TRIMS FOR MASS ASSIGNMENTS

The fundamental measurements of momentum and velocity provide an improved approach to mass spectrometer calibration. Typically, with magnetic sector or TOF mass spectrometers an empirical calibration is performed with a compound that fragments in a known and reproducible manner. The instrument is empirically adjusted to allow mass assignments under the assumption of constant ion energy. Metastable and CAD ions are by definition not directly assignable under these conditions. The TRIMS instrument has a unique advantage with its capacity to distinguish ions that result from unimolecular and/or CAD processes and assign their mass even if they have a significant energy spread. Stable and daughter ion profiles do not overlap with each other. Energy independence for the mass assignments is not possible in typical magnetic or TOF instruments.

# Calibration simplicity

Conversion of the entire MS/MS map to accurate masses is simplified with the TRIMS approach. Only three values are required to calibrate both the magnetic and TOF data fields: k3, toff, and Halloff voltage. This fact is borne out by the linearity observed in the time-of-flight and *Hall voltage* versus *mass* 1/2 plots. The residuals observed in both the time and Hall analyses are of sufficient variability and small magnitude to indicate lack of trends in the data. Since only these values are required, substantial improvements in speed of the mass determination are possible. Thus, an overall calibration process is much easier than with conventional approaches.

## CHAPTER III

## **REFERENCES**

- 1. Volkov, V.V. Nucl. Instr. Meth. 1979, 162, 623-636.
- 2. Betts, R.R. Nucl. Instr. Meth. 1979, 162, 531-538.
- 3. Purser, K.H.; Litherland, A.E.; Gove, H.E. *Nucl. Instr. Meth.* 1979, 162, 637-656.
- 4. Stults, J.T.; Holland, J.F.; Enke, C.G. Anal. Chem. 1983, 55, 1323-1330.
- 5. Sheil, M.M.; Derrick, P.J. Org. Mass Spectrom. 1988, 23, 429-435.
- 6. Bricker, D.L.; Russell, D.H. J. Am. Chem. Soc. 1986, 108, 6174-6179.
- 7. Wiley, W.C.; McLaren, I.H. Rev. Sci. Instrum., 1955, 26, 1150.
- 8. Shannon, T.W.; Mead, T.E.; Warner, C.G.; McLafferty, F.W. *Anal. Chem.* 1967, 39, 1748-1754.

#### CHAPTER IV

#### MS/MS ON THE CHROMATOGRAPHIC TIME SCALE

What lies behind us and what lies before us are small matters compared to what lies within us.

Ralph Waldo Emerson

## Introduction

As the problems facing analytical chemists become more and more complex, the demand is increasing for instrumentation that can provide lower limits of detection, greater selectivity, and structure-related information in a shorter period of time, especially during the analysis of transient samples [1,2]. MS/MS, by its multidimensional nature, has proven to be a key instrumental technique for many analytical problems. If chromatography is used to separate mixture components and deliver pure compounds to the ion source in sequence, the combination of GC and MS/MS, (GC-MS/MS), offers the potential to obtain extensive fragmentation information on each component. This potential for GC-MS/MS has not heretofore been realized because collecting the full MS/MS data field on the time scale of a packed column chromatographic peak requires an instrument with very rapid collection of mass spectral data and high sensitivity. If packed or wide-bore capillary chromatographic columns are used, the complete MS/MS data field must be obtained in times from two to twenty seconds. Conventional tandem mass filter instruments have not provided the data rates necessary for acquisition of the complete MS/MS data field on the chromatographic time scale. Figure 1.7 of chapter one illustrates the strategies required by conventional MS/MS instruments to collect a complete MS/MS data field. This figure is an indication of the inherent shortcomings of these instruments with regard to data acquisition due to the need for multiple scanning of analyzers for MS/MS analysis.

Although an additional dimension of selectivity can be obtained with MS/MS, discrete MS/MS scans (e.g., a daughter scan of a particular parent ion) remain insufficient for identifying a compound. Quite often complex structure elucidation problems require the maximum amount of spectral information available on a compound. For MS/MS this can mean measurement of all daughter ions of all parents, i.e., the complete data field. When all the parent ions of a compound are subjected to collisionally activated dissociation (CAD) an array of daughter ion spectra can be collected to provide a complete fragmentation map. From this data matrix specific mass spectral information can be extracted. For example, parent, daughter, and neutral loss scans can be reconstructed. The added dimension of information in the MS/MS data field can provide an analyst with empirical verification for a proposed arrangement of substructures within an unknown molecule and thus can facilitate an overall structure determination. All this information is available after a single experiment and the analyst is relieved from the concern of acquiring more measurements in real-time.

TRIMS answers the chromatographic challenge discussed above. A schematic representation of the second generation TRIMS instrument employing post-sector beam deflection is shown in Figure 2.10 of Chapter two. This figure is a modified version of Figure 1.10. The improved version has enabled the

exploration of high speed GC-MS/MS analyses by removing the limitations of the first generation TRIMS instrument.

#### TRIMS WITH TIME-ARRAY DETECTION

Connecting the output of the TRIMS instrument to the ITR allows for high speed GC-MS/MS analysis. The maximum rate for generation of TOF spectra is 10 kHz. The minimum number of transients that can be summed is 10 due to computer constraints. Therefore, the instrumental limit for the acquisition of data on the time axis is 1000 TOF spectra/sec. If each TOF spectrum acquisition is to be correlated with a point on the scan of the magnet, the magnetic field scan rate will determine the resolution of scans along the magnetic field axis (see Figure 4.1). For example, if one wishes to scan the magnetic field axis (B) from mass 200 to 300 in *one* second, up to 1000 complete TOF spectra can be recorded over this mass range. If this resolution is greater than needed, the magnetic field scan rate could be increased to give multiple MS/MS spectra per second, or the number of TOF transients per TOF spectrum could be increased to improve the signal-to-noise ratio (S/N) of the data.

## Trade-offs for TRIMS-TAD in resolution, detectability and acquisition time

Because the ITR can collect spectra much faster than needed to represent the chromatographic fidelity with the stored information, the rate of spectra generation can be reduced by performing longer intervals of averaging, thereby enhancing other analytical parameters. The trade-offs for TRIMS-TAD in

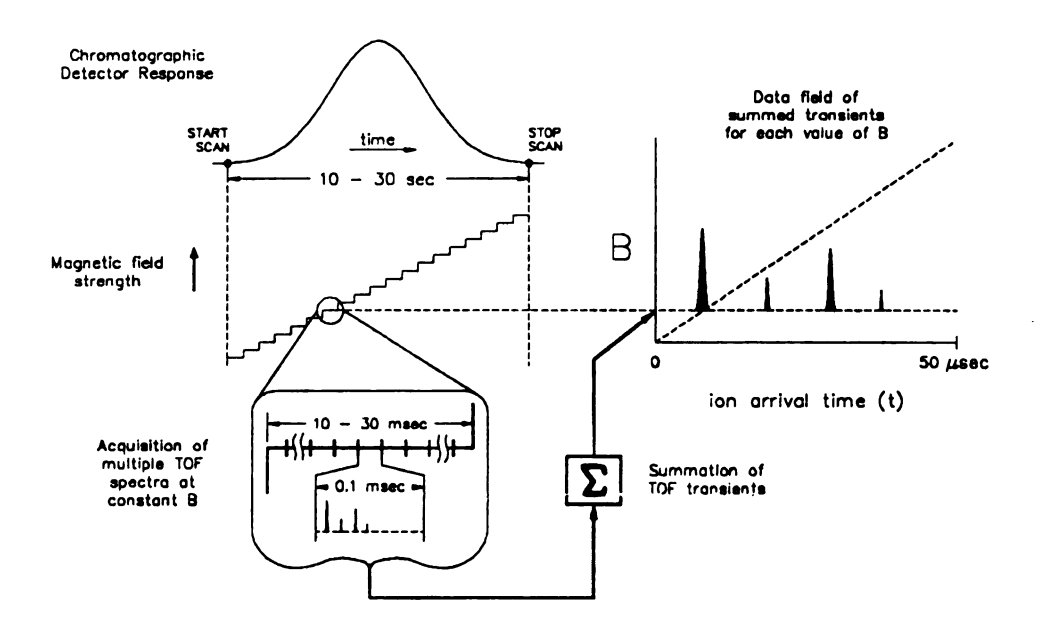


Figure 4.1 Detailed diagram of the *B-t* data field acquisition process. At each magnetic field strength increment, multiple TOF transients are summed to produce a scan. The full *B-t* data field thus consists of several scans for a single sweep of the magnetic field strength.

resolution, detectability and acquisition time can be related with the following equations:

(transients/scan)/(transients/sec) = sec/scan (4.1)

TOF scans/sweep = mass range/mass resolution (4.2)

mass range/mass resolution x sec/scan = sec/sweep (4.3)

where scan is defined as the summation of a number of transients, and sweep represents a single magnetic field transit over the desired mass range. Equation (4.1) is related to the S/N at each momentum setting. Equation (4.2) is related to the desired mass resolution and is dependent on the nature of the sample and the objectives of the analysis. Equation (4.3) represents the time for a complete MS/MS map acquisition with TRIMS-TAD and is determined by the temporal characteristics of the chromatographic analysis. For example, if one is limited to 10 seconds for a complete map acquisition and the desired mass range is 500 daltons with approximately unit mass resolution, then 20 msec per scan is available. In 20 msec at 10,000 transients/sec, 200 transients can be summed. The summation of two hundred transients provides a theoretical S/N improvement of approximately four over that with only 10 summed transients. Clearly, if better resolution or faster acquisition is desired, fewer transients can be summed.

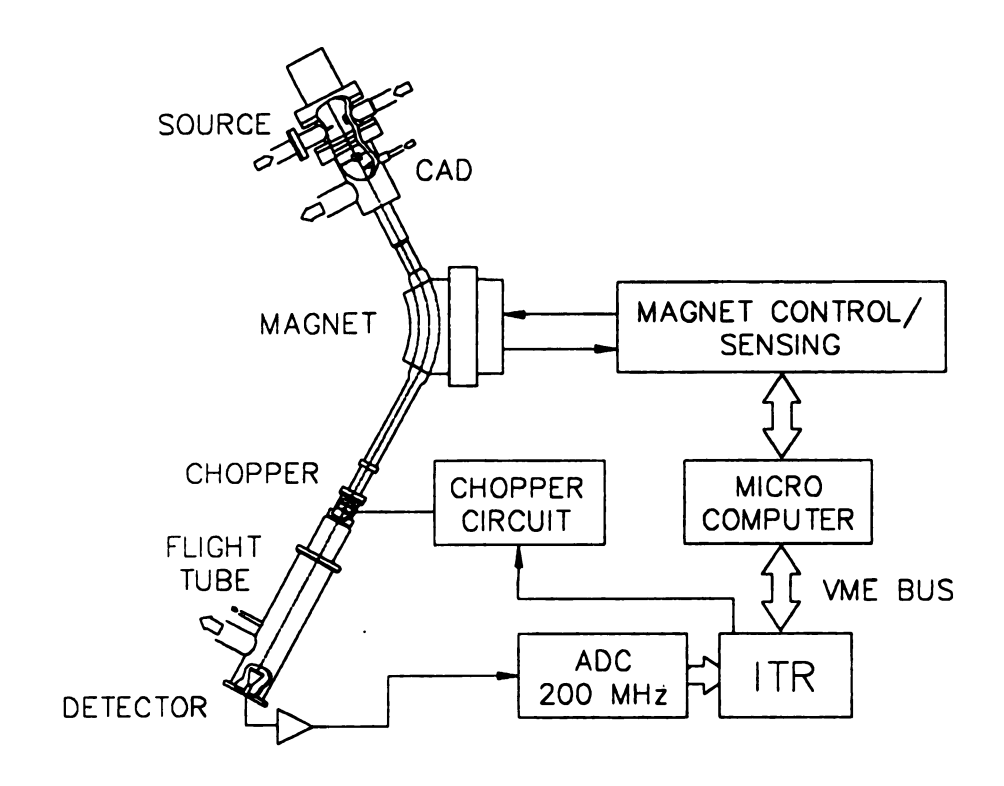
The potential for acquiring the entire MS/MS map on compounds as they elute from capillary columns may be realized on an instrument other than the LKB-9000 employed in this research. If wide-bore capillary chromatography is used, several MS/MS maps can be acquired and averaged over the elution of a single component. With improved ion sources and, thus, improved signal levels,

the time for an analysis can be reduced. Also, transient events in the source can be monitored more accurately and efficiently with improved instrumentation.

#### **INSTRUMENTATION FOR TRIMS-TAD**

A pulse from the ITR control circuitry is used as the trigger for deflection of the ion beam; in this way synchronization of data generation and acquisition is established. A block diagram of the TRIMS-TAD configuration is shown in Figure 4.2. The DAC and ADC described in Chapter two provide control/sensing for the magnet and an interface to a status-in, command-out board allows incrementing/sensing of the magnetic field after each scan file has been prepared. The output current of a channel electron multiplier array (CEMA) is amplified by a model 342 wideband non-inverting DC-coupled current amplifier (Analog Modules, Inc., Longwood, Fla.) in tandem with an inverting CLC 220 DC amplifier (Comlinear Corp., Loveland, CO). The second amplifier serves to provide the ITR with the proper signal polarity and also increases the gain. The signal is terminated with 50 ohms at the ADC input of the ITR.

The interface, discussed in Chapter two, between the Hall probe and the ITR was constructed to remove the step-function inherent with DAC control of the magnet. This allows the magnet to be scanned in its conventional manner. Transient summation occurs on a much faster time scale than the magnet sweep through a magnetic field range encompassing one dalton and therefore a factor of approximately four in speed is gained relative to DAC operation.



<u>Figure 4.2</u> A schematic of the TRIMS-TAD instrument. The TAD data system is comprised of an integrating transient recorder (ITR) and control hardware.

#### The ITR

The core of the ITR consists of a flash ADC with high-speed sum and store circuitry. Figure 4.3a illustrates the main features of the ITR data system. All modules communicate over a common An 8-bit 200 bus. megasample/second ADC (LeCroy Research Corp., Spring Valley, N.Y.) digitizes the transient data. An ADC of 8-bit resolution is sufficient for this application since the arrival at the detector of more than 15 ions (each accounting for approximately 15 ADC counts) in 5 nsec is not likely to occur. The custom sum and store circuitry contains two banks of memory and adders as shown in Figure 4.3b. This circuitry sums the ion current at each arrival time following each deflection of the ion beam for a preset number of digitized transients. The summing circuitry can sum from 10 to several thousand complete TOF spectra employing high speed emitter-coupled logic (ECL). While one bank of memory (random access memory (RAM) A or RAM B in Figure 4.3b) collects and sums successive transients, the other bank transfers the previous summed spectrum (scan file) to the reduction hardware [3]. As the ITR continuously collects the ion current in each transient with 5nsec resolution over an 80 µsec range, all the spectral information from each pulse is recorded.

The number of transients to be summed, scans (magnet increments) to be collected, and mass range per transient (related to the TOF for the ions of interest) are pre-determined and input into a parameter file for the ITR. A VME 68000 based (Motorola,Inc.) control system communicates with the ITR through a common bus as illustrated in Figure 4.3c. Dual-ported RAM provides data rate advantages and facilitates the data reduction process. Raw data are stored on a 300 Mbyte (Priam, Inc.) hard disk and post-processing is performed in software.

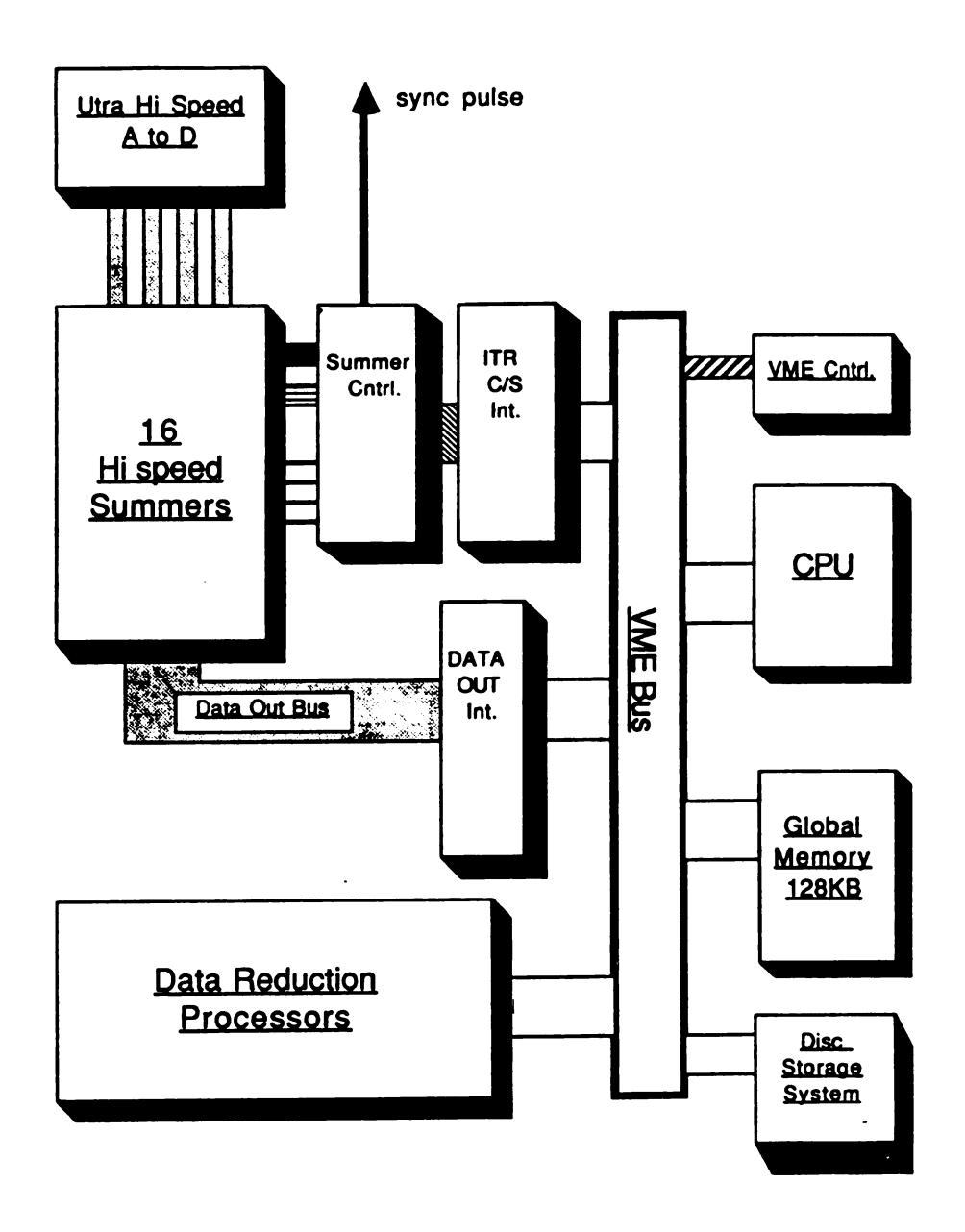


Figure 4.3 a The ITR data system consists of several modules which all communicate over a VME bus. Data flow begins at the top with transient digitization and summation occurring via "command-status" control modules. The data-out board can move data across the bus to a reduction module or to disk for storage.

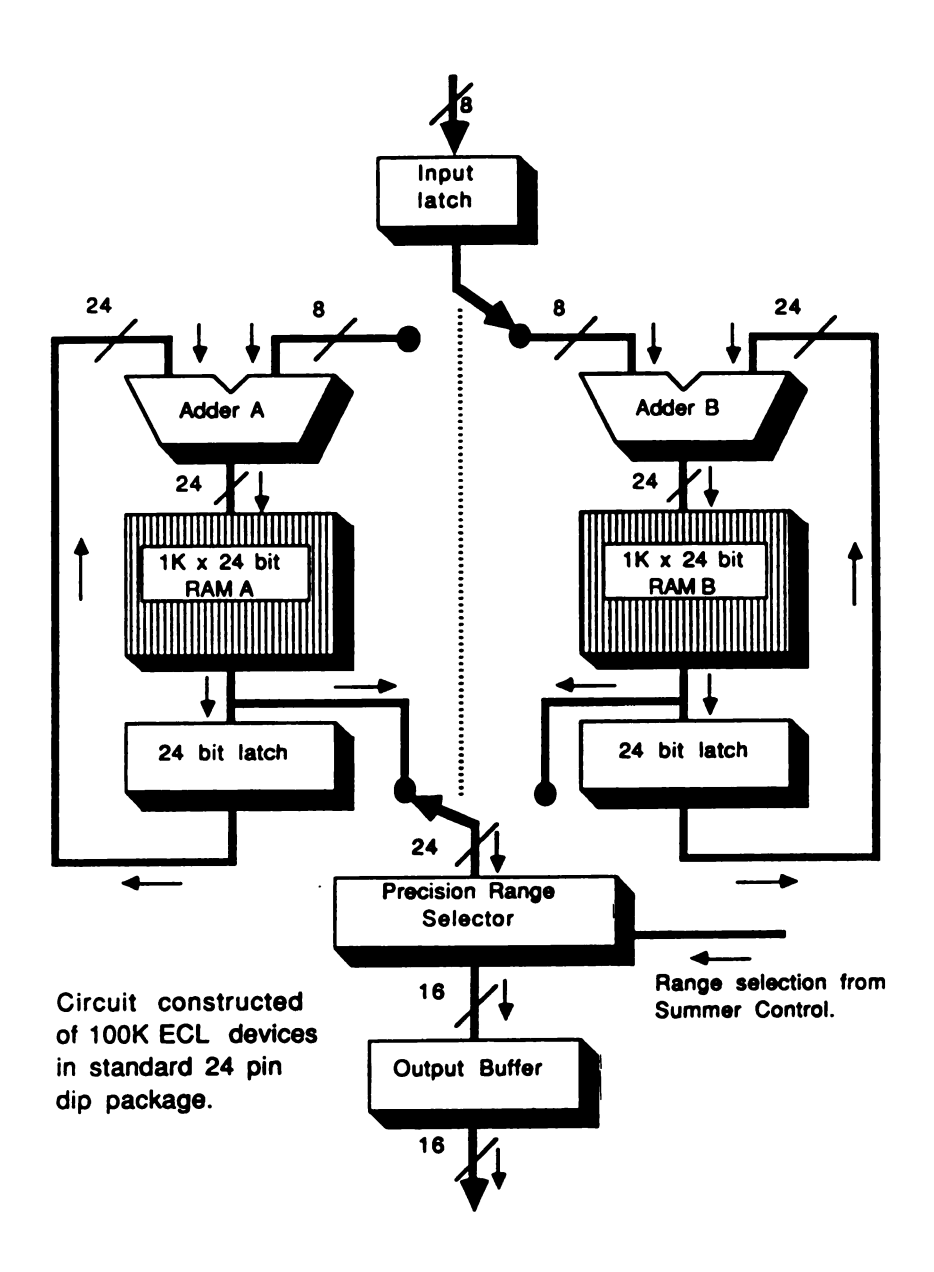
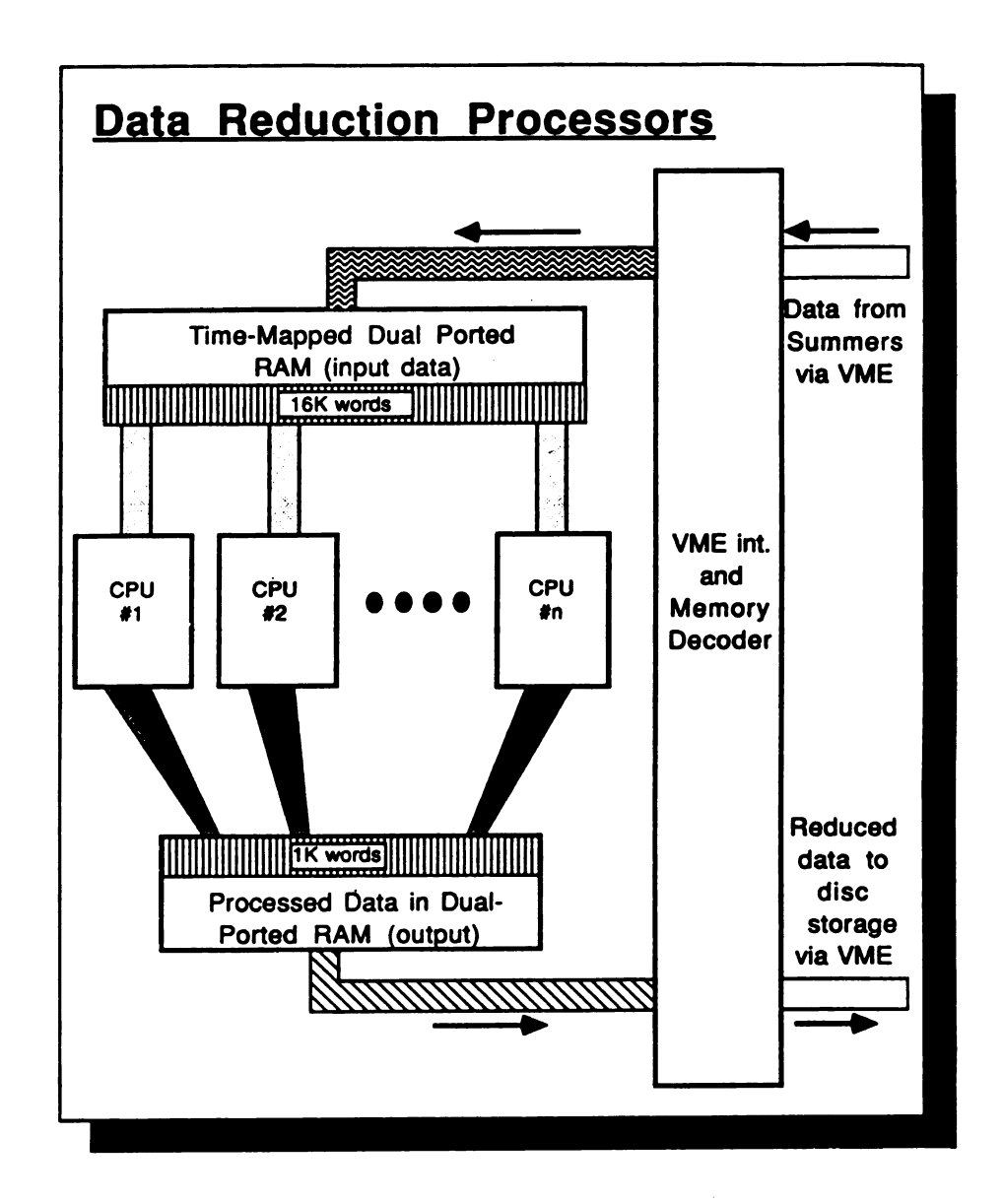


Figure 4.3 b The custom sum and store circuitry module of the ITR data system. Each bank contains an adder, RAM (1K x 24-bit) and a 24-bit latch. One bank sums successive transients while the other bank outputs the previously summed spectrum to the reduction hardware or storage.



<u>Figure 4.3 c</u> The data reduction processor module of the ITR data system. RAM is configured so that specific addresses correspond to specific time windows. This time-mapped memory is operated on by several contral processing units (CPUs) in parrallel. The Hall voltage value is read from the VME bus via the TRIMS-ITR Hall interface board. The processed data are then moved to storage in a Hall voltage, flight time, intensity triplet format.

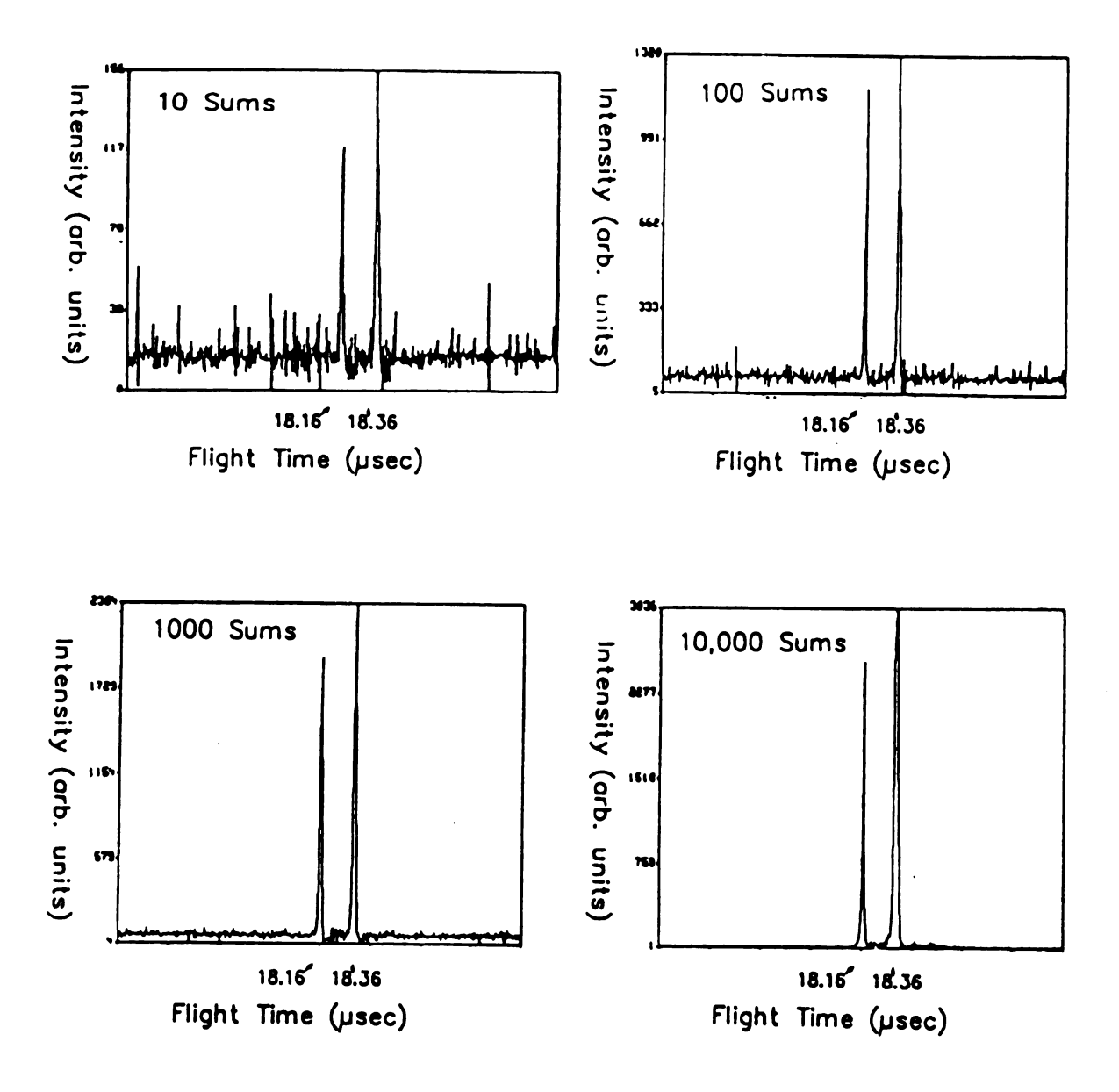
Data reduction to triplets (Hall voltage, flight time, intensity) can be performed in real-time by parallel processing with three VME133A 20 MHz (Motorola, Inc.) microprocessors on a common bus. Time centroiding and peak integration is performed "on the fly" in the parallel processing mode.

An example of the summation capability of the ITR is shown in Figure 4.4. The 90+ stable ion and the 92+-->91+ metastable decomposition of toluene were monitored with different periods of transient summation. This figure shows a definite reduction in noise when comparing the summation of 10 transients and 1000 or 10,000 summed transients. A plot of the S/N for mass 41 of n-decane versus the square root of the number of transients summed is shown in Figure 4.5. If the noise is truly random, then the S/N should increase linearly with the square root of the number of summed transients. The relationship observed approximates linear behavior, and thus, agrees with statistical theory.

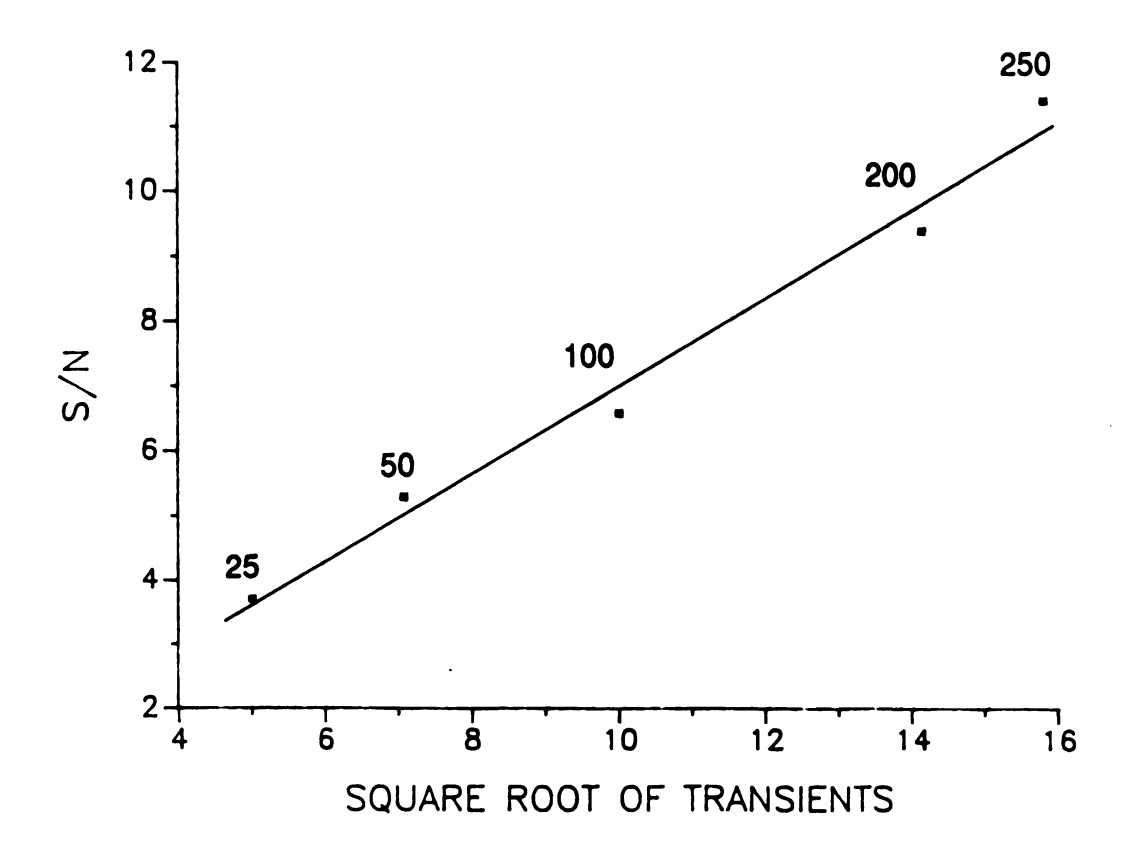
## Experimental Setup for TRIMS-TAD

The ion source pressure for steady state samples leaked into the instrument was typically 1.2 x 10-6 torr measured by a Penning gauge directly below the source housing and the source temperature was 230 C. The trap current was 60  $\mu$ A and the accelerating voltage was 3500 V. The front plate of the CEMA detector was typically maintained at a setting of 7 corresponding to a voltage of -2.65 kV.

The compounds analyzed were from Chem Service (West Chester, PA) and not further purified. Compounds were introduced either via a heated gas



<u>Figure 4.4</u> Transient summation capability of the ITR. The magnet is set to pass ions of mass 90 and the stable ions at this mass are observed (at 18.16  $\mu$ sec) as well as the 92 to 91 metastable ions (at 18.36  $\mu$ sec). Different numbers of sums (as indicated) were acquired and compared.



<u>Figure 4.5</u> S/N versus the square root of the number of summed transients for mass 41 of n-decane. Each data point was determined from the average of three separate measurements of the variation in the ion peak height. The reciprocal of the peak height relative standard deviation is the S/N value.

inlet or a gas chromatograph. The column used was a methyl silicone wide-bore capillary column (5m x 0.53mm x 2.65 $\mu$ m). The capillary column was fitted to the LKB-9000 with a conversion kit purchased from Supelco, Inc. (Bellefonte, PA).

CAD was accomplished by adding helium through a collision cell located in the first field-free region of the just beyond the source slit of the mass spectrometer. The ion beam represented by the base peak of n-decane was reduced to approximately 70 percent of its intensity by adjusting the helium gas pressure before the GC-MS/MS map acquisitions were started.

#### **MULTI-DIMENSIONAL DATA PRESENTATION**

After an MS/MS data map for n-decane (unimolecular decompositions) was acquired there was a need for a convenient means of determining where in the large data field significant fragmentation reactions might be found. One way to view the data and locate scan files that contain relevant information is to plot the maximum minus the minimum intensity within each scan versus scan number producing a function which resembles a total ion current plot. The scan number directly corresponds to a position on the magnetic field axis.

## Graphical Display Algorithm

Peak-finding is done on the VME system and subsequently the data are downloaded to an IBM-AT for further processing. A three-dimensional (3D) plotting algorithm facilitates display of the MS/MS data. Software was written to

present the data in a graphical form with the perspective viewing capability. The tri-dimensionality of the data require its presentation on a two-dimensional xy plane with intensity projecting into the z direction.

In representing the MS/MS data field, commercial software packages were only able to handle a data grid measuring 100 x 100. Even with such a limited grid size, several hours were required to perform the necessary calculations. The graphics software developed in our lab can accept data grids typically as large as 1000 x 1000 with display generation execution time on the order of seconds. The algorithm rapidly draws the data on an xy plane using the appropriate product of the respective x, y, and z rotational transformation matrices (see Figure 4.6). The original coordinates are represented as [x,y,z] while the transformed coordinates are [x,y,z]'.

The general transformation matrix [C] is given by the following equation [4]:

## [C] = [S][RZ][RX][RY][T]

The coordinates 0,0,0 are assigned to the center of the grid and the x, y, and z axes will all intersect at this point. The program accepts values for the grid rotation and the tilt after rotation. The x, y, and z scaling factors elongate or reduce the grid in those respective dimensions while translation factors perform global grid shifts.

The software permits multiple variables governing tick mark frequency, tick mark length, axis label sizes and placement, grid line frequency, global scaling, and data thresholding. The software will accept user supplied vectors in an ASCII file in the x y z data space. This allows generation of isomass lines or

## x y z transformation matrices

<u>Figure 4.6</u> These are the rotation matricles which transform the original x, y, z data coordinates. For the RX, RY or RZ matricles the x, y, and z values are in radians.

S = global scaling factor

T = absolute x, y, z global translation constant

other user defined annotations. The output can be sent to a HPGL (Hewlett Packard Graphics Language) compatible output device or to a file for later inclusion into documents. Companion programs allow limited editing of the data and transforming the graphical output to a standard format acceptable to most computer-aided design software for more intricate manipulations. The 3D display software is written in the C and assembly programming languages and requires an IBM or compatible microcomputer with at least 256 Kb of memory, an enhanced graphics adaptor card, and a color monitor.

#### TRIMS-TAD INSTRUMENT ASSESSMENT

Evaluation of the TRIMS-TAD instrument was performed in two stages. Confirmation of MS/MS data quality was assessed with n-decane; data integrity and speed were assessed with n-decanol. Both analyses were performed under raw data field acquisition (inherently slower than real-time peak-finding) conditions. N-decane was selected because a large number of metastable ions have been observed for this compound. The n-decane sample was introduced into the mass spectrometer at a constant rate via the heated inlet. This established an approximately constant sample pressure which lasted for several minutes before more sample was required. Under these conditions the TRIMS-TAD instrument was evaluated for daughter ion detection, mass range, and signal-to-background capabilities.

## MS/MS data quality determination

The complete MS/MS data field was collected for n-decane; 1280 scans were acquired at regular intervals along the magnetic field axis for a mass range of 15-150 daltons (with the magnet under DAC control). The ITR summed 200 transients at each magnetic field strength to provide a good signal-to-background (S/B) ratio. The complete MS/MS field was acquired in 30 seconds. A plot of the maximum minus the minimum intensity versus scan number is illustrated in Figure 4.7.

Scans taken at three different magnetic field strength values are shown in Figures 4.8a-c. Scans 599 (Figure 4.8a) and 973 (Figure 4.8b) show only one peak each at m/z 56 and 100, respectively, representing stable ions. Scan 474 (Figure 4.8c) shows two peaks; the first corresponds to a stable ion of mass 44, the second (at longer arrival time) corresponds to the metastable decomposition of m/z 113 to m/z 71 at an apparent mass of approximately 44.

Each of the scans shown provide information on the performance of the TRIMS-TAD instrument. The stable ions at mass 56 and 100 are found in a conventional mass spectrum of n-decane to be approximately 40% and 1% of the base peak, respectively. The same relative intensities are observed with the TRIMS-TAD instrument. In addition, the background is expected to be low due to the MS/MS measurement process [5] and consequently the S/B is very good. The stable and daughter ions observed in Figure 4.8c indicate the mass range potential of the ITR. A 40 μsec scan interval is illustrated, but the full time-array capability extends to 80 μsec (a mass range of approximately 1000 daltons) with 5 nsec resolution making it superior to current spatial array detectors. The range

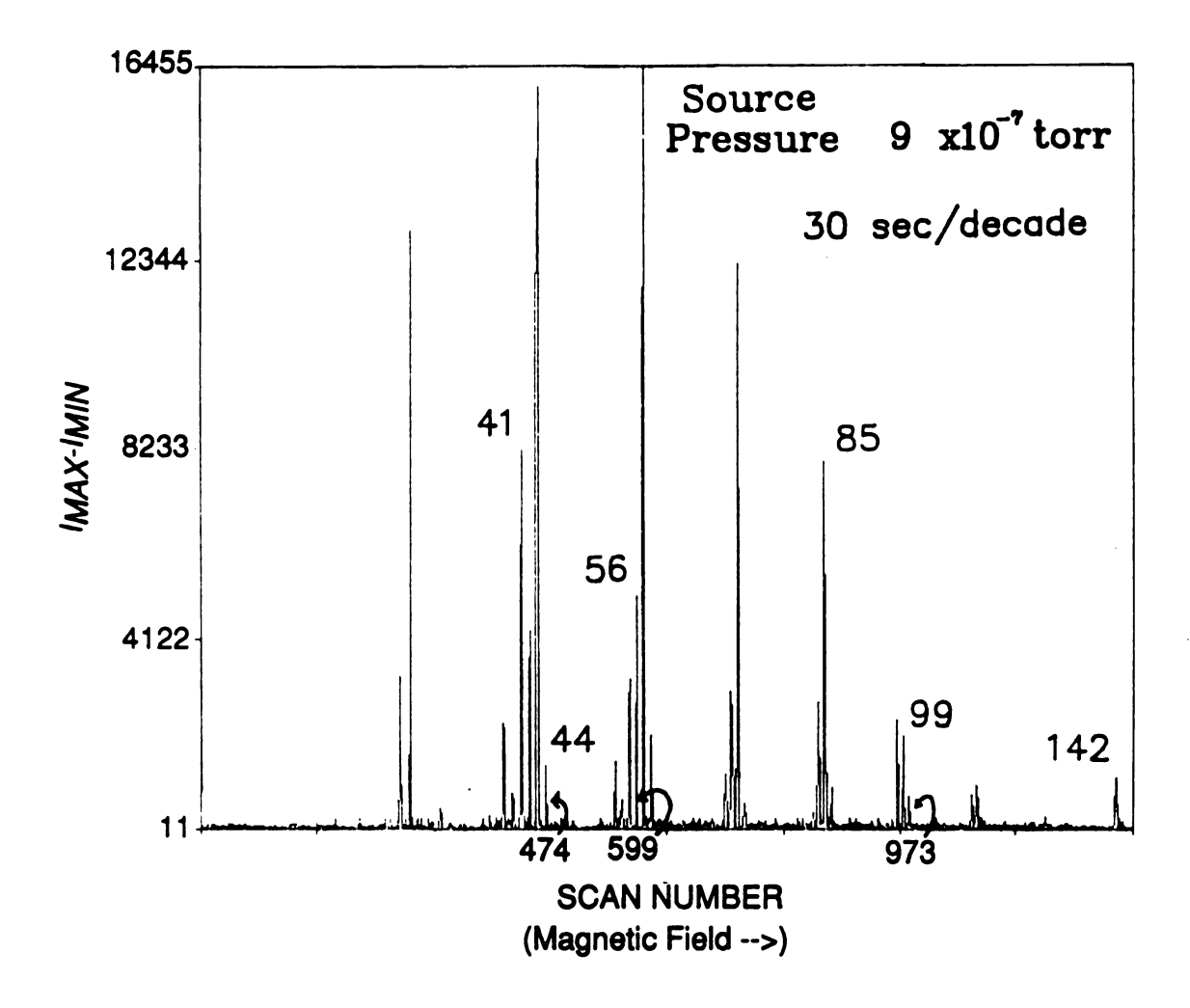


Figure 4.7 Composite plot of IMAX-IMIN (the "total ion current") as a function of the magnetic field strength. At each value of the magnetic field strength the difference between the maximum and the minimum intensity is plotted. This type of plot is convenient for examining the full MS/MS data field.

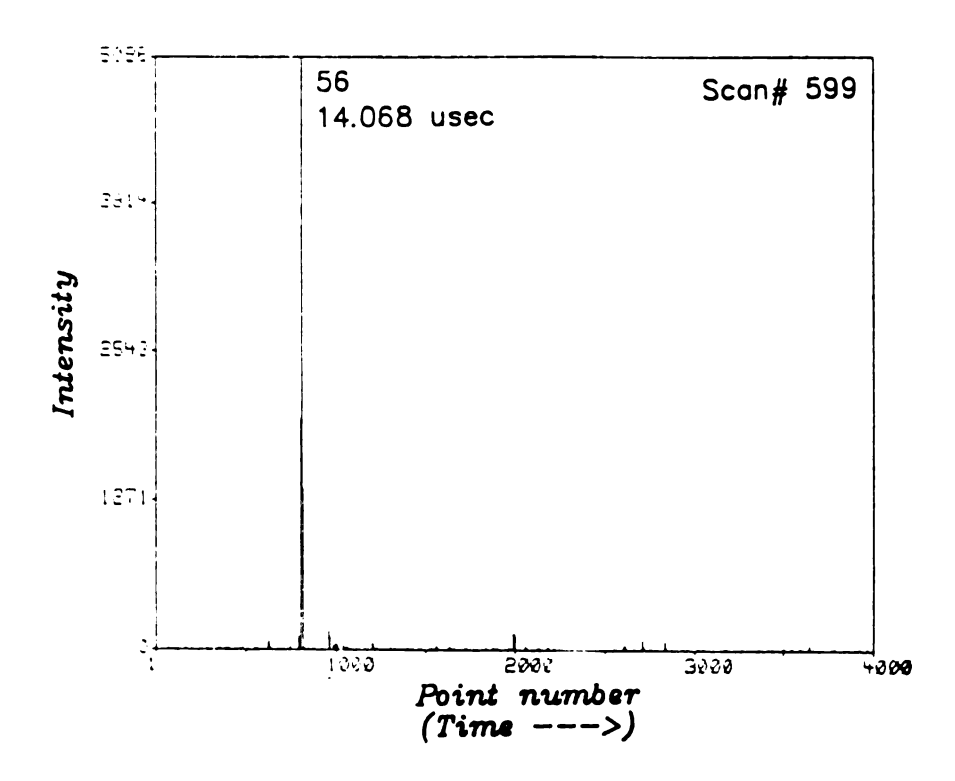


Figure 4.8 a Scan #599 was selected from the composite data of Figure 4.7. This scan shows a peak at m/z 56 for a stable ion.

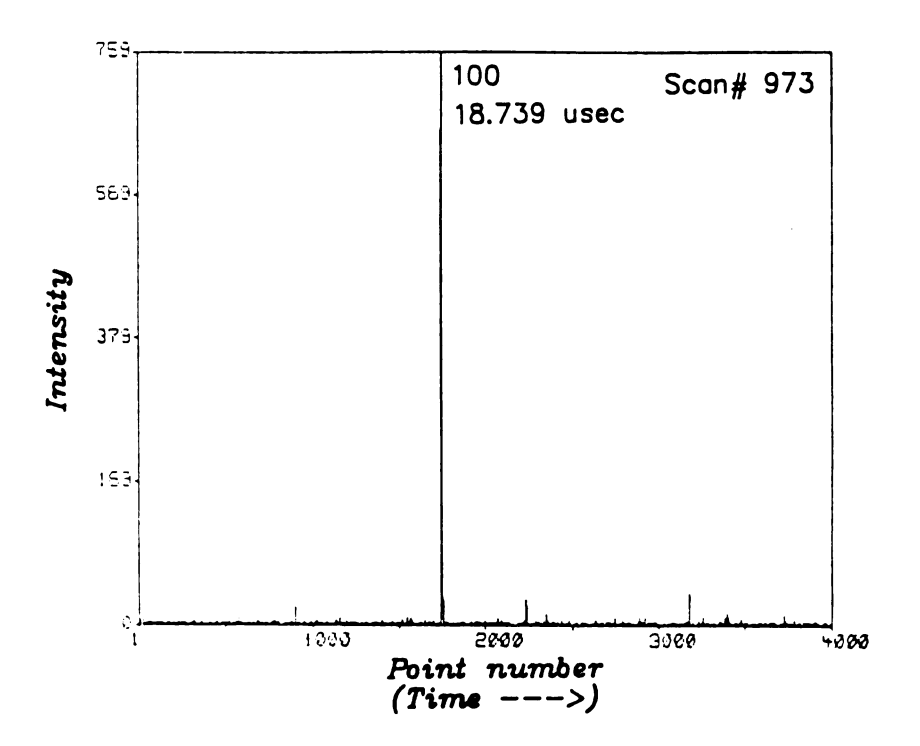


Figure 4.8 b Scan #973 was selected from the composite data of Figure 4.7. This scan was selected to observe the signal-to-background for ion current of reasonably low intensity at m/z 100.

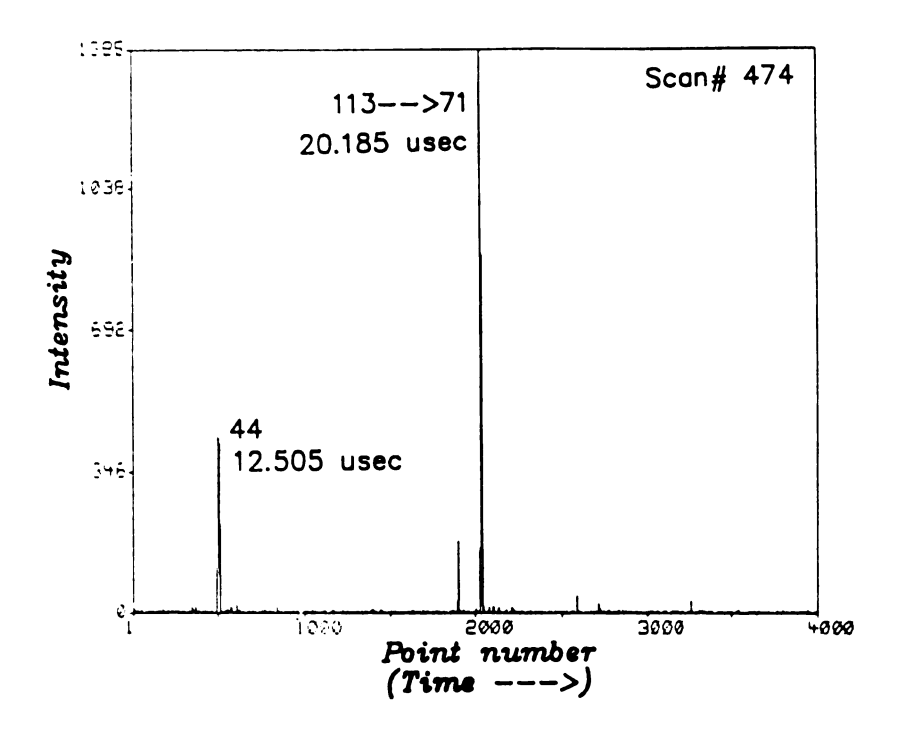


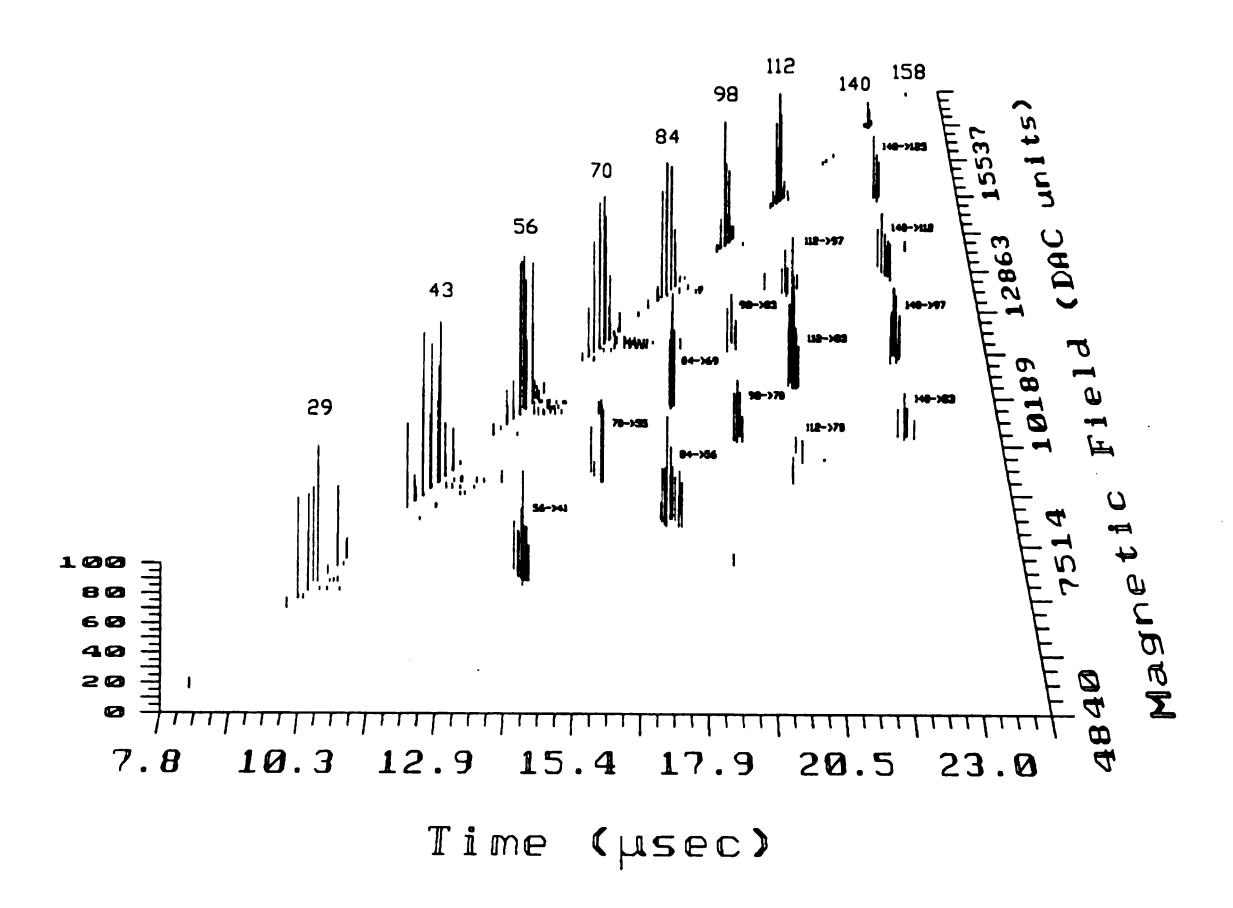
Figure 4.8 c Scan #474, also selected from the data in Figure 4.7, shows a peak at m/z 44 for a stable ion, as well as a peak at nearly the same m\* value which corresponds to the metastable reaction 113 --> 71.

of the TOF acquisition will depend on the highest mass anticipated for a compound and is user defined. These data also indicate from the high S/B that fewer transients could have been summed (equations 4.1-4.3) and, thus, the total MS/MS map acquisition time could have been reduced by approximately a factor of three. For this steady state sample, the acquisition time was not a concern and the 30-second acquisition time for this MS/MS map was quite sufficient for the initial assessment of TRIMS-TAD.

## MS/MS data integrity and speed assessment

Data integrity and speed of the complete MS/MS data field acquisition were studied with the unimolecular decompositions of n-decanol. Farncombe and co-workers [6] had successfully mapped the fragmentation reactions of this compound employing a forward geometry double-focusing mass spectrometer; these data provided a good basis of comparison for the TRIMS-TAD study.

The results for the MS/MS map acquisition for n-decanol under steady state conditions are shown in Figure 4.9. The large data field presented was drawn using the graphical algorithm discussed earlier. This is a tilted view with perspective of the full field with the masses and observed reactions (see Figure 4.10) labeled. The mass range is slightly greater than one decade (15-168 daltons); the magnetic field strength was controlled by the DAC. The acquisition time was 43 seconds as compared to the several minutes required by Farncombe and co-workers [7,8]. Under raw data acquisition conditions (no real-time peak finding) this experiment produced 12.1 Mbytes of data, forcing the disk controller to operate at a sustained data rate of 2.26 Mbits/sec.



<u>Figure 4.9</u> Complete unimolecular fragmentation field observed for n-decanol. The daughter (metastable) ion intensities have been multiplied by five.

Figure 4.10 Postulated fragmentation reactions in n-decanol.

All of the reactions observed in the literature for n-decanol were observed in this 43-second experimental acquisition time with TRIMS-TAD. This was found to be the shortest acquisition time possible for n-decanol (under DAC control, raw data acquisition and processing, and with the LKB-9000) at which the less abundant metastable ions could still be observed. Newer instruments with improved sensitivity would allow increased acquisition speeds for comparable data integrity. A factor of four or five is estimated as the possible degree of improvement in acquisition speed.

From these experiments it is apparent that the write-speed of the hard disk for data storage is an additional time factor to consider with TRIMS-TAD in its raw data acquisition configuration. Raw data are downloaded to the storage circuitry of the ITR data system. It was found that the acquisition time can vary by as much as 2 seconds depending on the distance the disk head has to move and the amount of data being downloaded. Peak finding in real-time via parallel processing improves data throughput and eliminates disk write speed as a contributing factor to the MS/MS acquisition time.

#### GC-MS/MS assessment of TRIMS-TAD

#### Selected Reaction monitoring

A mixture of benzene and chlorobenzene was injected into an OV-101 packed column and subjected to selected reaction monitoring with the TRIMS-TAD instrument. The reaction monitored was the 78+-->77+ metastable decomposition of benzene. Figure 4.11 illustrates the results of this experiment. Each data point in the ion current chromatogram represents 250 summed TOF spectra. These scans were produced by setting the magnetic field strength to pass mass 76. Scan numbers 70, 214, and 140 show the stable ion mass 76 in addition to the daughter mass 77 of the parent mass 78 of benzene. Scan number 595 shows the stable ion mass 76 of chlorobenzene. Scan number 595 does not show the reaction that is observed with benzene.

Another observation can be made from inspection of Figure 4.11. Scans 70, 214, and 140 are from different regions of the chromatographic peak and all contain identical mass spectral data (barring baseline noise). The ITR collected and integrated transients at a rate far greater than the ion source pressure changed. This acquisition rate avoids the peak skew that would otherwise occur with conventional data systems in GC-MS instruments.

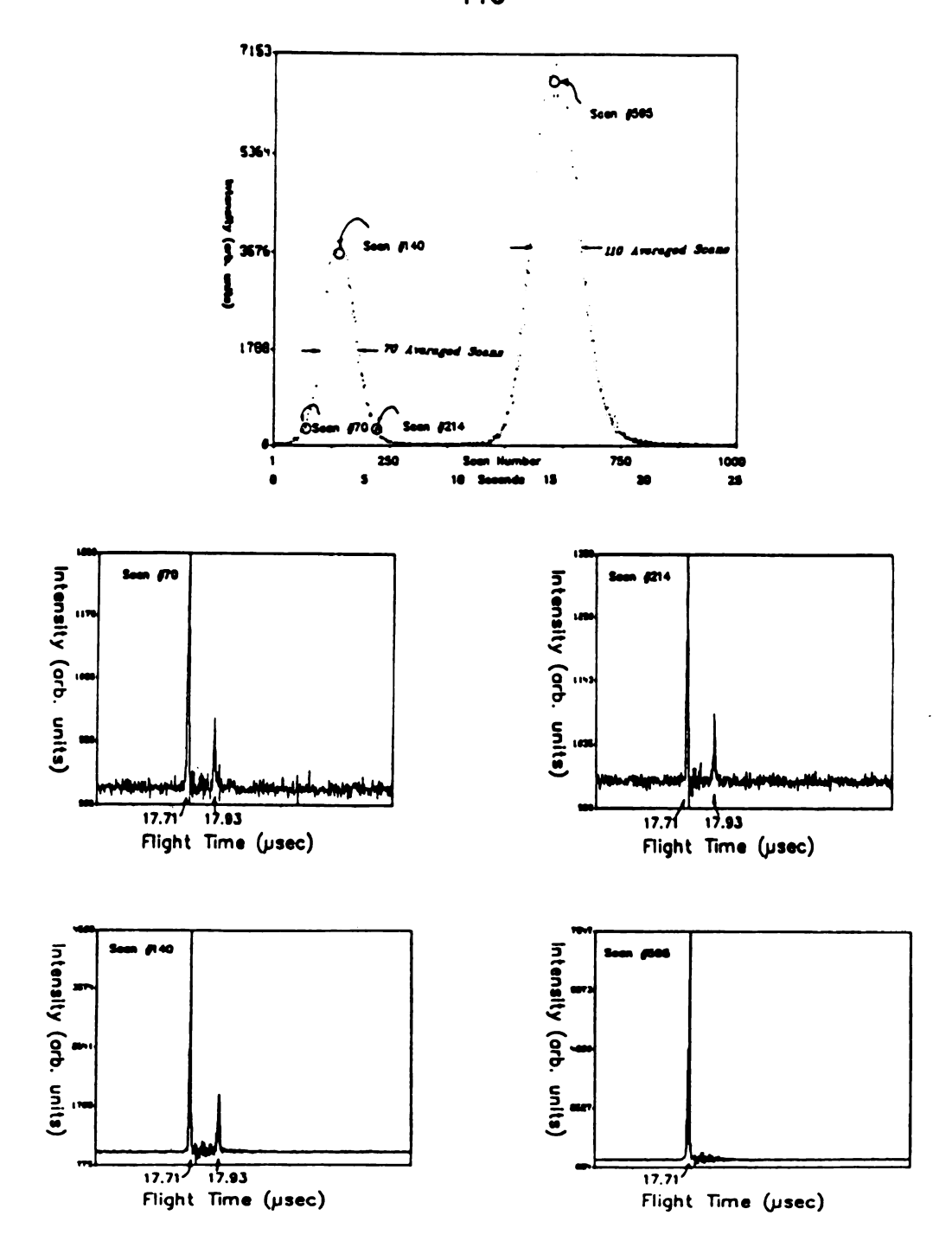


Figure 4.11 A selected reaction monitoring experiment with TRIMS-TAD. A mixture of benzene and chlorobenzene was separated by gas chromatography and subjected to MS/MS. The selected reaction was the 78 --> 77 metastable decomposition of benzene (peak at 17.93  $\mu sec$ ); the stable ion of mass 76 is represented by a peak at 17.71  $\mu sec.$ . Four scans were chosen from the 1000 total scans and the data are described in the text.

## Complete MS/MS field acquisition

The GC-MS response was most dramatically affected by the quantity of sample required for an MS/MS acquisition. Sample sizes of less than one microgram produced GC peaks that caused sample pressure changes in the source that were too rapid for a full MS/MS map to be acquired. The actual sample amount required by the TRIMS-TAD instrument for a discernible MS/MS map for methyl stearate, after separation from solvent and other impurities by the GC, was 5.3 µg. The complete MS/MS data field for this compound is shown in Figure 4.12. The mass range is slightly less than a decade, but approximately 10µsec of TOF information (2000 data points over a mass range from m/z 45 to 310)) was acquired per scan. The total time for acquisition of this MS/MS data field was 10 seconds with unit mass resolution along both the magnetic field and time axes. The stable ions and some of the observed fragmentation (by CAD) reactions (see Figure 4.13) have been labeled. The minimum sample requirement of 5.3 micrograms represents at least two orders of magnitude lower sample than that reported in the literature for the same type of analysis [6,7]. More typical are the milligram quantities reported by Farncombe and co-workers [8].

These experiments indicate that the TRIMS-TAD approach to MS/MS structure problems is feasible on the time frame of chromatography and therefore can lead to the acquisition of the complete MS/MS data field for components of complex mixtures separated by this method.

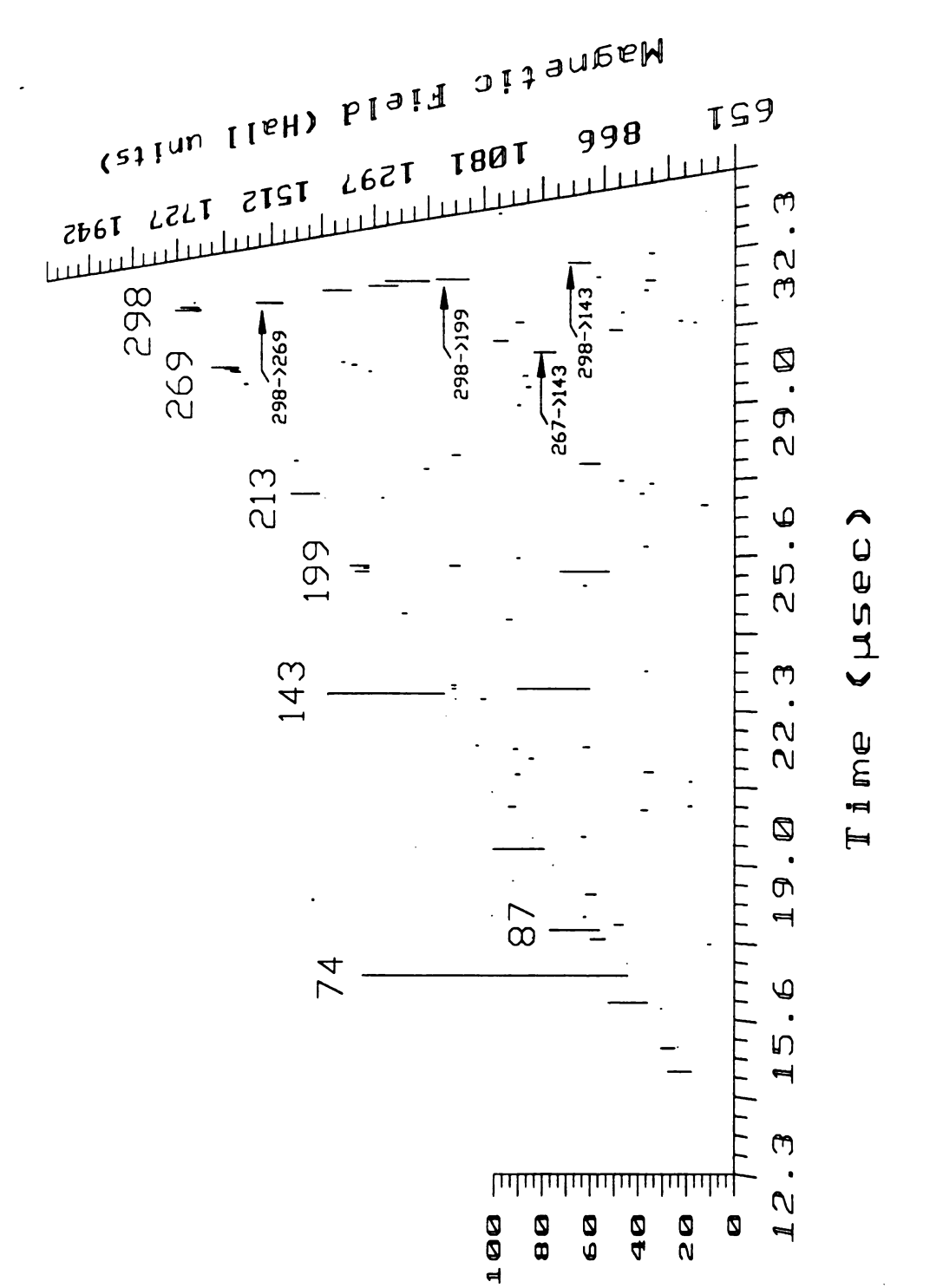


Figure 4.12 A complete MS/MS map of methyl sterate acquired in 10 seconds. This is a top view of the B-t data field. A wide-bore capillary column was used for the chromatographic introduction to the TRIMS-TAD instrument.

#### **FUTURE OPPORTUNITIES FOR TRIMS-TAD**

The rapid acquisition of an MS/MS data matrix will open up new opportunities for the full use of MS/MS. The ability to collect MS/MS spectra without interference from other components in an impure sample will allow highenergy MS/MS data bases to be constructed [8]. Other applications of MS/MS not utilizing on-line chromatographic separation, such as structure elucidation and studies of fragmentation pathways, could be carried out significantly more rapidly and consequently with much less sample. As liquid chromatographic-mass spectrometric interfaces improve it will be possible to map constituents generated from biochemical digests. As the TRIMS-TAD instrumentation improves the ability to monitor even less transient events in the source of a mass spectrometer will be possible.

#### **CHAPTER IV**

#### REFERENCES

- 1. Holland, J.F.; Enke, C.G.; Allison, J.; Stults, J.T.; Pinkston, J.D.; Newcome, B.H.; Watson, J.T. *Anal. Chem.* 1983, 55, 997A-1012A.
- 2. Glish, G.L.; Shaddock, V.M.; Harmon, K.; Cooks, R.G. *Anal. Chem.* 1980, 52, 165-167.
- 3. Enke, C.G.; Newcome, B.H.; Holland, J.F. U.S. Patent #4, 490, 806.
- 4. Mark Victor is responsible for coding the graphical algorithm
- 5. Cooks, R.G.; Glish, G.L. Chem. and Eng. News 1981, Nov. 30, 40-52.
- 6. Farncombe, M.J.; Mason, R.S.; Jennings, K.R.; Scrivens, J. Int. J. Mass Spectrom. Ion Phys. 1982, 44, 91-107.
- 7. Farncombe, M.J.; Jennings, K.R.; Mason, R.S.; Schlunegger, U.P. Org. Mass Spectrom. 1983, 18, 612-616.
- 8. Jennings, K.R.; Mason, R.S. Ch. 9 "Tandem Mass Spectrometry," Ed. F.W. McLafferty, Wiley, 1983.
- 9. Enke, C.G.; Wade, A.; Palmer, P.; Hart, K.J. *Anal. Chem.* 1987, 59, 1363A-1371A.

#### CHAPTER V

# KINETIC ENERGY RELEASE PROFILE MEASUREMENT WITH TRIMS-TAD

Tribulation brings about perseverance; and perseverance proven character; and proven character, hope.

Romans 5:3-4

#### Introduction

The TRIMS technique can be used to determine the energy distribution profiles for both parent and daughter ions. The product of *B* and *t* is a constant for all ions of the same m/z. Therefore, a spread in ion energies for a single m/z is manifest as a spread in ion abundance along a curve of constant *Bt* when plotted on the *B-t* plane (see Figure 5.1). From the parent or stable ion profiles, the energy resolution of the instrument can be determined. The additional spread in the daughter ion energy profiles yields the additional energy distribution caused by the fragmentation process.

The magnitude of the kinetic energy released by the ion dissociation process can be related to the potential energy surface for the metastable dissociation and to the internal energy of the metastable ion activated complex [1,2]. Since the potential energy surface is characteristic of a particular reaction, the kinetic energy release is often also characteristic of a particular reaction. This fact has been exploited to investigate ion structure and to differentiate

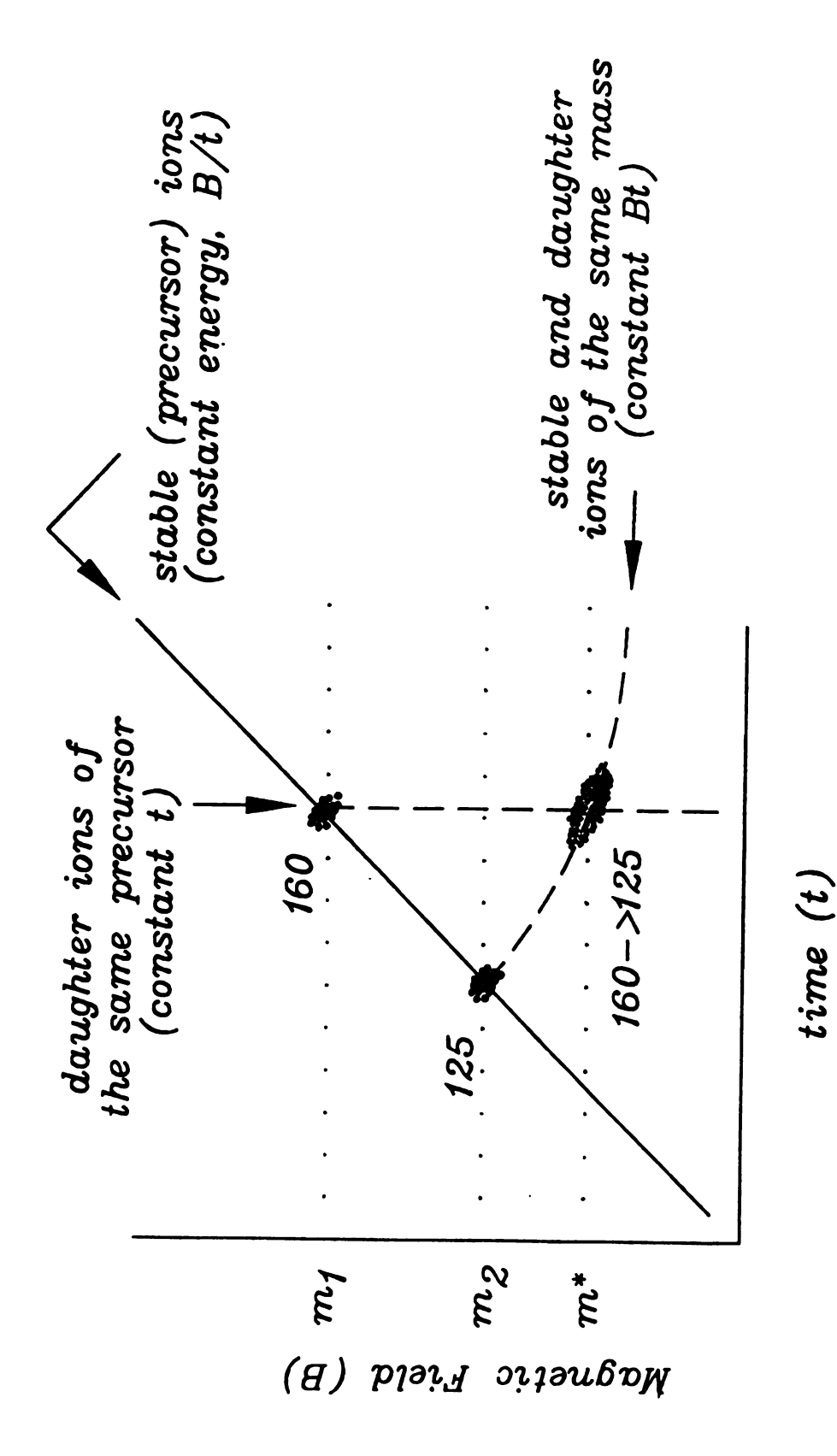


Figure 5.1 Representation of the B-t data field for the metastable loss of chlorine from the molecular ion of 2,4 dichlorotoluene.

isomeric species by mass spectrometry [3-6]. For example, kinetic energy release has been used to differentiate epimeric steroids [7], and to identify a wide variety of isomeric halogenated compounds [8,9].

Several techniques have been used to measure kinetic energy release. The most common are ion kinetic energy spectrometry (IKES) [10] and mass-analyzed ion kinetic energy spectrometry (MIKES) [11-14]. In these techniques the energy determination is performed with an electric sector or with a magnetic sector/electric sector combination in reverse geometry (BE), respectively. A recently developed technique with considerable promise utilizes an electric sector/quadrupole combination (EQ) [15].

Kinetic energy release has also been measured by magnetic sector instruments [16,17] and time-of-flight (TOF) instruments [18,19]. However, these techniques cannot resolve the kinetic energy release for daughter ions of similar mass which are derived from the same parent. The electric sector functions as the daughter ion mass analyzer, i.e., the mass analysis and kinetic energy release measurement occur along the same measurement axis. In many cases, peak overlap requires sophisticated deconvolution techniques to separate the energy contributions from each daughter mass.

In TRIMS, daughter ions are formed in the field-free region between the source and the magnet and essentially maintain the velocity of their parents. Thus, the flight time measurement for a daughter serves to identify its parent. lons of different energy, but the same mass, will be assigned to the correct mass through equation [1.1] but, will appear at different values of *B* and *t*. Therefore, regardless of the magnitude of the kinetic energy release, the ion intensity for

daughter ions of similar mass will be completely resolved [20]. TRIMS has successfully been applied by Lifshitz et al. to measure kinetic energy release as a function of ion lifetime [21].

## Equations for energy release measurement by TRIMS

The kinetic energy of an ion can be obtained from its position on the *Bt* line for its mass in the following way. The ion energy, *E*, is proportional to the quotient *B/t* and can be derived as shown below:

$$E = 1/2 \text{ mv}^2 \tag{5.1}$$

$$v = d/t ag{5.2}$$

substituting equations (1.1) and (5.2) into equation (5.1) yields

$$E = B/t(k_1) \tag{5.3}$$

where  $k_1$  is equal to (erdz/2). The values of B and t thus serve not only to identify the parent and daughter masses, but they also indicate the energy of the ion. If the ion current profile for a selected daughter mass in the B-t data field is plotted as ion abundance vs. B/t, a direct measure of the ion energy distribution is obtained. This is very similar to the method of data treatment in IKES.

The kinetic energy release, T, is a function of the observed energy distribution, as given by equation (5.4)

$$T = (m_1 2eV/16m_2m_3)(\Delta E/E)^2$$
 (5.4)

[22,23] where  $m_1$ ,  $m_2$  and  $m_3$  are the parent, daughter, and neutral masses, respectively, E is the energy of the stable ions, and  $\Delta E$  is the energy value obtained from the corrected energy distribution of the daughter ions. This correction is related to the energy spread of the stable ions by equation (5.5) below:

$$\Delta E = \Delta E_{obs} - (m_2/m_1) \Delta E_{stable}$$
 (5.5)

where  $\Delta E_{obs}$  is the observed energy value obtained from the width at half-height measurement of the daughter ion energy distribution and  $\Delta E_{stable}$  is the value obtained for the same measurement from the energy distribution of parent ions that did not fragment.

#### INSTRUMENT OPERATION WHEN STUDYING KINETIC ENERGY RELEASE

The ITR data system described in Chapter four is used for the energy release measurements with slight modification to the parameter table. The magnet range is set to encompass the calculated apparent mass, for the particular parent to daughter reaction, by  $\pm 2$  daltons. The TOF range is set to encompass the parent ion's arrival time  $\pm 1\mu sec$ . When the parameter table is

set, data collection commences upon execution of a program written in 68010 assembly language. At each momentum setting, arrival time spectra are summed in the selected region of the *B-t* data field. The raw data are then extracted from the data field and downloaded to a PC-AT (for post-processing).

From the data field, which contains intensity vs arrival time for a range of momentum values, a contour can be plotted showing the curved profile in the *B-t* field (see Figure 5.2). The energy spread in the daughter ions causes the intensity of the peak to be distributed along this curve. By conversion of these data to mass and energy for each point (equations 1.1 and 5.3), selecting the mass, and replotting the data as ion abundance vs. energy, an energy distribution profile is obtained (see Figure 5.3).

#### KINETIC ENERGY RELEASE RESULTS

To arrive at an accurate value of energy at a particular B,t coordinate it was necessary to correct for observed offsets in the Hall voltage and time measurements and to determine  $k_1$  in equation (5.3). The beam chopping synchronization has a constant time offset and was determined from a linear least-squares regression of t vs m<sup>1/2</sup>. The value of the intercept is then subtracted from all measured ion arrival times. A Hall voltage offset was observed as well and a regression of hall vs m<sup>1/2</sup> yielded the Hall voltage correction factor. The value of  $k_1$  was determined by solving equation (5.3) for several stable ions at a nominal energy of 3.5kV.

The kinetic energy release, T, is a function of the observed energy distribution. It is important to note that an energy correction must be made

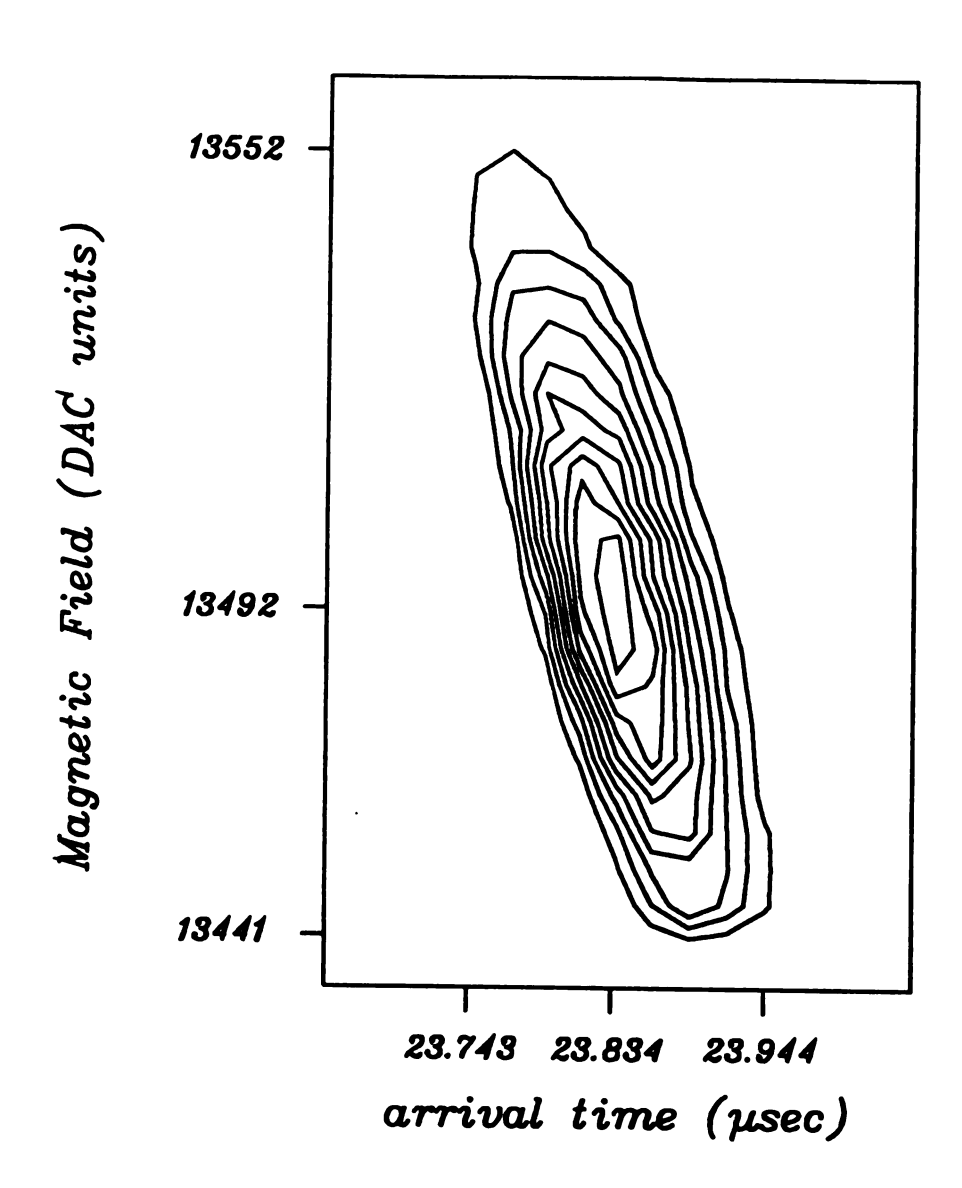


Figure 5.2 Observed contour in the *B-t* data field for the reaction represented in Figure 5.1.

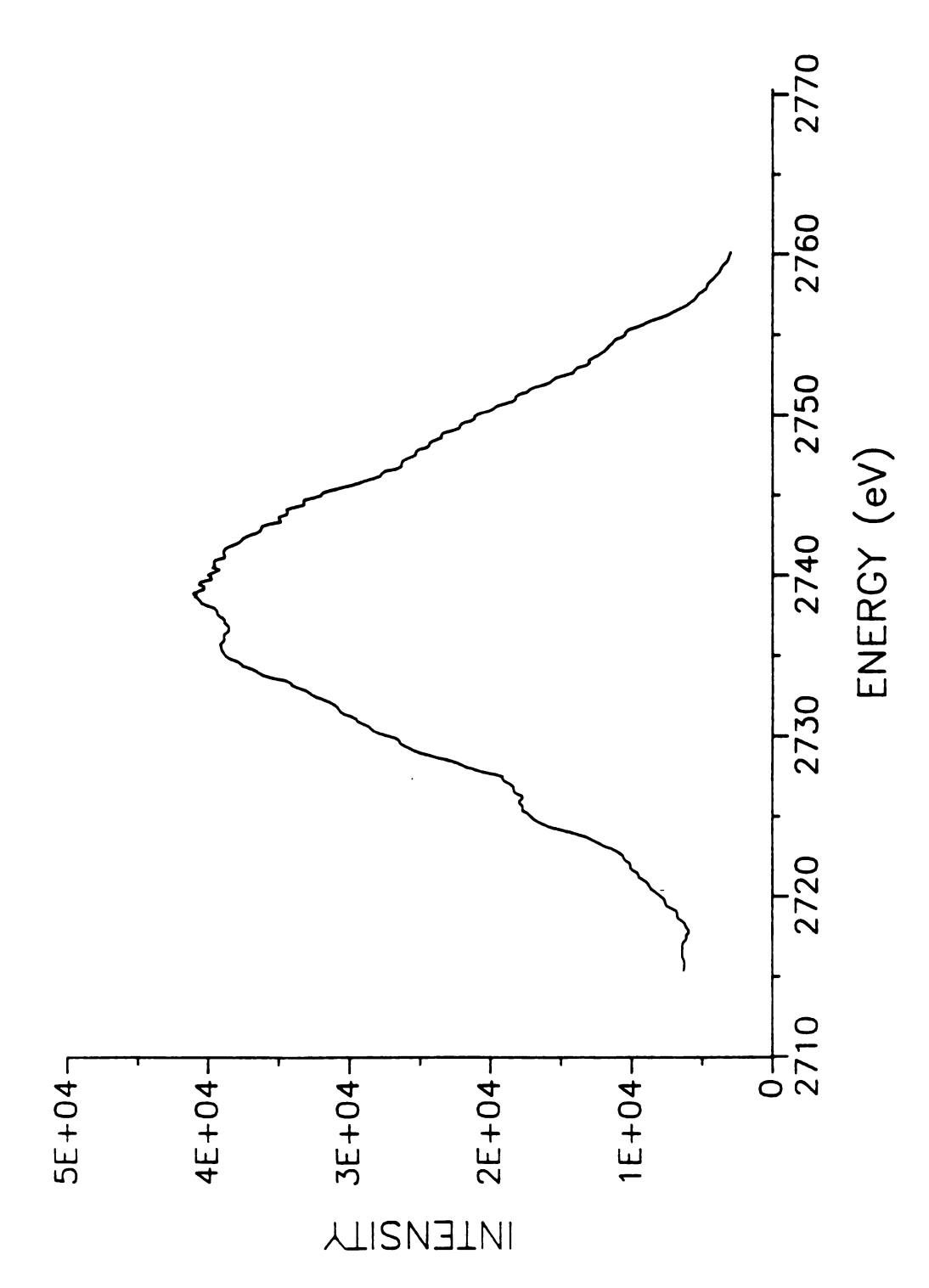
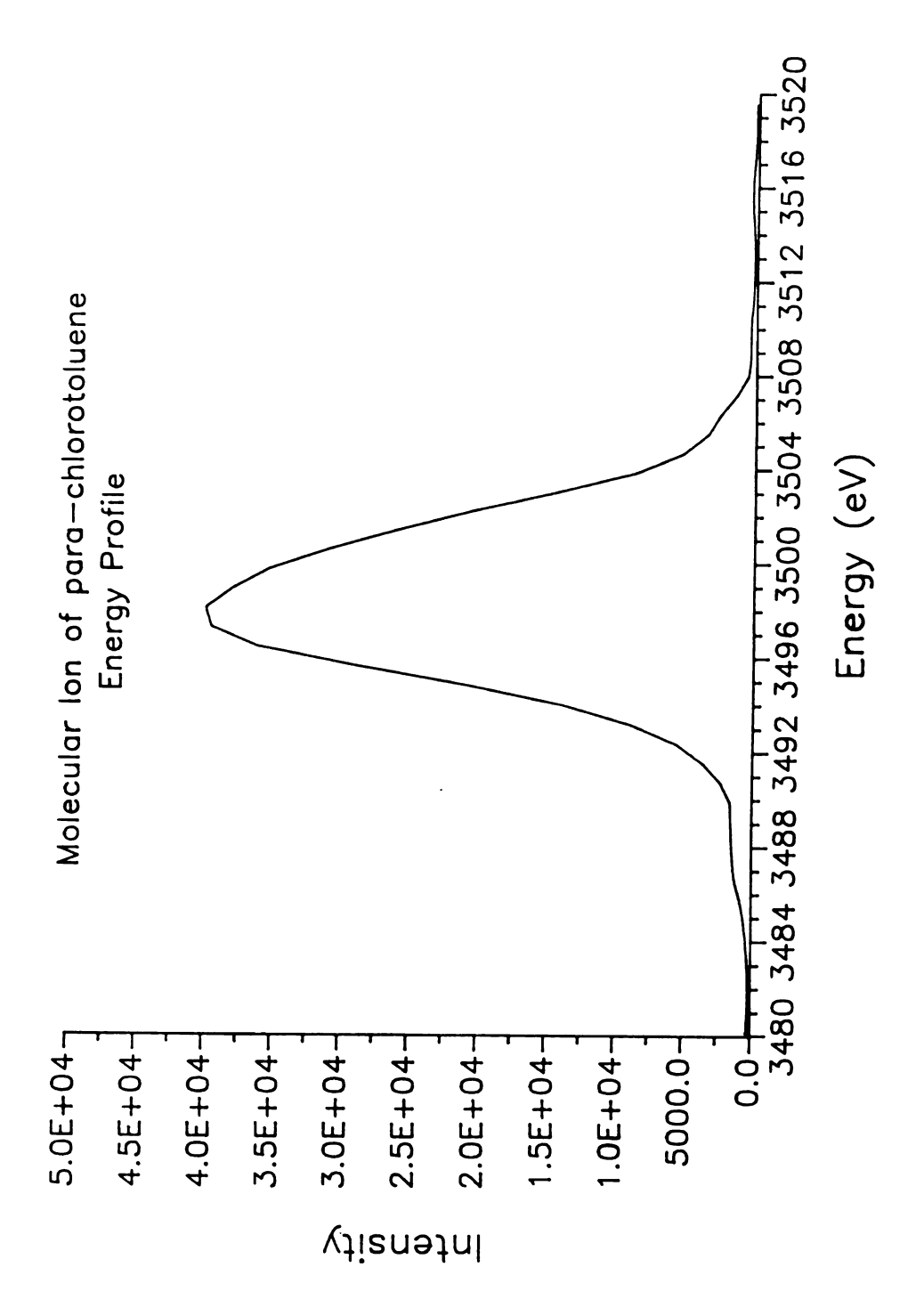


Figure 5.3 Energy release profile from the metastable loss of chlorine from 2,4 dichlorotoluene.

because some of the daughter ion kinetic energy distribution is due to the inherent energy distribution of the parent ions from the source. An example of this energy distribution is shown in Figure 5.4. If there were no kinetic energy release upon fragmentation, the daughter ions should display the same relative energy distribution as their parent ions [1]. All the kinetic energy release data presented here has been corrected for parent ion energy distribution using equation (5.5).

Table 5.1 shows the measured energy releases for two selected compounds. These results compare favorably with the values in the literature. The energy profile for the loss of chlorine from benzyl chloride is shown in Figure 5.5.



Eigure 5.4 Energy profile for the molecular ion of para-chlorotoluene. The energy width at half-height is approximately 7 electron volts.

TABLE 5.1

ENERGY RELEASE FOR LOSS OF CHLORINE UNDER UNIMOLECULAR CONDITIONS

COMPOUND	UNIMOLECULAR (meV)	LIT (meV)a
2,4 dichlorotoluene	28.4	28.6
benzyl chloride	7.7	7.4

a Ref. [9]

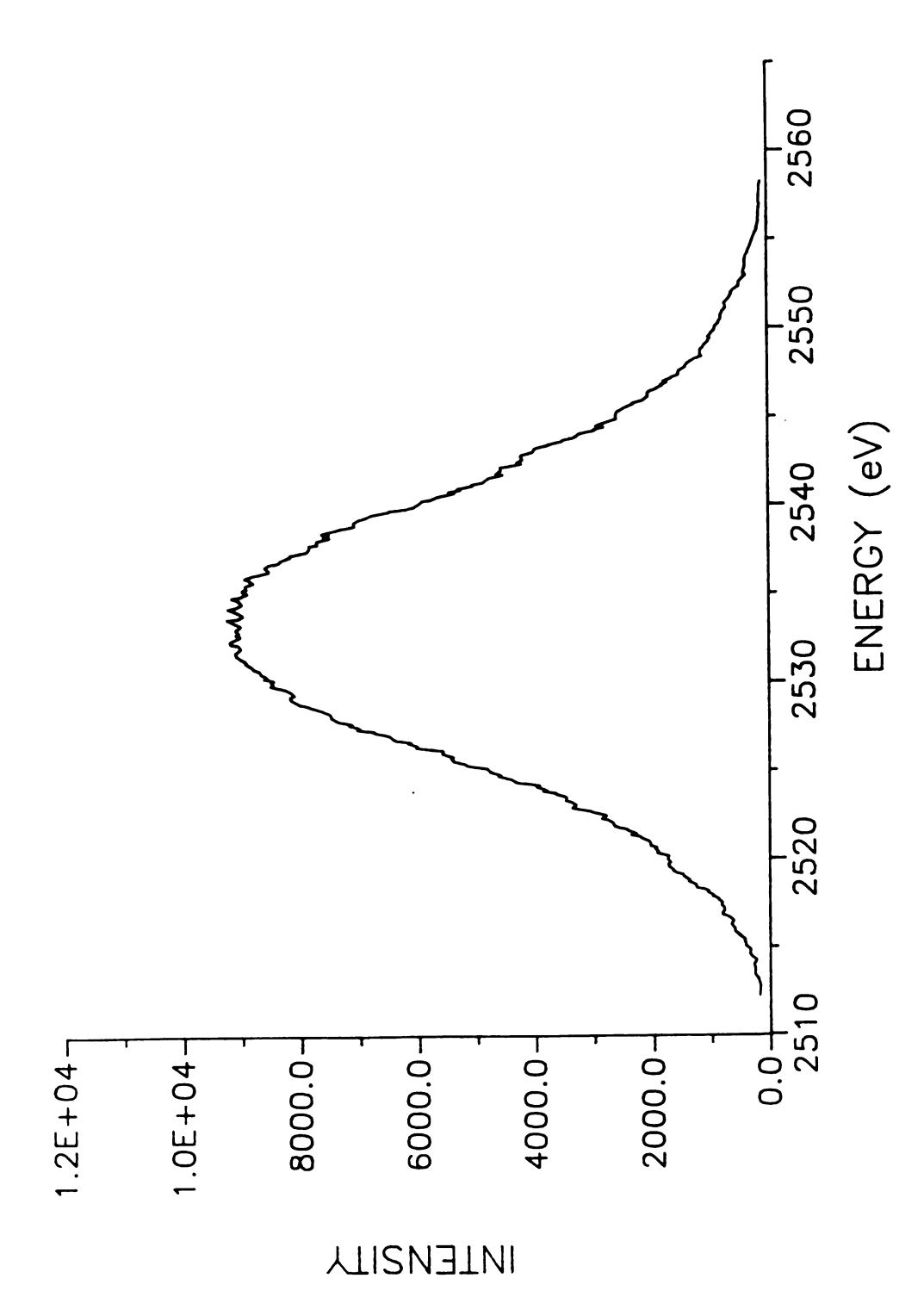


Figure 5.5 Energy release profile of the metastable loss of chlorine from benzyl chloride.

The observed kinetic energy distribution will be a combination of ion thermal energy spread, kinetic energy release, and instrumental parameters such as flight time pulse width, ion path variations and slit width. Thus the difference between our measurements and the literature values for the energy release are most likely due to slight temporal variations in the measurement and physical variation in ion optical and instrument design. The profile shown in Figure 5.2 of the daughter ions in the *B-t* field gives an idea of how the instrumental parameters affect the overall profile. A finite thickness to the *B-t* curve is observed. This thickness is the result of a convolution of slit width, thermal energy variations and other instrumental parameters and will change slightly, for example, upon slit adjustment or deflection assembly adjustments. The ultimate daughter ion resolution will be limited by this distribution. An excellent discussion and analysis of these effects for kinetic energy release determination is given by Derrick *et al.* [24].

The length of the *B-t* curve for particular isomass daughter ions represents their range of kinetic energy spread. This spread can reduce the precision with which the parent ion is identified. By centroiding the energy peak for a daughter ion, the mean energy and hence mean arrival time can be obtained. This process increases the precision for parent mass identification.

TAD was employed for the collection of energy profiles because of its speed and summing capabilities over that of TSD. The ITR's electronic architecture allows vast improvements in the speed/signal-to-noise tradeoff. In TSD, generation of a similar signal-to-noise has to occur sequentially over each channel in time. For example, to collect the data from a 200 nsec time region at

10,000 integrations (10 kHz pulsing rate) per 10 nsec interval requires twenty seconds with TSD. The ITR requires only one second for this same acquisition.

## **CONCLUSION**

In conclusion, the results indicate that the TRIMS technique is useful for kinetic energy release measurements. TRIMS in combination with TAD can fulfill a special niche in energy release measurements. The energy distributions for both stable and daughter ions can be measured accurately and rapidly with TRIMS-TAD system. The daughter ions consistently show a greater magnitude of energy spread, and they appear as predicted on the appropriate line of constant *Bt*.

#### **CHAPTER V**

#### REFERENCES

- 1. Cooks, R.G.; Beynon, J.H.; Caprioli, R.M.; Lester, G.R. "Metastable lons", Elsevier: New York, 1973, pp. 57-70 and 104-121.
- 2. Jones, E.G.; Beynon, J.H.; Cooks, R.G. J. Chem. Phys. 1972, 57, 2652-58.
- 3. Shannon, T.W.; McLafferty, F.W. J. Am. Chem. Soc. 1966, 88, 5021-22.
- 4. Jones, E.G.; Bauman, L.E.; Beynon, J.H.; Cooks, R.G. Org. Mass Spectrom. 1973, 7, 185-192.
- 5. Holmes, J.L.; Terlouw, J.K. Org. Mass Spectrom. 1980, 15, 383-396.
- 6. Levsen, K."Fundamental Aspects of Organic Mass Spectro-metry", Verlag Chemie: New York, 1978, pp. 237-242.
- 7. Zaretskii, Z.V.I.; Dan, P.; Kustanovich, Z.; Larka, E.A.; Herbert, C.G.; Beynon, J.H.; Djerassi, C. Org. Mass Spectrom. 1984, 19, 321-325.
- 8. Hass, J.R.; Tondeur, Y.; Voyksner, R.D. Anal. Chem. 1983, 55, 295-297.
- 9. Voyksner, R.D.; Hass, J.R.; Bursey, M.M. Anal. Chem. 1983, 55, 914-920.
- 10. Beynon, J.H.; Caprioli, R.M.; Baitinger, W.E.; Amy, J.W. Int. J. Mass Spectrom. Ion Phys. 1969, 3, 313-321.
- 11. Beynon, J.H.; Cooks, R.G. J. Phys. E 1974, 7, 10-18.
- 12. Beynon, J.H.; Cooks, R.G. Int. J. Mass Spectrom. Ion Phys. 1976, 19, 107-137.
- 13. McLuckey, S.A.; Glish, G.L. Int. J. Mass Spectrom. Ion Proc. 1987, 76, 41-46.
- 14. Beynon, J.H.; Cooks, R.G.; Amy, J.W.; Baitinger, W.E.; Riley, T.Y. Anal. Chem. 1973, 45, 1023A-1031A.
- 15. Harris, F.M.; Keenan, G.A.; Bolton, P.D.; Davies, S.B. Singh, S.; Beynon, J.H. Int. J. Mass Spectrom. Ion Phys. 1984, 58, 273-292.
- 16. Beynon, J.H.; Saunders, R.A.; Williams, A.E. Z. Naturforsch 1965, 20A, 180.

- 17. Sensharma, D.K.; Franklin, J.L. Int. J. Mass Spectrom. Ion Phys. 1974, 13, 139-150.
- 18. Franklin, J.L.; Hierl, P.M.; Whan, D.A. J. Chem. Phys. 1967, 47, 3148-53.
- 19. Haddon, W.F.; McLafferty, F.W. Anal. Chem. 1969, 41, 31-36.
- 20. Stults, J.T.; Enke, C.G.; Holland, J.F. presented at the 32nd Annual Conference on Mass Spectrometry and Allied Topics, San Tonio, TX, May 27 June 1, 1984, bound volume pp. 519-520.
- 21. Lifshitz, C.; Gefen, S.; Arakawa, R. J. Phys. Chem. 1984, 88, 4242-46.
- 22. Beynon, J.H.; Caprioli, R.M.; Baitinger, W.E.; Amy, J.W. Org. Mass Spectrom. 1970, 3, 661-668.
- 23. Terwilliger, D.T.; Beynon, J.H.; Cooks, R.G. Proc. R. Soc. London, Ser. A 1974, 341, 135.
- 24. Rumpf, B.A.; Derrick, P.J. Int. J. Mass Spectrom. Ion Proc. 1988, 82, 239-257.

#### **CHAPTER VI**

#### **FUTURE APPLICATIONS OF TRIMS-TAD**

In my end is my beginning.

Brian Eckenrode

#### Introduction

TRIMS has proven itself as a viable analytical technique with a bright future. Post-sector beam deflection is a simple modification to a single sector mass spectrometer yielding enhancements in resolution and sensitivity over those of source pulsing. The simplicity of this instrumentation provides adaptability to older instruments and, thus, revives their use and utility. The deflection circuitry, add-on flight tube, and associated electronics (not including the ITR) can be purchased for under \$10,000 [1]. With the addition of the ITR, rapid acquisition of an MS/MS map will open up new opportunities for the full use of MS/MS. The capability for energy-independent mass assignments paves the way for high mass CAD mass assignment accuracy. TRIMS can be used for kinetic energy release studies for analytical or physical chemistry purposes. Modification of instruments with alternate ionization sources for TRIMS provides possibilities only limited by the analytical chemist's imagination and ingenuity.

## Potassium ion desorption spectrometry (KIDS)

An analytical study with TRIMS-TAD of compounds ionized by K+IDS [2] was initiated. A direct insertion probe (DIP) and the ion source of the LKB-9000 was modified by Karen Light and myself so that we could try K+IDS-TRIMS-TAD. The ion source DIP inlet was bored to 1/4" diameter. The probe itself was modified for K+IDS, but still needs to be extended for easier rough pumping. A viewport mounted on the source block would facilitate probe entry into the source. Experimentation with organic acids placed on the probe were planned. The sample lifetime was typically 6 to 10 seconds, and therefore, TRIMS-TAD for MS/MS analysis was elected as the instrument of choice.

#### CI/MS/MS

Also planned was an experiment introducing methane into the source via the GC, to as high a pressure as possible, and, thus, performing chemical ionization (CI) on a sample. MS/MS, in this manner, in a TOF instrument has not been done by anyone to my knowledge. This experiment would illustrate the use of an alternate ionization technique in TRIMS.

# Pulsed secondary ion mass spectrometry (SIMS)

A couple of years ago I proposed a pulsed SIMS system. The sample duty cycle would improve markedly over beam deflection and the possibility to study surface reactions by MS/MS existed. I realized that the large energy spread would reduce resolution (but not cause errors in mass assignments) and that I would be better off with an electric sector placed before the magnet. Since the LKB-9000 does not have an electric sector, this idea was abandoned. Modification of a double-focusing instrument for TRIMS will allow experiments with this ionization technique.

#### **GENERAL SYSTEM IMPROVEMENTS**

The present instrumentation can be further improved with a little time and effort. One area is with the deflection assembly electronics. Experimentation with increased repetition rates is suggested. Development of faster and more easily controllable (computer interface) electronics will facilitate analyses. An improved gas chromatograph with temperature control programming and capillary column capability will be necessary. Magnetic field strength scanning control via ITR will be required to allow several MS/MS map acquisitions and averaging.

The alignment of the deflection slit and the detector is crucial to the success of this technique. An adjustable slit mask would be a much needed improvement so that beam positioning and background signal could be controlled and investigated.

# <u>Automated Chemical structure Elucidation System (ACES) and TRIMS-TAD</u>

A long term goal of the TRIMS-TAD project is to incorporate it with the ACES project [3]. The TRIMS-TAD instrument can rapidly produce MS/MS maps, but there remains the task of correlating fragmentation patterns with chemical structure. Figure 6.1 shows the TRIMS-TAD element in an analysis flow. The top of the figure begins with an unknown sample mixture which is first separated by gas or liquid chromatography. The separated component then can enter the TRIMS-TAD system for generation of a complete MS/MS fragmentation map. The TRIMS-TAD region has been expanded to reiterate the processes occurring over a sample lifetime. This MS/MS data are then downloaded to ACES for structure elucidation.

## **CLOSING COMMENT**

The future of TRIMS is very bright. Several hurdles have been overcome, but several still remain. Continuing improvements in technology combined with the imagination and effort of analytical scientists will prove this technique's farreaching capabilities.

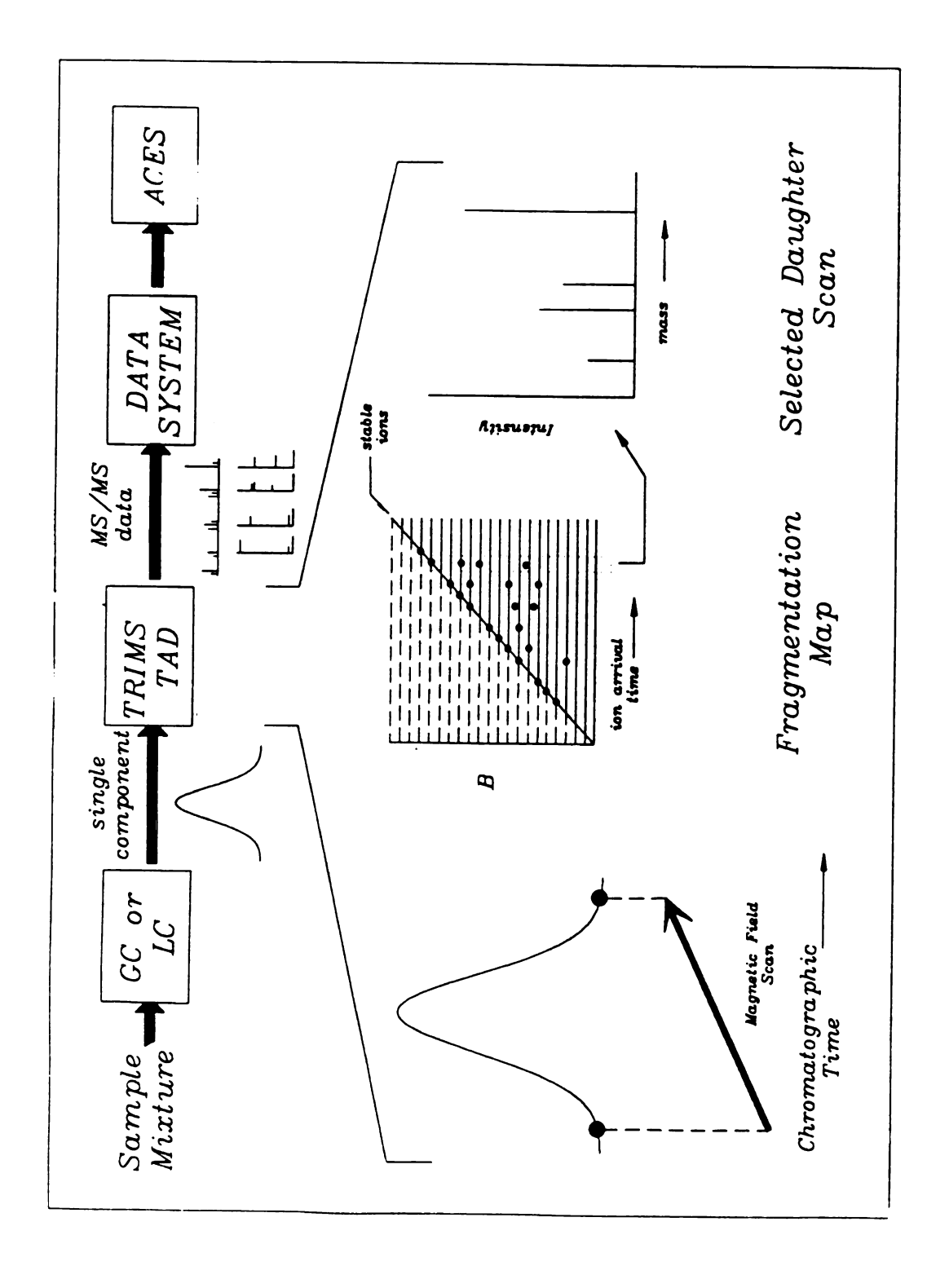


Figure 6.1 Overall chemical structure elucidation scheme incorporating TRIMS-TAD.

## **CHAPTER VI**

## REFERENCES

- 1. Eckenrode, B.A.; Watson, J.T.; Enke, C.G.; Holland, J.F. Int. J. Mass Spectrom. Ion Processes 1988, 83, 177-187.
- 2. Bombick, D.; Pinkston, J.D.; Allison, J. Anal. Chem. 1984, 56, 396-402.
- 3. Enke, C.G.; Wade, A.; Palmer, P.; Hart, K.J. *Anal. Chem.* 1987, 59, 1363A-1371A.